



## **Progetto S4 - Titolo esteso del progetto**

*Responsabili: Dr. Luca Malagnini (INGV) e Prof. Daniele Spallarossa (UniGe)*

### **Rendiconto conclusivo (periodo 1 giugno 2005 - 31 luglio 2007)**

#### Abstract/goals of the project

The most important goal of this project is the implementation of the ShakeMap code (Wald et al., 1999a,b) in an automatic configuration, and the validation of such quasi-real time product. This goal includes the successful conclusion of a number of other subprojects, including: i) designing the data flux of the entire regional network; ii) correcting for the effects of the shallow geology at each and every recording site; iii) automatically characterizing the seismic source, in terms of location, magnitude, geometry and orientation, and, if needed, finite dimensions; iv) calibrating regional predictive relationships for the ground motion induced by an earthquake, starting at a minimum magnitude of interest, for a wide magnitude range; v) quantifying the effects of the surface geology on the ground motion for every location within the entire monitored region.

Without going now into the details of the ShakeMap code, its purpose is the definition of quasi-real-time scenarios of ground shaking, shortly after the occurrence of an earthquake. It is clear what could be the implications and the advantages for the Dipartimento di Protezione Civile of having some prompt and detailed information about an earthquake occurred just a few minutes earlier, summarized in a detailed shake map (the mentioned scenario) and directly viewable and usable using sophisticated tools such as Google Earth or similar ones.

The ShakeMap project represented an important chance of cooperation for all the institutions involved, and with the former Servizio Sismico Nazionale (SSN) of the Dipartimento della Protezione Civile (DPC). The national accelerometric network (Rete Accelerometrica Nazionale (RAN), in fact, is run by the former SSN. The cooperation between all the participants (all the Research Units, RS's) should have occurred, whenever possible, on the most important task of the entire ShakeMap project: data exchange. Unfortunately, for reasons other than technical or scientific in nature, the data exchange never happened between the RAN and the main data center at INGV, nor between the Rete Accelerometrica del Friuli (RAF, funded by the regional branch of Protezione Civile), and neither between the stations of the OGS-CRS and the main data center at INGV. Data exchange is active only between the RU of the University of Genova (UniGe) and INGV.

The null contribution of the most important accelerometric networks to the INGV-located, integrated, real-time data set had the important effect of making all the future ShakeMaps from large earthquakes largely unstable, until INGV will deploy a sufficient number of strong-motion instruments throughout out national territory, especially in the NE part of Italy (see Figure I.1 in the next section), where the data coverage is particularly sparse.

The natural evolution of the present project must be towards an Early Warning (EW) tool, which in essence, is no more than a super-fast scenario producer. A significant part of S4 (not in terms of budget) was about EW applications in Italy. Our conclusion, beyond the obvious usefulness of EW applications, is that the future of real-time application in seismology must go through a real integration of seismic and accelerometric networks.

## 1. Risultati del progetto: aspetti generali (*max 6 pagine*)

The most important achievement of this project is the implementation of the complex system of codes that are necessary for the near-real time analysis of the seismicity of the entire Italian region, and of the adjacent areas. This plethora of computer codes, and of huge amounts of information of different kinds that are necessary for the correct use of such codes, has been installed and finely tuned at a number of different institutions that participate to the project. Specifically, ShakeMap is presently run in real-time at INGV, UniGe, UniTri, OGS-CRS.

Although redundancy is always an excellent characteristic of all the tools that are used in the seismic monitoring of the national territory, it is not clear at the moment the use that will be done of the ShakeMaps that will be produced for the region of overlap (i.e., the Italian NE), since three different institutions will be able to go public with their scenarios shortly after an earthquake occurs, and most likely all such scenarios will differ slightly, due to different attenuation relationships, different focal solutions obtained by different seismologists, and, most important of all, due to substantially different data fluxes available to each different data center. We will come back to the issue of data exchange later on, but, since the idea of the national data set of accelerometric and velocimetric waveforms has failed due to the existence of policies of unclear logic that effectively prevented any real-time data exchange, we give up on dealing on anything related to inter-institution data fluxes, and leave the solution of such problem to the representatives of DPC, INGV, UniTri, OGS-CRS, and of the regional DPC of Friuli-Venezia Giulia.

We, however, stress the fact that the Rete Accelerometrica Nazionale (RAN) does not exchange data with the main data center at INGV, nor does the Rete Accelerometrica del Friuli-Venezia Giulia (RAF). The cited accelerometric networks are the two main players in strong-motion monitoring in Italy. Moreover, they both belong to a set of tools for seismometric monitoring funded by agencies of civil defense and, one way or the other, they both are monitoring networks directly related to the present project (RAN belongs directly to DPC, whereas RAF is run and maintained by one of our partners). It is also very clear that there are no stringent technical difficulties that prevent the effective data exchanges.

The project was organized in five tasks:

- Task 1. Data exchange and organization of the main data center at INGV. This task has been considered critical for the success of the entire project. Our goals have only partially been achieved, because the data exchange is effectively active only between INGV and UniGe. With OGS-CRS we will be able to implement, before the end of the project, the data flux generated by a few low-cost accelerometric stations from OGS-CRS to the main data center at INGV. The internal organization of the main data center at INGV has been achieved through a sophisticated architecture that will be described in details later on.
- Task 2. Generation of a new velocity model of Italy that is suitable for the computation of realistic Green's functions to be used in the automatic procedures for the characterization of the seismic source. The Task has been considered marginal for the success of the project by the revision committee, but still a lot of work has been done by the different RU's for the definition of regional sets of Green's functions to be used for the waveform inversion codes for the determination of the moment tensor solutions. A subproject on the analysis of the cross-correlation of the ground noise started at the end of the first year; its

goal was the joint inversion of the group velocity dispersion curves computed along interstation paths, together with the available receiver functions computed at a large number of broadband stations for the national network run by INGV.

- Task 3. Design of the data centers and installation of all the computer codes for the real-time analysis of the earthquakes within the Italian territory and the adjacent regions. Design and implementation of the procedures to be used for the data exchange and the generation of the integrated data set. Installation of new codes for the event location (NonLinLoc), and extension of the use of the latter for the daily monitoring activities. Design and implementation of a web site for the visualization of the near-real time results, and for the distribution of seismic data to the outside world. Design of a web-based tool for the remote handling of the procedures for the source characterization. One of our RU's (RU 6, UniRm1, Dept. of Electronic Engineering headed by N. Pierdicca) has worked on some tools for the automatic analysis of satellite images in various bands of the electromagnetic spectrum (from radar to visible). Results obtained by RU 6 are very promising, although the computer codes developed are of limited use at present, due to the long time windows between satellites' passages. Applications were performed in regions struck by strong recent earthquakes. An Italian version of a web-based macroseismic survey called "Did you feel it?" has been developed and is automatically running on the INGV web site. The most important addendum to the initial version of the present project is represented by the activities named "Early Warning" (EW) that have been performed in cooperation with UC Berkeley. Such activities should continue in a future framework, and should include a participation of INGV in the design of an acquisition/monitoring system of new generation, where both the flux of information, and the decision-making algorithms, would be specifically tailored on the EW needs. The EW results obtained within S4 are very promising and deserve a special attention.
- Task 4. Determination of regional predictive relationships for the ground motion. Gathering of significant data sets for the regions of Italy where a modern analysis has not been performed yet on high-quality digital data (southern Italy, northern Sicily). Investigation on the capabilities of weak-motion-based predictive relationships to predict the ground motion induced by larger earthquakes. Investigation of the scaling properties of the seismic sources. Determination of absolute site terms in some regions. Determination of predictive relationships for specific site classes (NEHRP, EUROCODE8). Calibration of tools for the automatic computation of the moment-rate spectra of earthquakes, and of their  $M_w$ 's. The Italian regional predictive relationships for the ground motion have been written in a tabular form and included in a modified module of the computer package ShakeMap. Among inter-RU's activities, predictive relationships of different nature have been compared against one another for the E Alps, and an inter-RU subproject has been initiated with the goal of producing a 2-D attenuation tomography of northern Italy.
- Task 5. Effect of the shallow geology on the ground shaking. Performance of seismic surveys on selected sites of regional and national seismic networks. Borehole-data acquisition and interpretation in terms of velocity structure for some sites of the Central Apennines. Performance of surface experiments and comparison with the information obtained by the borehole analyses (SASW, MASW, H/V, etc.). Determination of absolute site terms using seismological techniques. Compilation of maps of the shallow geology for the Italian territory, to be used for the correction of the ground motion scenarios generated by ShakeMap.

Results for earthquakes occurred in our region of interested are posted on the following INGV web page: <http://earthquake.rm.ingv.it/>, where the events are described in terms of source characteristics, shaking scenarios, and general regional information. Both automatic and

revised moment tensor solutions are shown. The Quick Regional CMT solutions generated by Silvia Pondrelli (INGV Bologna) are also posted. Waveforms used for the source characterization can also be downloaded, together with all the information necessary for the instrument deconvolutions. ShakeMaps for larger events are not published automatically, as asked by Mauro Dolce during a specific meeting, but they are first transmitted to DPC.

The UniGe also publishes automatically a web page with all the information on the last event: <http://www.dipteris.unige.it/geofisica/AutoLoc.php>. This page contains the location and its quality, some ground-motion parameters, magnitude ( $M_L$ ), and a figure with the waveforms and picks. In case the event is important, a button can be hit to go to the ShakeMap (it requires a login username and password). The xml files to build the ShakeMap can be downloaded by an authorized user, and are also automatically emailed to INGV.

Early Warning (EW) activities were very useful to us for understanding the capabilities of the available real-time network, and the needs for future cooperation for the institutions that operate on the regional and national seismic monitoring in Italy. Since EW is, by definition, a super-fast reaction to a seismic event, based on a scenario produced very rapidly, there are two critical issues: i) the information flux, i.e., the softwares that are currently used for the data acquisition need to be redesigned completely, since reaction times are, at present, way too long for EW purposes; ii) distribution of stations on the monitored region, i.e., since a fast magnitude-location point can be computed using four observations, the time needed for the fourth arrival to be detected for an earthquake occurring anywhere within a region (roughly, the distance of the fourth closest station to any point of a given region divided by the P-wave velocity) is a measure of the upper bound of the promptness of our network. Figure I.1, taken from a study by Olivieri et al. (2007), shows, for each location over the entire Italian territory, the distance of the fourth closest broadband seismic station of the INGV National Digital Seismic Network. Figure I.1 basically quantifies the goodness of the coverage of the national region, based on the needs of a modern network, and clearly highlights the necessity of an effective data exchange, especially for what concerns the poorly covered NE Italy.

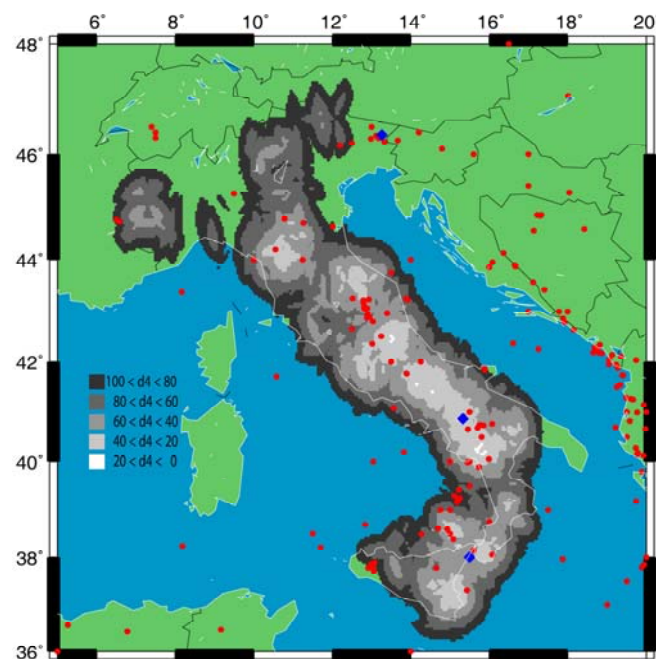


Figure 1: Map showing the density of INGV National Digital Seismic Network stations across Italy. The gray scale indicates the distance of the fourth closest station to all points in Italy.

Black indicates that the fourth closest station is 80 to 100 km away, white indicates a distance less than 20km. Where there is no gray scale there are not four stations within 100 km. Red dots are  $M > 5.0$  earths reported in the ISC catalogue for the last century. The blue diamonds indicate three representative earthquakes discussed by Olivieri et al.(2007). From north to south they are the 1976 Friuli, 1980 Irpinia and 1908 Messina earthquake locations.

## 2. Risultati del progetto aspetti di dettaglio per singoli task (max 20 pagine)

- **Task 1 – Data organization, integration and exchange**

Although this task has been considered critical for the success of the entire project, our goals have only partially been achieved. In fact, the real-time data exchange is effectively active only between INGV and UniGe. At the moment, all real-time, digital, 3C stations deployed in North Western Italy and managed by UniGe are shared with the INGV: at the same time, some INGV stations transmit on real time to UniGe allowing for a fast and efficient data exchange. With OGS-CRS we will be able to implement, before the end of the project, the data flux generated by a few low-cost accelerometric stations from OGS-CRS to the main data center at INGV.

Moreover the internal organization of the main data center at INGV and at UniGe has been achieved through a sophisticated architecture that will be described in some details.

The data archiving-distribution system of the INGV and UniGe system allow the users to access the data in various ways, depending on the analysis needs. Because of their complexity, the systems are still under development. The archived data to be distributed consist of both full waveforms and of various types of parametric data (e.g., station location coordinates, instrumental response, filtering procedures, arrival time of phases, earthquake locations).

INGV Archiving-distribution system:

Real-time data. It has been developed a continuous data stream procedure that allows, in principle, for the distribution of all the data acquired by the national network. Core to the data stream distribution is the implementation of the *SeedLink Server* that gathers in real-time all the data acquired by the CNT.

Station Data-base. During the course of the project, the station metadata database (DB) has been completed. This DB has been designed to keep track of the day-to-day functioning of the station. This is of great benefit to the technical personnel that can promptly recover the history of the stations, as well as their performance.

Event Data-base. The event DB has been populated with the revised earthquake locations obtained by the seismologists on duty in the seismic centre. In less than 30' (often in less than 15') the DB is adjourned as a new event has been recorded and located by the seismologists on H24 duty in the INGV seismic centre. The data of the DB are used to generate maps published on the INGV recent earthquake web page.

Continuous Data Archiving. The data recorded in real time are transferred to the waveform archive after checking for possible data gaps. A more thorough checking of the waveforms is postponed to a later stage of the data processing

Event Data Archiving. It has been developed a procedure that, after each earthquake determination, prepares the waveform event data in SAC format together with the station response functions as poles-and-zeros and sensitivity. These data are distributed on the web as gzipped tar ball for each event.

- **Task 2 – Definition of crustal models**

The ultimate goal of this task is that of determining the Green's functions (GFs) over the entire Italian territory and neighboring areas in order to be able to model the observed ground motion. To this purpose it is necessary to determine the velocity structure of both P- and S-waves for the Crust and the Upper Mantle. During the project this goal has been pursued in various ways – broadband waveform inversion for velocity model parameters, cross-correlation of seismic noise at pairs of stations, travel-time tomography, receiver functions.

### ***GF Regionalization***

As anticipated, the GFs are the main ingredients for forward waveform modeling of arbitrary focal mechanisms (point and finite fault sources) and/or for retrieving the moment tensor (or the finite fault) through inversion of the data of the Italian broadband stations. To this end, it has been completed a study (Li et al., BSSA in press) in which the Italian territory has been subdivided in laterally homogeneous regions (i.e., 1D velocity models). This regionalization has been accomplished through inversion of broadband data of the recently installed Italian broadband network and MedNet, together with several thousands of P- and S-wave arrival times. In order to obtain the regionalized 1D models, we have used the genetic algorithm (GA) to search the velocity model parameters from a set of 39 earthquakes with known focal mechanism (Figure 2.1). This study, however has highlighted the limitations of the 1D regionalization just described for geologically complex areas such as the Italian peninsula.

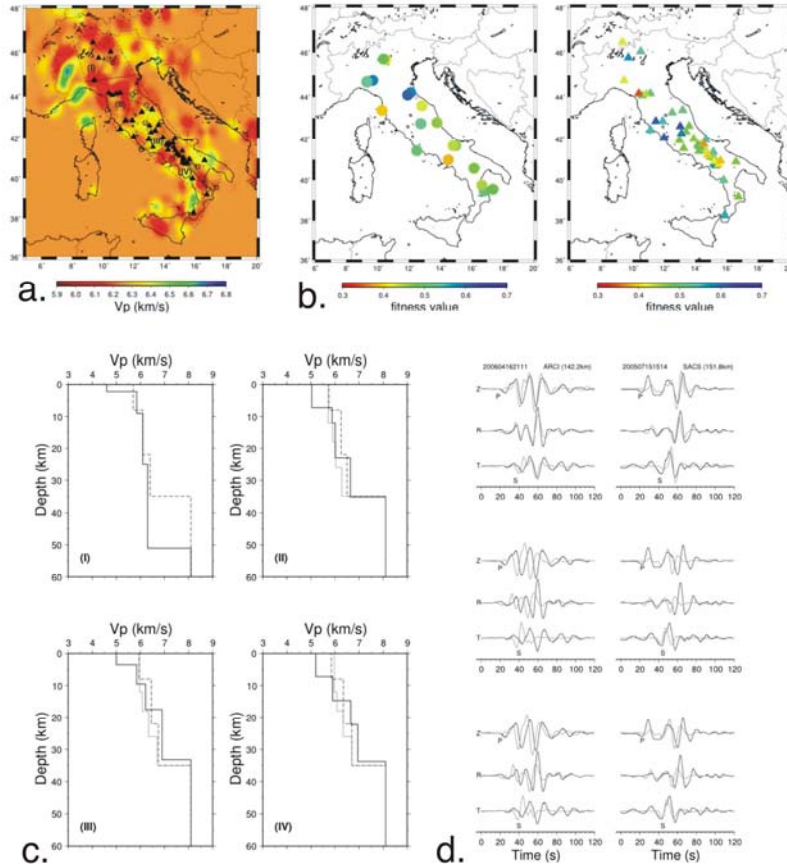


Figure 2.1: Results of the regionalization in laterally homogeneous velocity structures of the Italian peninsula. a.) Polygonal areas and paths used to determine the velocity models; b.) Fitness values calculated from the velocity models (P) determined in this study for all events (left) and stations (right) used in the Genetic Algorithm (GA) inversions. c.) 1-D velocity models obtained from the GA for the four regions (solid line), plotted together with previously proposed models. d.) Comparison of synthetic waveforms with observation for Region (II), the northern Apennines. Top: Comparison of synthetic waveforms from the best-fit velocity model obtained in this study (gray) with observed waveforms (black). Middle: Comparison of synthetic waveforms from the velocity model averaged from recent P-wave tomography results (gray) with observed waveforms (black). Bottom: Comparison of synthetic waveforms from the minimum 1D velocity model from Chiarabba and Frepoli (1997) (gray) with observed waveforms (black).

### ***Receiver Function***

The followed approach consists of two separate steps:

Step 1: The computation of the Moho depth underneath each seismic station with Receiver Function (RF) technique. This technique uses the P-S conversion at the velocity interface to produce 1D S-wave velocity models and the depth of the conversion (the Moho, in our case).

Step 2: The integration of Moho depth information from RF and Controlled Seismic Sources (CSS) data and 3D P-wave velocity model of the area. The final result is a 3D image of the Moho depth underneath the Italian peninsula.

In detail, in this work it has been addressed the crust-mantle boundary under the Apennines, using teleseismic receiver function (RF). We analysed teleseismic records of the National Seismic Network, together with data from temporary networks (mainly RETREAT and CATSCAN campaigns). The data set used comprises about 7700 high s/n ratio waveforms

from 138 broadband seismic stations. The RF data-set was investigated using different methods. We started with a single station analysis of the RF dataset computed for each seismic station, to provide a S-velocity profile under each station. As an example, in Figure 2.2 we illustrate the results for seismic stations deployed along the CROP-04 seismic line, during the CATSCAN experiment (Steckler et al, 2007, submitted to Geology).

The well known stacking method of Zhu and Kanamori (Zhu and Kanamori, 2000) has been also applied to extract first-order information about the bulk crustal seismic properties. We obtained results for a dense linear array deployed during the RETREAT campaign (Piana Agostinetti et al, 2007, in preparation).

Finally, we have integrated results from the RF with those independently obtained by controlled seismic sources (CSS) experiments all over Italy. The Moho depths derived from both CSS and RF are used, weighted accordingly with the estimation errors, as observational points to fit the Moho topography. The P-wave velocity model, continuous through the area, is used both to define the boundary between the Adriatic and the Tyrrhenian plates and to introduce constraints on the mean P-wave velocity in the crust (Figure 2.3).

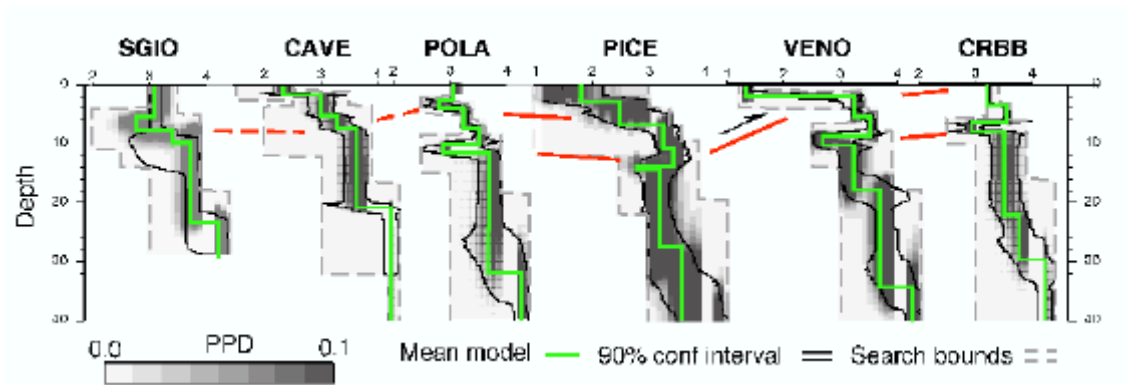
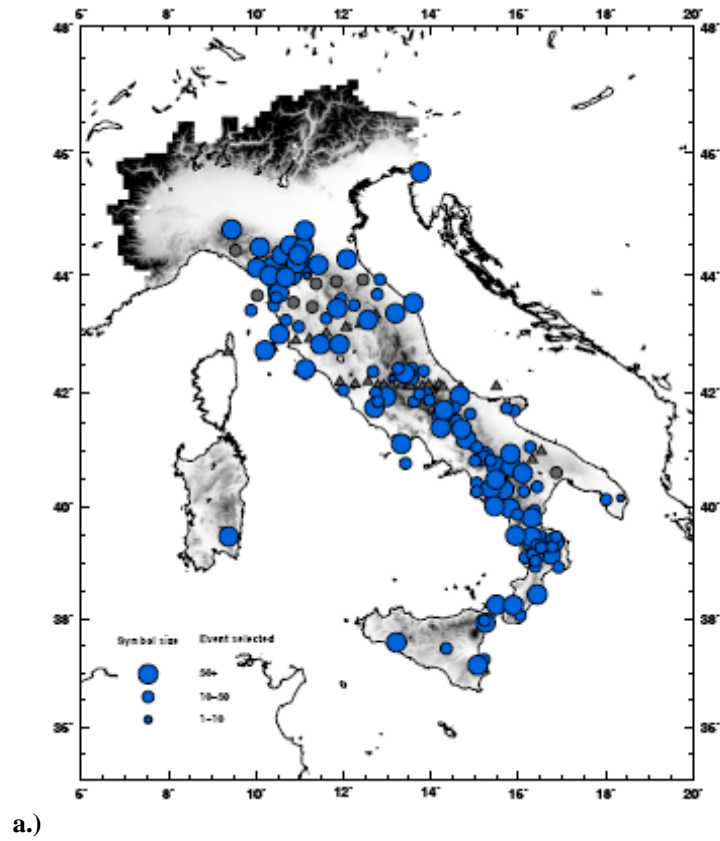


Figure 2.2: a.) Map showing the seismic stations selected for the RF study. The circle dimension scales with the number of data available for each station. The triangles are selected stations from temporary experiments. b.) Example showing a profile of 1D Vs models across the southern Apennines.

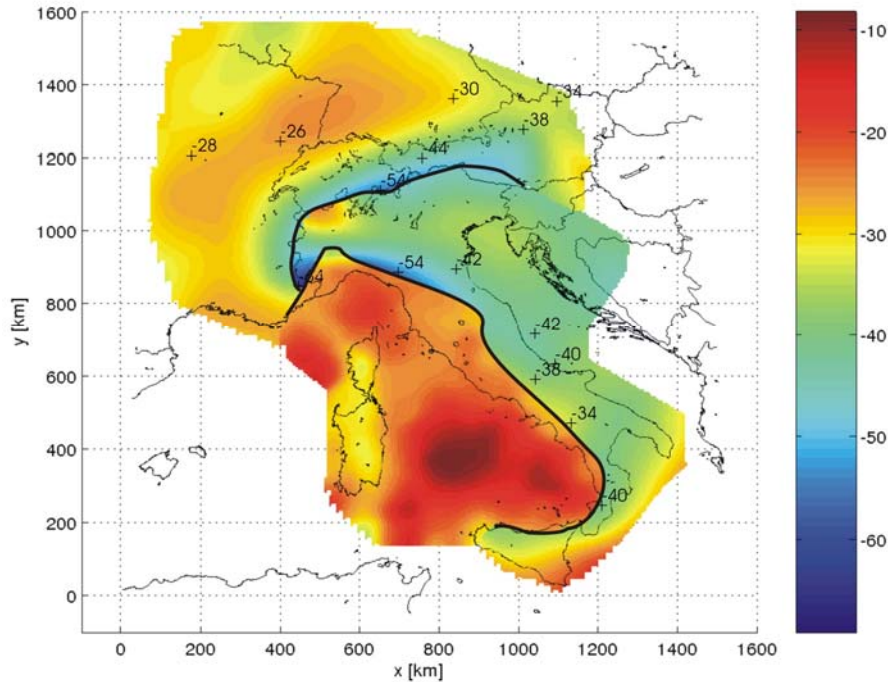


Figure 2.3: The Moho depth underneath Italy.

**Travel-time inversion**

According to the project, for Task2 the UR3 performed a seismic zonation of NE Italy into 6 areas by taking into account results from tomographic inversion as well as other geophysical and geological data available from the literature (Bressan, 2005). For each zone we defined a mono dimensional layered model between 0 and 35/40 km depth, depending on the Moho location, for which we estimated the P wave velocity ( $V_p$ ), the ratio  $V_p/V_s$ , the density and the quality factor  $Q_p$  and  $Q_s$ , all parameters that are used in the Task 3 for the computation of the Green functions. See Figure 2.4

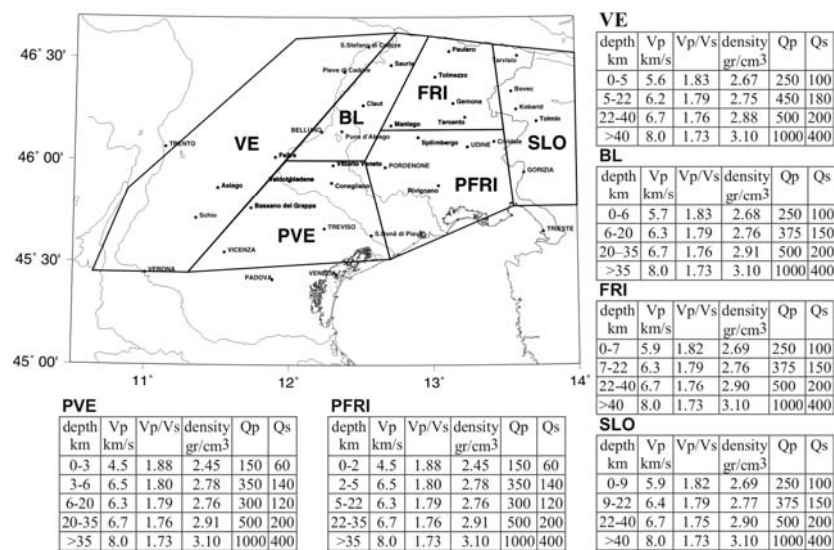


Figure 2.4: Structural model Proposed by RU3, with tables describing the velocity structure for each region.

Moreover the application of tomographic inversion methods has allowed to accurately define both 1D and 2D models for South-Western Alps and Northern Apennines (Figure 2.5). The tomographic study covers an area of about 380 x 460 km extending in latitude from about 43° N to 46°N 50' and in longitude from 6° E to 12° E. 3958 local events have been used for a total of 59.781 P phase first arrivals and 44.863 S phase first arrivals.

The P velocity distribution was widely studied in the past, and it is reasonably possible to consider it sufficiently known, at least at large scale. On the contrary, the S waves 3D velocity model and consequently the Vp/Vs ratio was not so well studied. The Vp/Vs ratio seems to increase in the shallow layers because of the presence of quaternary sediments, while more deeply, a high Vp/Vs ratio area is observed, corresponding to the Ivrea body. This anomaly extends to 16-20 km in deep. A second high Vp/Vs ratio zone extending to ~ 30 km in deep, has been noticed corresponding to the Northern Apennines.

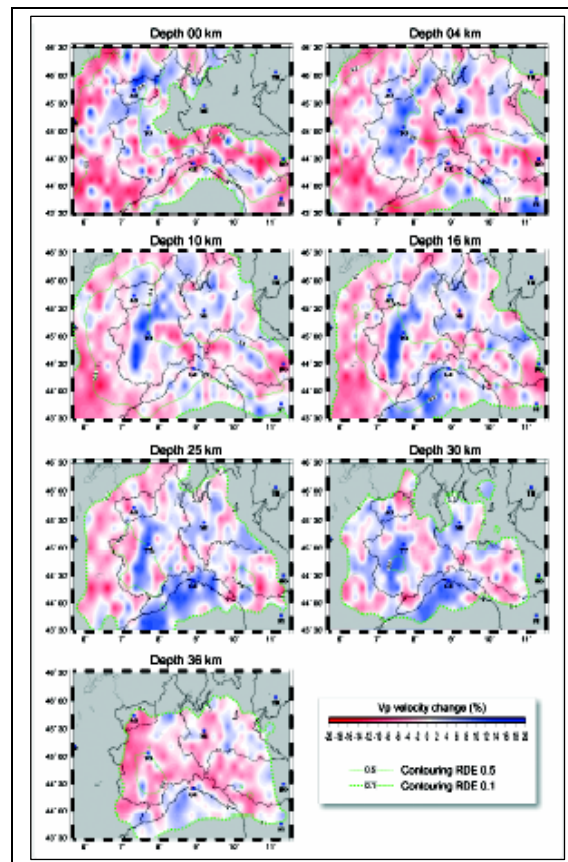


Figure 2.5: Tomographic model for the North Italy

### ***Cross-correlation of the ground noise***

In a second work (still underway) similarly driven toward determination of the velocity structure, we have employed a recently proposed technique which exploits the seismic noise recorded at pairs of stations for long periods of time (Shapiro and Campillo, 2004; Shapiro et al., 2005). In practice, the technique is based on stacking the cross-correlation of ambient noise between pairs of stations. As result, the true Green's function between the station pairs are obtained. From all these GFs it is then possible to determine the inter-station group velocities for periods comprised between 5 and 30 s (Figure 2.6).

In detail, digital waveforms from the RSN satellite telemetered broadband seismic network

were used in an initial determination of the inter-station Green's function through the cross-correlation of ground noise. Two months of digital data were used. Because of the available inter-station distances, focus was made on the 0.05 – 1 Hz frequency band. The network digital data were prepared by deconvolving the instrument responses to permit the use of all stations and by down-sampling to a 20Hz sample rate to speed the processing. Inter-station Green's functions were estimated for each of the 1278 station pairs; This initial study demonstrated the promise of the technique. We learned that we should consider the 0.02 – 1 Hz frequency band since there seems to be adequate long period signal related to mid-crustal structure. An example of interstation Green's functions as derived by the cross-correlation of ground noise is reported in Figure 2.7. The interpretation of the observed Green's function as simple surface-wave propagation is affected by scattering of the signal for many of the station pairs. For a few paths, selection of the fundamental mode group velocity is easy. However, in order to interpret all of the inter-station Green's functions, the expected dispersion for typical crustal profiles must be understood on the basis of other work on the three-dimensional nature of the crust.

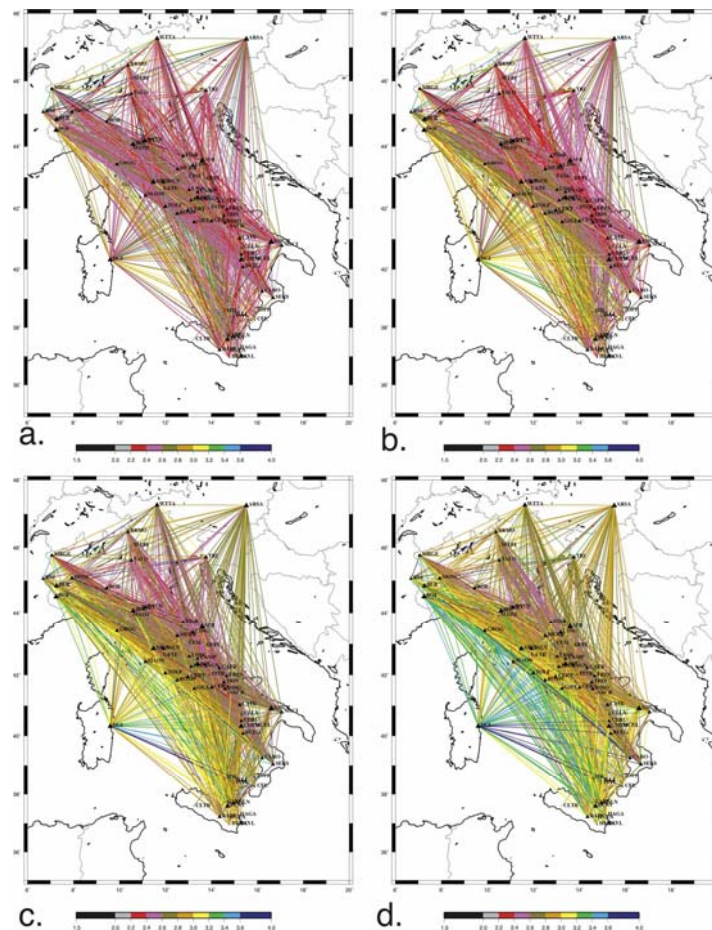


Figure 2.6: In Average Rayleigh wave group velocities at different periods between the station pairs used in the ambient noise cross-correlation analysis. a) 10.2 s; b) 14.6 s; c.) 20.5 s and d.) 24.9 s.

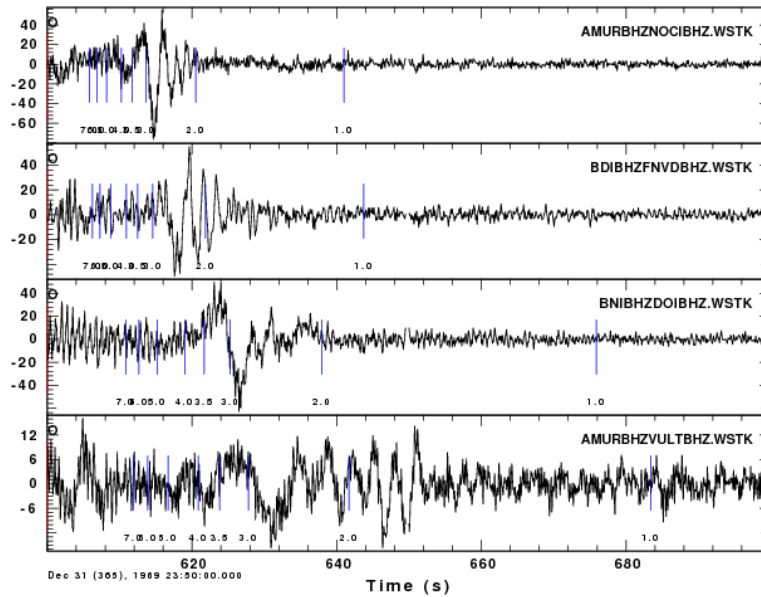


Figure 2.7: Interstation Green's functions from the cross-correlation of ground noise. All traces start at zero lag. The ticks indicate signal group velocities

### *Crustal rheology in peninsular Italy and Sicily*

One of the goals of this task is the definition of a first-order resistance model of the crust. The maximum deviatoric stress and the expected rheological behaviour (brittle vs. ductile behaviour) at depth were computed by means of rheological profiles (Ranalli and Murphy, 1987). Several 1-D rheological profiles, or strength envelopes, along DSS and Crop seismic profiles (Figure 2.8) were computed using the Coulomb-Navier criterion to describe the brittle behaviour and the Power Law Creep to represent plastic flow.

To compute the rheological profiles, crustal stratification, temperature, gross composition, tectonic regime, and strain rate have been derived as in the following:

- Depth of the main interfaces in the crust and allowed velocity ranges come from DSS and/or CROP profiles.
- Temperature has been computed assuming stationary uniform vertical conduction of the heat (Dragoni et al., 1996) and using regional or local heat flow data (Pasquale et al., 1997; Della Vedova et al., 2001).
- Based on the projected velocities and computed temperatures at depth, the possible composition for each layer in each of 40 points has been computed by means of tabulated literature data (Rudnick and Fountain, 1995, Christensen and Mooney, 2005).
- Tectonic regime comes from ZS9 seismic zonation (Meletti and Valensise, 2004) and, for Umbria and Sicily, from Lavecchia et al. (in preparation).
- Regional and local strain rate, based on long-term (~100 y) triangulation and short-term GPS data, have been derived by Hunstad et al. (2003) and Serpelloni et al. (2005).

From Coulomb-Navier criterion and Power Law Creep (Ranalli and Murphy, 1987) the yield strength profiles at depth were computed. All the needed parameters are shown in Table 2.2.

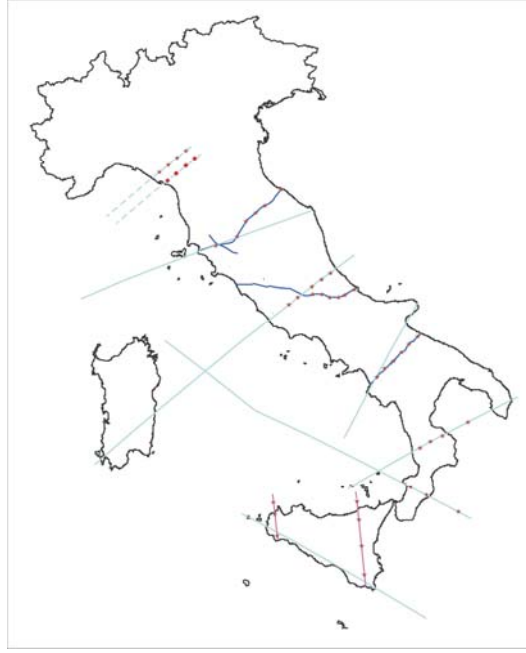


Figure 2.8: Locations of the rheological 1-D profiles (stars) and CROP-DSS lines.

| Layer | Lithology           | Code | Density (kg/m <sup>3</sup> ) | A (MPa <sup>-n</sup> /s)   | n   | E (kJ/mol) |
|-------|---------------------|------|------------------------------|----------------------------|-----|------------|
| UC    | Solnhofen limestone | SOL  | 2500                         | 1E-0.12 (s <sup>-1</sup> ) | /   | 197        |
| UC    | Solnhofen limestone | SOL  | 2500                         | 2.5E+3                     | 4.7 | 297        |
| IC    | DRY QUARTZITE       | QZd  | 2620                         | 6.7E-6                     | 2.4 | 156        |
| IC    | WET QUARTZITE       | QZw  | 2620                         | 3.2E-4                     | 2.3 | 154        |
| IC    | GRANITE             | GR   | 2750                         | 1.8E-9                     | 3.2 | 123        |
| IC    | WET GRANITE         | GRw  | 2750                         | 2.0E-4                     | 1.9 | 137        |
| IC    | QUARTZ-DIORITE      | QZD  | 2750                         | 1.3E-3                     | 2.4 | 219        |
| IC    | WET QUARTZ -DIORITE | QZDw | 2750                         | 3.16E-2                    | 2.4 | 212        |
| LC    | FELSIC GRANULITE    | GRF  | 2706                         | 8.0E-3                     | 3.1 | 243        |
| LC    | MAFIC GRANULITE     | GRM  | 3038                         | 1.4E+4                     | 4.2 | 445        |
| LC    | DIABASE             | DIA  | 2850                         | 2.0E-4                     | 3.4 | 260        |
| LC    | ANORTHOSITE         | AN   | 2850                         | 3.2E-4                     | 3.2 | 238        |
| UM    | WET PERIDOTITE      | PW   | 3250                         | 2.0E+3                     | 4.0 | 471        |
| UM    | DRY PERIDOTITE      | PD   | 3250                         | 2.5E+4                     | 3.5 | 532        |

Table 2.1: Assumed rheologies, density, and creep parameters A, n, and E. The code indexes Table 2.2 results. UC, IC, LC, UM: upper-intermediate-lower crust and upper mantle.

| Name     | lon   | lat   | Hf (mW/m <sup>2</sup> ) | hr (k m) | Strain rate (10 <sup>-15</sup> ) (s <sup>-1</sup> ) | Zs9 | Kine - mati cs (Zs9) | Use d Kine - mati cs | Bottom of interfaces (km) |    |     |                | Rheologies |
|----------|-------|-------|-------------------------|----------|---|-----|----------------------|----------------------|---------------------------|----|-----|----------------|------------|
|          |       |       |                         |          |   |     |                      |                      | U C                       | 2  | I C | L C            |            |
| pt 1 Lun | 10.00 | 44.10 | 70                      | 8        | 0.786 (G)   | 916 | NF                   |                      | 7                         | 16 | 34  | SOL-QZD-GRF-PW |            |

|                   |             |             |     |    |                  |             |         |           |     |               |      |                           |                |
|-------------------|-------------|-------------|-----|----|------------------|-------------|---------|-----------|-----|---------------|------|---------------------------|----------------|
|                   | 20          | 00          |     |    |                  |             |         |           |     |               |      |                           |                |
| pt 2 Lun          | 10.22<br>68 | 44.23<br>72 | 60  | 8  | 0.786 (G)        | 915         | NF      |           | 9   | 18            | 37   | SOL-GR o QZD-DIA-PW       |                |
| pt 3 Lun          | 10.45<br>27 | 44.37<br>39 | 50  | 8  | 0.786 (G)        | 913         | UN<br>K | NF        | 9   | 19            | 37   | SOL-GR o QZD-GRF-PW       |                |
| pt 4 Lun          | 10.67<br>08 | 44.50<br>50 | 40  | 8  | 1.3-15 (G)       | 913         | UN<br>K | TF        | 7   | 19            | 36   | SOL-GR o QZD-AN-PW        |                |
| pt 1 Lun I        | 9.795<br>0  | 44.25<br>89 | 70  | 8  | 0.786 (G)        | 916         | NF      |           | 8   | 15            | 32   | SOL-GR o QZD-QZd-PW       |                |
| pt 2 Lun I        | 10.03<br>01 | 44.40<br>08 | 60  | 8  | 0.786 (G)        | 915         | NF      |           | 9   | 18            | 38   | SOL-GR o QZD-QZd-PW       |                |
| pt 3 Lun I        | 10.24<br>09 | 44.52<br>75 | 50  | 8  | 0.786 (G)        | 913         | UN<br>K | NF        | 9   | 17            | 37   | SOL-GR o QZD-GR-PW        |                |
| pt 4 Lun I        | 10.45<br>70 | 44.65<br>49 | 40  | 8  | 1.3 -15 (G)      | 913         | UN<br>K | TF        | 9   | 18            | 37   | SOL-GR o QZD-GR-PW        |                |
| pt 1 Crop03       | 11.19<br>68 | 42.91<br>70 | 110 | 8  | 0.18 (H)         | 921         | NF      |           | 2   | 14            | 21   | SOL-GR-DIA-PW             |                |
| pt 2 Crop03       | 11.74<br>84 | 43.12<br>27 | 110 | 8  | 0.18 (H)         | 921         | NF      |           | 4   | 15            | 26   | SOL-GR-DIA-PW             |                |
| pt 3 Crop03       | 11.96<br>04 | 43.38<br>90 | 70  | 8  | 1.6 (H)          | 920         | NF      |           | 4.5 | 15            | 26   | SOL-GR-DIA-PW             |                |
| pt 4 Crop03       | 12.24<br>12 | 43.55<br>36 | 50  | 8  | 1.6 (H)          | 919         | NF      |           | 8   | 21            | 38   | SOL-GR o QZD-DIA-PW       |                |
| pt 5 Crop03       | 12.45<br>79 | 43.66<br>99 | 40  | 8  | 1.6/ 1.3 -15 (G) | 918         | UN<br>K | NF/<br>TF | 10  | 26            | 45   | SOL-GR o QZD-DIA-PW       |                |
| pt 6 Crop03       | 12.76<br>43 | 43.90<br>65 | 40  | 8  | 1.3 -15 (G)      | 917         | TF      |           | 10  | 19            | 35.5 | SOL-GR-DIA-PW             |                |
| pt 1 Crop11       | 13.58<br>73 | 42.03<br>21 | 45  | 10 | 1.8 (H)          | 923         | NF      |           | 18  | 25            | 38   | 44                        | SOL-QZD-GRM-PW |
| pt 2 Crop11       | 13.80<br>28 | 42.04<br>12 | 40  | 10 | 1.8 (H)          | 923         | NF      |           | 16  | 22            | 34   | 42                        | SOL-QZD-GRM-PW |
| pt 3 Crop11       | 14.00<br>41 | 41.98<br>40 | 40  | 8  | 1.8 (H)          | 923         | NF      |           | 14  | 19            | 32   | 39                        | SOL-QZD-GRM-PW |
| Crop11            | 14.21<br>66 | 41.97<br>92 | 40  | 8  | 1.8 (H)          | 918         | UN<br>K | TF        | 12  | 16            | 29   | 37                        | SOL-QZD-GRM-PW |
| pt 5 Crop11       | 14.38<br>26 | 42.02<br>95 | 35  | 8  | 1.27 (H)         | ND<br>(917) | OUT     | TF        | 10  | 15            | 27   | 35                        | SOL-QZD-GRM-PW |
| pt 6 Crop11       | 14.61<br>89 | 42.12<br>94 | 35  | 8  | 1.27 (H)         | ND<br>(917) | OUT     | TF        | 9   | 13            | 25   | 35                        | SOL-QZD-AN-PW  |
| pt 1 Crop04       | 15.16<br>73 | 40.52<br>60 | 40  | 10 | 0.76 (H)         | ND<br>(927) | OUT     | NF        | 8   | 22            | 28   | SOL-GR o QZD-GRF o DIA-PW |                |
| pt 2 Crop04       | 15.36<br>22 | 40.68<br>01 | 40  | 8  | 3.21 (H)         | 927         | NF      |           | 9   | 20            | 39   | SOL-GR o QZD-GRF o DIA-PW |                |
| pt 3 Crop04       | 15.57<br>77 | 40.82<br>16 | 40  | 8  | 3.21 (H)         | ND<br>(927) | OUT     | NF        | 6   | 18            | 32   | SOL-QZD-GRF o DIA-PW      |                |
| pt 4 Crop04       | 15.77<br>80 | 40.97<br>20 | 45  | 8  | 0.1 (G)          | 925         | SS      |           | 8   | 18            | 29   | SOL-QZD-AN-PW             |                |
| pt 5 Crop04       | 15.96<br>73 | 41.11<br>83 | 45  | 8  | 0.1 (G)          | 925         | SS      |           | 10  | 28            | 36   | SOL-QZD-AN-PW             |                |
| pt 6 Crop04       | 16.18<br>42 | 41.26<br>53 | 45  | 8  | 0.1 (G)          | 925         | SS      |           | 9   | 27            | 33   | SOL-QZD-AN-PW             |                |
| pt 1 Calabria     | 16.22<br>70 | 39.25<br>12 | 60  | 7  | 0.825 (S)        | 929         | NF      |           | 9   | 22            |      | SOL-QZD o DIA-PW          |                |
| pt 2 mid Calabria | 16.48<br>93 | 39.35<br>79 | 60  | 7  | 0.825 (S)        | 929         | NF      |           | 7   | 24            |      | SOL-QZD o DIA-PW          |                |
| pt 2 Calabria     | 16.78<br>33 | 39.47<br>10 | 50  | 7  | 0.444 (S)        | 930         | UN<br>K | NF        | 5   | 21<br>-<br>25 | 35   | SOL-QZD o DIA-PW          |                |
| pt 2 bis Calabria | 17.42<br>84 | 39.71<br>96 | 50  | 7  | 0.444 (S)        | ND          | OUT     | TF        | 3   | 15            | 30   | SOL-GR o QZD-DIA-PW       |                |
| pt 3 Calabria     | 15.99<br>46 | 38.53<br>81 | 50  | 7  | 0.825 (S)        | 929         | NF      |           | 7   | 17            |      | SOL-QZD-PW                |                |
| pt 4 Calabria     | 16.39<br>67 | 38.38<br>64 | 50  | 7  | 0.444 (S)        | 930         | UN<br>K | NF        | 5   | 18            | 36   | SOL-GR o QZD-DIA-PW       |                |
| pt 4 bis Calabria | 17.18<br>03 | 38.08<br>30 | 50  | 8  | 0.444 (S)        | ND          | OUT     | SS        | 9   | 27            | 32   | SOL-QZD-DIA-PW            |                |
| pt 1 Sicily       | 12.61<br>09 | 38.24<br>86 | 50  | 8  | 0.63 (S)         | ND          | OUT     | TF        | 9   | 18            | 28   | SOL-QZD-GRM-PW            |                |
| pt 2 Sicily       | 12.65<br>83 | 38.05<br>88 | 50  | 10 | 0.1 -1 (S)       | ND          | OUT     | TF        | 9   | 24            | 34   | SOL-QZD-GRM-PW            |                |
| pt 3 Sicily       | 12.72<br>01 | 37.64<br>89 | 80  | 10 | 0.1 -1 (S)       | ND          | OUT     | TF        | 10  | 24            | 33   | SOL-GR o QZD-GRM-PW       |                |

|             |             |             |    |    |             |     |     |    |    |    |    |                         |
|-------------|-------------|-------------|----|----|-------------|-----|-----|----|----|----|----|-------------------------|
| pt 4 Sicily | 14.68<br>99 | 38.27<br>36 | 80 | 8  | 0.63 (S)    | 933 | TF  |    | 6  | 15 | 24 | SOL-GR o QZD-DIA-<br>PW |
| pt 5 Sicily | 14.73<br>14 | 37.94<br>51 | 50 | 10 | 0.1 – 1 (S) | ND  | OUT | NF | 12 | 23 | 38 | SOL-QZD-DIA-PW          |
| pt 6 Sicily | 14.79<br>35 | 37.45<br>60 | 70 | 10 | 0.1 – 1 (S) | ND  | OUT | TF | 10 | 20 | 32 | SOL-GR o QZD-GRM-<br>PW |
| pt 7 Sicily | 14.86<br>28 | 36.93<br>94 | 70 | 10 | 0.1 – 1 (S) | 935 | SS  |    | 10 | 22 | 32 | SOL-GR o QZD-GRM-<br>PW |

Table 2.2: Resulting parameters for rheological profile construction. Profile locations, heat flow (hf), characteristic depth for radioactive heat productivity (hr), strain rate (S = Serpelloni et al., 2005; H = Hunstad et al., 2003; G=Lavecchia et al. (personal communication); ZS9 area code; ZS9 kinematics and used kinematics if undetermined (UNK) by ZS9 or outside (OUT) from the zonation (NF Normal, TF Thrust, SS Strike slip); depth of interfaces; code for rheological parameters (see Table 2.1).

- **Task 3 ShakeMap**

This task involves many activities for the accurate representation of the earthquake source and of its effects on the resulting ground motion. The core of the task is the implementation of the USGS-ShakeMap package (Wald et al. 1999) for the monitoring of the Italian region, but a

number of other different procedures were also implemented for a better, rapid understanding of the earthquake process. The latter include phase picking, fully nonlinear algorithms for earthquake location, early warning estimates of source location and magnitude, automatic magnitude, moment tensor, and finite source determinations, and the development of a web portal where the results can be published. As a corollary, a method for the calculation of the space-temporal estimates of seismic hazard has been also put under testing. In the following is provided a brief description of the activities and of the results accomplished.

### ***Phase Picking***

During these two years, the UniGe developed and tested several automatic picking procedures. During the first stage, a “two-step” procedure was developed, based on the APK algorithm (Allen 1978), and on the re-picking algorithm “Mannekenpix 1.7” (Alderson, 2004). More recently, a new automatic picking procedure was introduced, based on the seismic signal envelope and on the Akaike Information Criterion (AIC). The P- and S-phase arrival time are detected selecting the minimum of the AIC function (Sleeman and Eck, 1999). In detail, the steps are:

- Event detection
- Preliminary signal filtering (BP 2.5 – 15 Hz) and envelope using a threshold of 0.16 (vertical component).
- Computation of the AIC function on the previously selected window and recognition of P arrival time as minimum of AIC function;
- Pick P validation based on S/N ratio analysis;
- Preliminary location based on the validated picks (only P phases) using the Hypoellipse and/or a non-linear procedure (see next paragraph);
- Validation of the location;
- Definition of the theoretical S arrival times through a simplified velocity model and selection, for each station, of a time window around the theoretical S arrival time;
- Computation of the AIC function on the window selected in the previous step and recognition of S arrival time as minimum of AIC function;
- Pick S validation based on S/N ratio.

Preliminary results indicate that the APK-based procedure is more selective, while the AIC function allows the detection of a larger number of S arrival time (Figure 3.1).

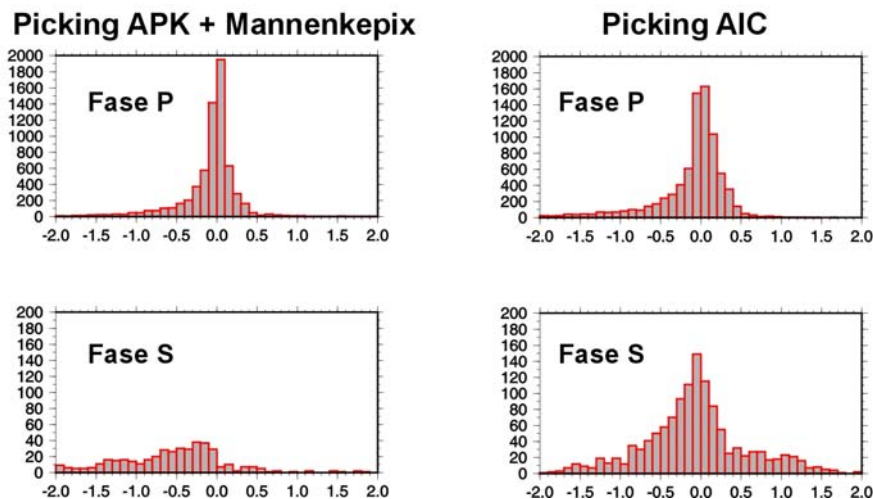


Figure 3.1: Differences between automatically and manually detected P-wave arrival times (upper panels) and between automatically and manually detected S-wave arrival times (lower panels). Right panels show results obtained using the AIC-based procedure, while the left ones using the APK-based one.

Event location is calculated using both the Hypoellipse computer code (Lahr, 1979) and the NonLinLoc method (Lomax et al., 2002, Lomax et al., 2001). The latter method is applied using a 3D velocity model coming from the tomographic inversion described in Task 2. Figure 3.2 shows a comparison among automatic locations obtained using the two different automatic picking procedures and the two location procedures.

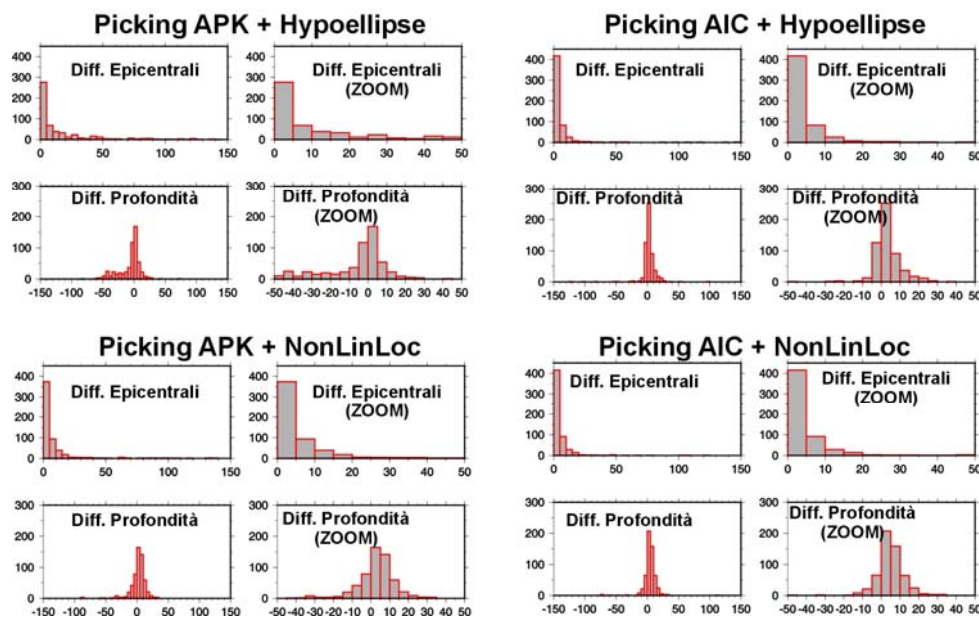
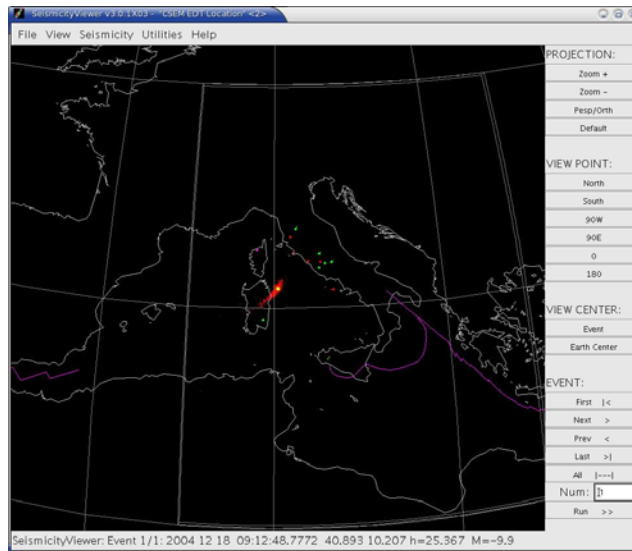


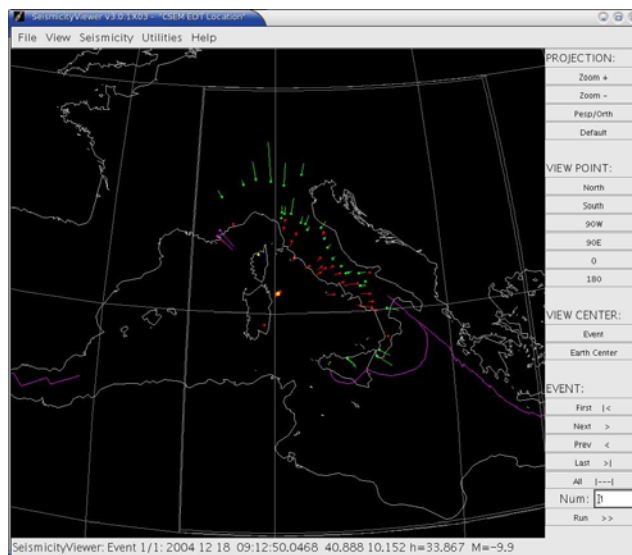
Figure 3.2: Differences between automatic and manual locations.

### *Non-linear earthquake location*

Both at INGV and at the UniGe it has been implemented the software NonLinLoc (Lomax, et al., 2000; Lomax, et al., 2001; Lomax, 2005; <http://www.alomax.net/nlloc>; NLL hereafter) and the Java visualization applet SeismicityViewer. NLL adopts the “Equal Differential Time” misfit function which is particularly robust in presence of data outliers (Lomax et al, submitted for publication). An example of NLL earthquake determination is provided in Figure 3.3, where an event off the coast of Sardinia is shown.



a.)



b)

Figure 3.3: Example of earthquake location obtained from the application of the program NLL. The event occurred near Olbia in Sardinia where very few stations are present. a.) location using the first stations recording the event only on the Tyrrhenian side of the Italian peninsula. It is clear the effect that fewer stations have on the location probability density function shown as a cloud of red points. b) Location with the complete set of stations that have recorded the event

### ***Real-time moment magnitude computation***

For northwestern Italy, an automatic procedure for the automatic moment magnitude computation has been implemented by applying the methodology described in Mayeda et al. [2003]. A set of correction parameters to be used in the automatic procedure have been carefully calibrated for the real time 3C stations of the RSNI, ETH and INGV within the Northwestern Alps and Northern Apennine.

Figure 3.4 shows an example of automatic  $M_w$  computation based on the coda waves analysis for three moderate events. Notice that although a large scatter characterizes the Salo' event, due to a location outside the network, the  $M_w$  value is comparable to the one obtained by

MedNet and SED.

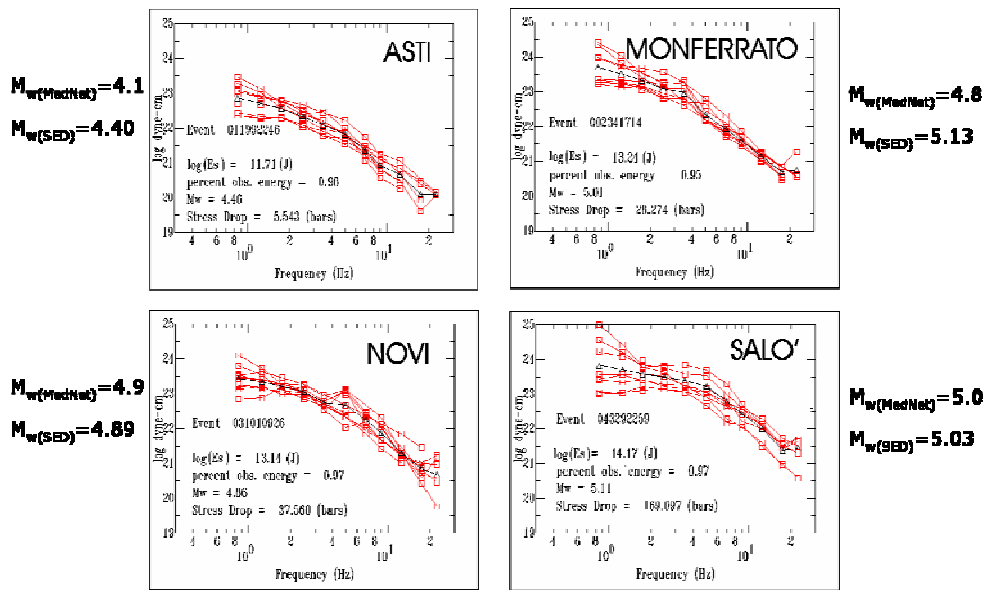


Figure 3.4: Example of automatically derived source spectra used for the Mw computation. Red curves are individual-station source spectra, while black curves are the averages over all stations. Automatic Mw's are computed on the average moment-rate spectra.

For northeastern Italy, an algorithm for the estimation of moment magnitude ( $M_w$ ) has been developed applying the methodology described in Andrews [1986]. This methodology uses the Brune spectrum and the corner frequency and is applied to the S waves. Broadband data and strong motion data relative to about 50 stations, 193 events, 3576 traces, has been analyzed in order to test the code (Figure 3.5). The standard deviation of the single station moment magnitude estimates with respect to the average event estimate is rather low and does not depend on distance. The method gives values of moment magnitude in very good agreement with independent estimates (moment tensor inversion). For all events, the retrieved moment magnitudes are also compatible, even for the smallest considered ones. In order to validate this approach, for about 143 events ( $1.0 \leq M_w \leq 4.0$ , hypocentral distance between 20 and 225 km, depths generally less than 15 km),  $M_w$ 's were also calculated by applying the empirical method based on coda envelope amplitude measurements described in Mayeda *et al.* [2003]. To calibrate the source moment-rate spectra, we used independent estimates of the moment magnitudes obtained from the long-period waveform modelling of two moderate-magnitude events in the region: Bovec 2004,  $M_w=5.2$  (Harvard) and Carnia 2002,  $M_w=4.7$  (MedNet). After calibrating these two stations,  $M_w$ 's were computed for the complete dataset (Figure 3.6).

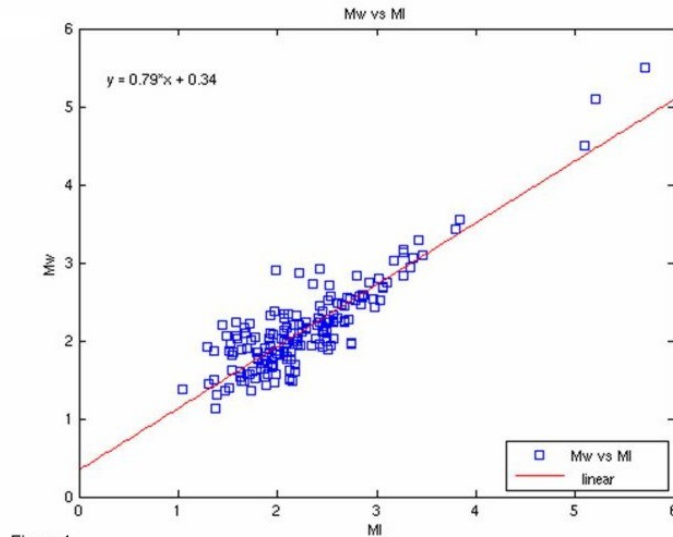


Figure 3.5: Moment magnitude (Brune Spectrum) versus Local Magnitude

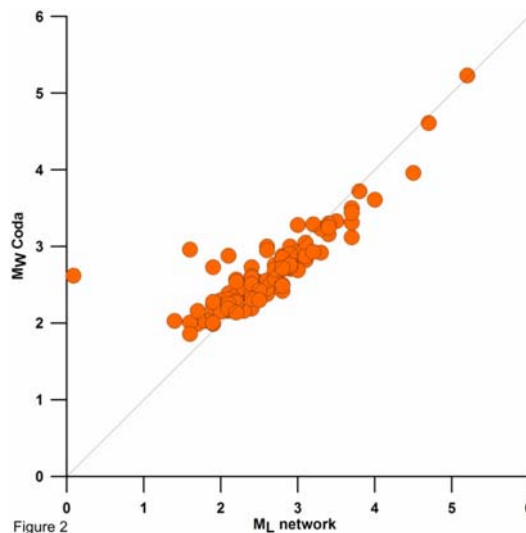
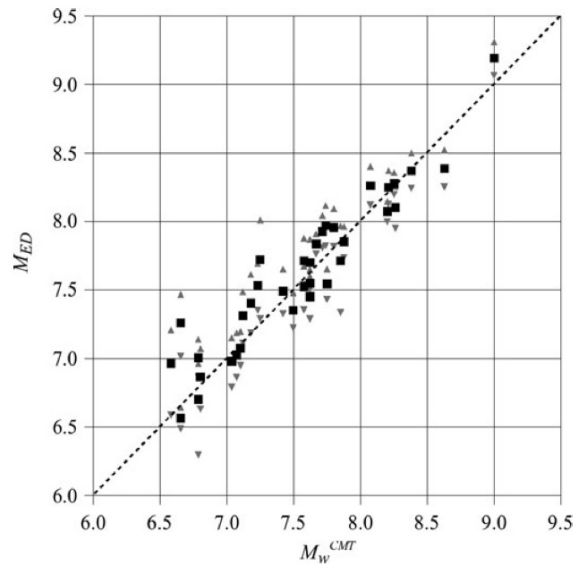


Figure 3.6: Moment magnitude (Coda Amplitude) versus Local Magnitude

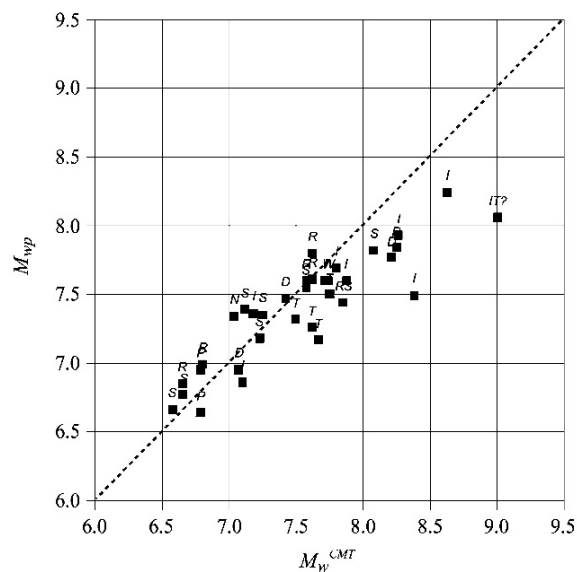
***Energy-duration magnitude.***

A new magnitude scale named  $M_{ED}$  (energy-duration magnitude; *Lomax et al., in press*) has been developed within the framework of S4. Such magnitude scale avails of estimates of short-period (1 Hz) duration and of seismic energy estimates determined between the arrival of P- and S-waves arrivals at teleseismic distances larger than  $30^\circ$ . It has been found that  $M_{ED}$  is particularly accurate for earthquakes  $M > 7.5$  and, through the determination of the energy-to-moment ratio, it is capable of indicating the tsunamigenic potential of a given earthquake. Noticeably,  $M_{ED}$  has shown to provide a magnitude of 9.2 for the great Sumatra earthquake (12/26/2004) less than 20 minutes after the earthquake occurrence. The correct magnitude estimate of the Sumatra earthquake was estimated several months after its occurrence by using the Earth's free oscillations whereas it is well known that only after several hours after the earthquake the magnitude was upgraded to M9 giving the true dimension of the

catastrophe. Similarly, after the 2006 July 17, Java earthquake, the initial magnitude was  $M=7.2$  (17 min after OT), the CMT magnitude, available about 1 hr after OT, was  $M_{CMT}=7.7$ ; the energy-duration results for this event give  $M_{ED} = 7.8$ , with a very long source duration of about 160 s, and a very low energy-to-moment ratio, indicating a possible tsunami earthquake. This estimate would have been possible within 17 minutes. In Figure 2.7, we show the comparison between the values of  $M_{ED}$  and those of  $M_{CMT}$ .



a.)



b.)

Figure 3.7 a.) Comparison of the performance of  $M_{ED}$  versus  $M_{CMT}$ . b.) Comparison of the performance of  $M_{wp}$  versus  $M_{CMT}$ . It is clear that  $M_{wp}$  saturates around M8 whereas  $M_{ED}$  does not. (from Lomax et al., in press).

### ***Real-time moment tensor estimation***

During these two years INGV developed an automatic moment tensor procedure capable of releasing, once the 24/7 INGV seismic center has located  $M_I \geq 3.5$  earthquakes, moment tensor solutions within about 5 minutes.

Moment tensor solution are computed for Italian earthquakes using data from the high quality INGV and MedNet regional broadband network, using the complete waveform inversion methodology, originally proposed by *Dreger and Helmberger (1993)* and later implemented by *Dreger (2003)*.

The algorithm inverts complete, three-component broadband displacement waveforms to estimate the point-source solution, while does not solve for the isotropic component that is constrained to zero. The goodness of the solution is determined by comparing synthetics with observed data, and it is measured through the variance reduction parameter (VR).

*The Real-Time Automatic Algorithm (AUTO-TDMT)* computation technique is triggered by a UNIX *crontab* command, which checks every 2 minutes for a new  $M_I \geq 3.5$  earthquake. The procedure starts by downloading the velocity waveforms from all the stations having recorded the event, within 300 km of epicentral distance. If the magnitude is higher that  $M_I=5.0$ , the distance range is extended to 500 km.

Data are corrected for the instrument response, integrated to obtain displacement, and band-pass filtered. The frequency band is chosen as follows: 0.02-0.05 Hz for events with  $M_I \geq 3.8$ ; 0.02-0.1 Hz for events with magnitude smaller than 3.8. The AUTO-TDMT procedure selects the optimal set of stations for applying the moment tensor inversion. Such procedure takes into account the signal to noise ratios of the data, and the stations distribution relative to the event location and magnitude.

To investigate the dependence of the solution on depth, the procedure repeats the inversion for several point-source depths. Among all the moment tensor solutions obtained for all the explored depths, the one with the largest overall variance reduction is chosen.

The AUTO-TDMT procedure determines earthquake focal mechanism, moment magnitude, percentage of double couple, preferred depth, and the solution quality value. The quality parameter (A to D with A best) depends on the number of the stations used, the azimuthal coverage, and the variance reduction.

All the moment tensor solutions with at least quality C are automatically published on the web-page <http://earthquake.rm.ingv.it>.

A seismologist subsequently reviews all the moment tensor solutions. Reviewing solutions implies the proper knowledge of how the inversion code, and the automatic procedure work. To make the revision procedure easier and accessible, we have developed a web-interface. This interface is presently under testing.

In Figure 3.8 is reported an example of how the AUTO-TDMT procedure worked for a small Apennine earthquake, the 2007 March 29,  $M_I = 3.9$  Monti Sibillini Earthquake.

The event has been recorded by 61 broadband stations within the distance range of 28-297 km. The results of the AUTO-TDMT are shown in Figure 3.8 and Figure 3.9. In Figure 3.8 is reported the moment tensor solution, while Figure 3.9 shows focal mechanism and associated variance reduction for each one of the inverted centroid depths. The quality of this solution is C.

Overall, this is a quite good automatic solution. It gives us a reasonable moment magnitude, a fair fit at 3 of the 7 inverted stations, a centroid depth consistent with the earthquake location given by the seismic center (lat 42.83°N, lon 13.21°E, depth 5.7 km). To improve the quality of the solution and the DC component we have replaced 3 stations with other stations of the correspondent sector and we have adjusted the *zcor* parameter, in particular for MAON. All

these steps result in better seismogram fits. In this example, the final depth is that one already selected by the AUTO-TDMT because it gives the better result.

The Reviewed MT solution (REV-TDMT) has Quality A and  $M_w = 3.9$  (Figure 2.10). The inferred moment tensor solution is consistent with the tectonics of the region.

During the second year of the project, INGV inserted in the project web portal the moment tensor solutions obtained by Pondrelli and co-authors using the Regional Centroid Moment Tensor (RCMT) technique. This method is based on the inversion of surface waves of intermediate period - 35 s – recorded at regional distance. INGV compute RCMT routinely since 1997 for intermediate- magnitude earthquakes (about  $4.5 < M < 5.5$ ) occurring in the Euro-Mediterranean region, and we maintain a catalog of solutions (Pondrelli et al., 2002, 2004, 2006; <http://www.ingv.it/seismoglo/RCMT/>).

The surface wave Quick Regional Centroid Moment Tensor (QRCMT) calculation is fast, allowing rapid determination of source mechanisms, a feature of great importance for scientific and relief operations following an earthquake (Ekström et al., GRL, 1998).

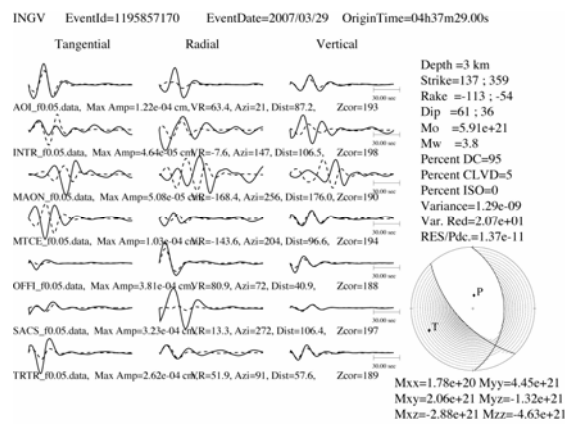


Figure 3.8 Automatic moment tensor solution for the Monti Sibillini earthquake

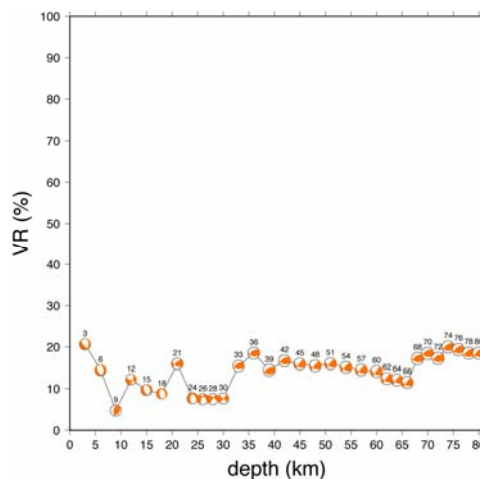


Figure 3.9 Depth versus variance reduction

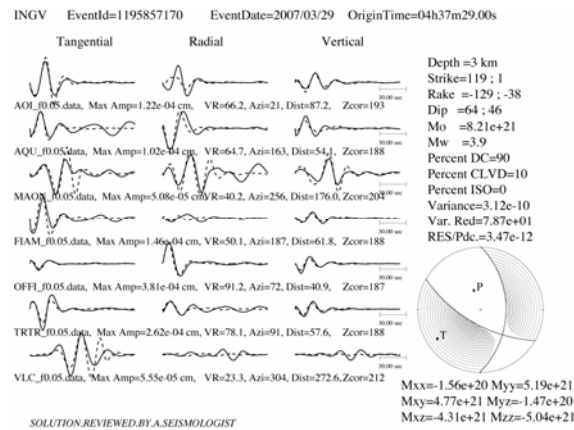


Figure 3.10 Reviewed moment tensor solution for the Monti Sibillini earthquake

For NE Italy, the RU3 has also developed an automatic procedure that uses the moment tensor (MT) inversion code originally proposed by Dreger and Helmberger (1993). MT for all the events with  $MD \geq 3.6$  occurred in the Friuli Venezia Giulia and surrounding area were computed using 6 broad band stations managed by CRS. Preliminary tests revealed that even one-station solutions prove quite effective in many cases though the minimum number of stations depends on the epicenter position and on the source radiation pattern. Moreover, the best double couple and the Mw are quite robust although the resolution depth is not always well constrained. The focal mechanisms obtained are plotted in Figure 3.11, together with (when available) the focal mechanisms obtained by other means. In Figure 3.12, an example of complete moment tensor solution is given.

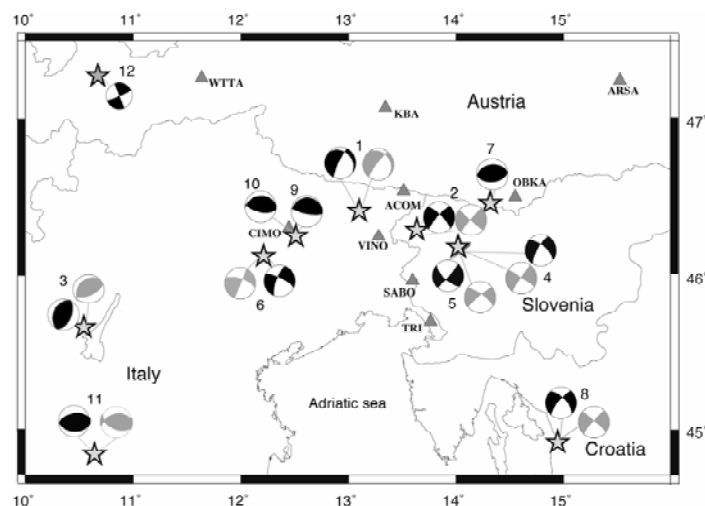


Figure 3.11. Map of earthquakes (stars) and focal mechanisms (black beach balls) retrieved. For the same event a focal mechanism retrieved by other means (grey beach balls) is plotted when available.

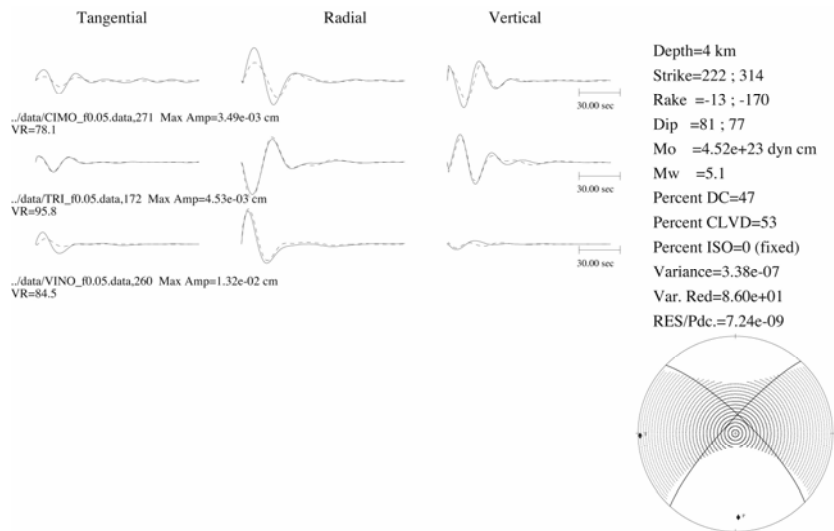


Figure 3.12. Moment tensor solution for event n. 2 as reported in Figure 2.9. The corresponding waveform fit between real (solid line) and synthetic (dashed line) data is also plotted (Saraò, 2007)

### ***Kinematic inversion on finite fault***

During the two years of the project, INGV has implemented and tested the kinematic inversion procedure on finite fault proposed by *Dreger and Kaverina (2000)*. The procedure uses mainly broadband and strong motion waveforms, but it can invert also for GPS and InSar data.

This procedure is able to rapidly determine earthquake source parameters (slip distribution, rise time, rupture velocity) through a non-negative least-squares solver. The inverse problem is simplified considering only source models with constant rise time and constant rupture velocity on the fault plane. To resolve the fault plane ambiguity, the procedure inverts the data testing for the two possible fault planes given by the moment tensor inversion.

The hypocentral location and moment magnitude are given by moment tensor inversion. The fault dimension are assumed 20% larger than those inferred by the empirical relationships of *Wells and Coppersmith (1994)* for the corresponding magnitude, allowing the rupture to be unilateral and bilateral. The rise time is set through the *Somerville et al. (1999)* empirical relationship.

Once the fault dimension and rise time are fixed, the inversion is performed for both planes over a range of constant rupture velocities: the best rupture velocity for each plane is that which gives maximum variance reduction (*Dreger and Kaverina, 2000*). Moreover, the variance reduction values allow for the determination of the causative fault plane.

The minimum magnitude to apply this procedure is approximately  $M_w \sim 5.5$ . The Green's functions have been computed using a frequency-wavenumber approach developed by *Saikia (1994)*.

INGV is finishing to implement a short procedure, triggered by the AUTO-TDMT tool (see above) that, when an earthquake with  $M_I > 5.5$  occurs, sets up directories and files to be used for the finite fault inversion.

The procedure has been tested for three real events: 2000, Western Tottori earthquake;  $M_w = 5.6$ ; 2002 Greece earthquake;  $M_w = 5.7$ ; 1980 Irpinia earthquake,  $M_w = 6.9$ . 2000, Western Tottori,  $M_w = 5.6$  (Figure 3.13).

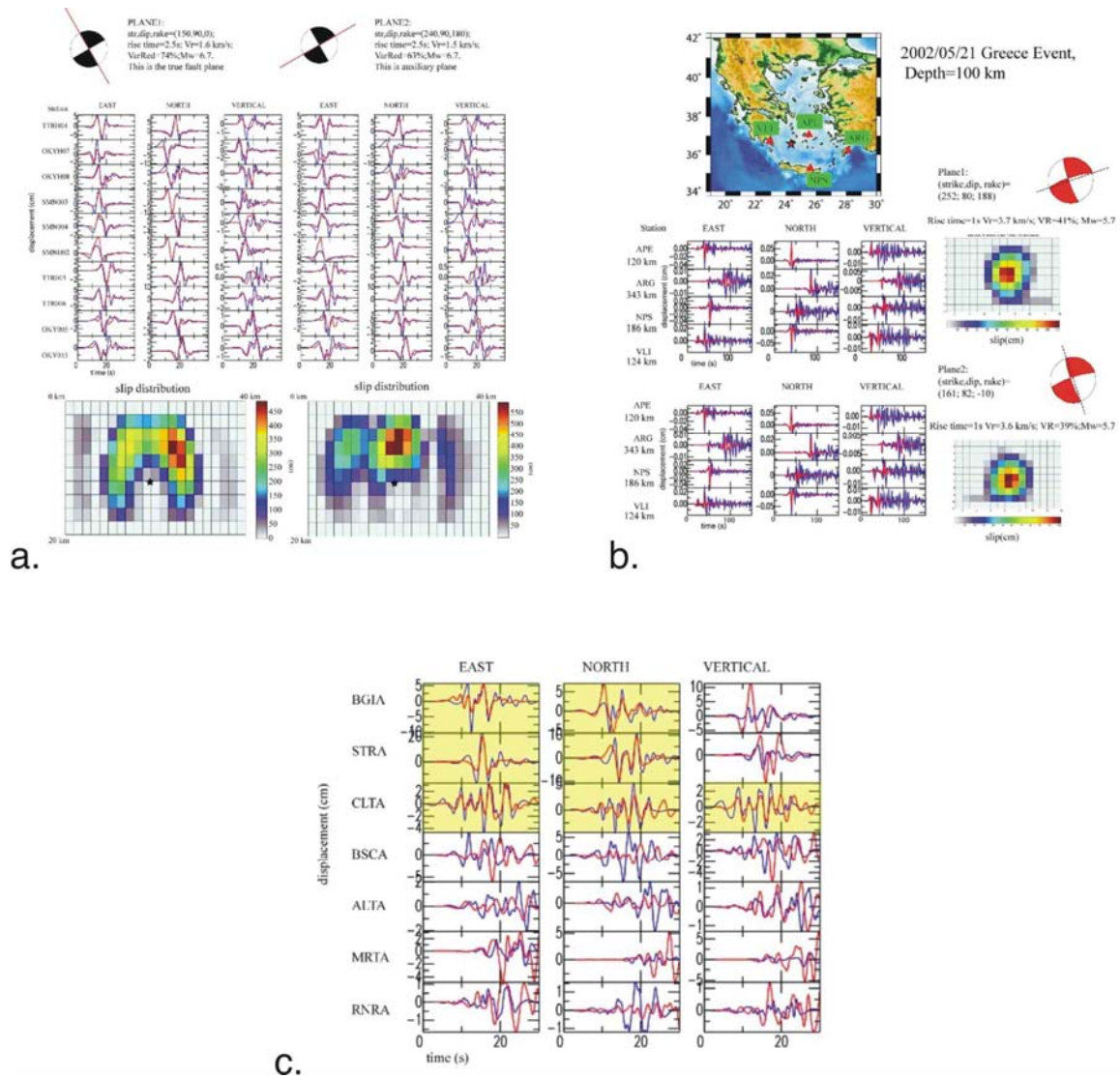


Figure 3.13. Kinematic inversion of the 2000 Western Tottori earthquake; comparison of strong motion (blue lines) with synthetic waveforms (red lines) for both planes (left: fault plane, right: auxiliary plane). The bottom panels show the slip distribution of the two planes. b.) Kinematic inversion of the 2002 Greece earthquake; comparison of strong motion (blue lines) with synthetic waveforms (red lines) for both planes. c.) Kinematic inversion of the 1980 Irpinia earthquake; comparison of strong motion (blue lines) with synthetic waveforms (red lines) for both planes

### ShakeMap

During these two years, RU1, RU3, RU4 and RU5 installed and tested the release 3.1 of the USGS-ShakeMap package. The package itself generates maps of ground shaking in terms of various peak ground motion (PGM) parameters (PGA, PGV, SA at 0.3, 1.0 and 3.0 s and instrumentally derived intensities). In practice, grossly simplifying the problem, ShakeMap can be assimilated to a seismology-based interpolation algorithm that exploits observed ground motion data and seismological knowledge to determine maps of ground motion at local and regional scales. Thus, and in addition to the data, fundamental ingredients toward obtaining accurate maps are i.) the attenuation relations for the ground motion with distance at different periods and for different magnitudes, and ii.) realistic descriptions of the

amplifications that the local site geology - the site effects – induce on the incoming seismic wavefield. In the current version of the package the generation of the peak ground motion maps relies on regional attenuation laws and on local site amplifications based on the S-wave velocities in the uppermost 30 m ( $V_{S30}$ ). Thus fidelity to the “true” ground motions depends heavily on the data available and on the attenuation and site corrections imposed.

In the implementation carried out at INGV, and for the purpose of near real-time generation of maps (few minutes from earthquake occurrence), data are mainly provided by the broadband network complemented by strong motion data when available (currently about 60 broadband stations include also strong motion sensors). With regard to the “seismological information” required for proper interpolation, the attenuation laws previously determined by Malagnini and co-authors have been used (Morasca, et al., 2006; Malagnini, et al., 2002; Malagnini, et al., 2000; ). For the site correction part, the  $V_{S30}$  have been initially taken from the rough classification of the Italian territory in terms of three litho-types – rock, stiff, and soft (1000, 600 and 350 m/s, respectively), and toward the end of the project a more detailed description of  $V_{S30}$  based on the geology (1:100,000 maps) and on five different site classification (A=1000, B=600, C=300, D=150 and E=250 m/s) has become available from the activities of the project (see Task 5).

Maps are all published on an INGV internal server (*wood.int.ingv.it*) and the official ones are “pushed” to the publicly accessible server *earthquake.rm.ingv.it*.

An example of the shakemap determined by INGV for a M3.8 earthquake in northern Italy (near Brescia) is provided in Figure 3.14 where it is made use, in addition to the CNT station data, of the strong motion data recorded by the strong motion network of the Milano INGV section..

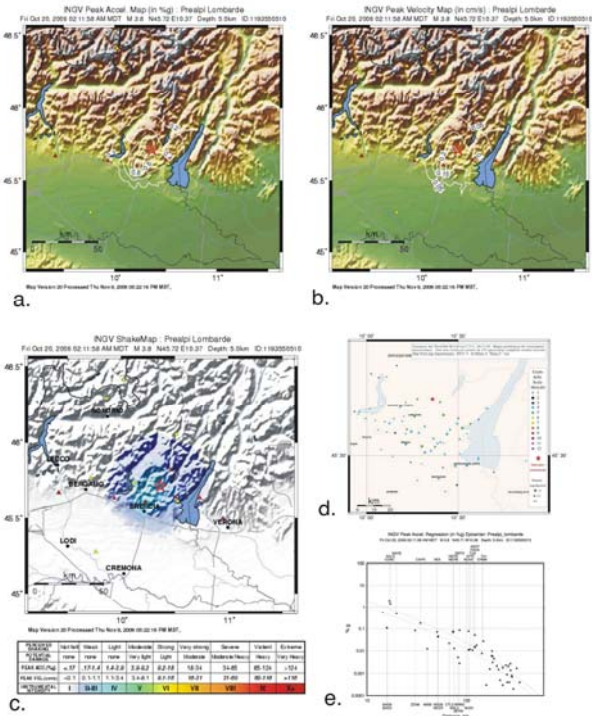


Figure 3.14. Shakemaps and macroseismic intensity maps determined for the October 20, 2006, M3.8 earthquake that occurred near Brescia (Northern Italy). a.) PGA; b.) PGV; c.) MII. d.) macroseismic intensity determined from web questionnaire. e.) plot generated with *plotreg* where The red solid curve indicates the PGA attenuation for a M3.8 earthquake whereas the green one is adjusted for the “bias” depending on the actual observed data.

### Early-warning

Real-time determination of earthquake location and size is a big challenge for immediate shutdown of, for example, high risk manufactories (chemical plants), high velocity trains, and, in general, anything that, as result of the strong ground motion shaking, can become particularly harmful to people and the environment. During the course of the project it has been implemented the software ElarmS proposed by *Allen and Kanamori (2003)* to determine within few seconds earthquake location and magnitude. The procedure as implemented at INGV (*Olivieri et al, submitted for publication*) relies on some of real-time modules of the earthworm package and, for testing purposes, it is triggered 10 minutes after the earthquake has occurred. ElarmS is capable to provide first locations (and magnitudes) after the 4<sup>th</sup> station has detected the first P-wave arrival time. In Figure 3.15, we show the detection capabilities of the Italian network applied to the set of  $M > 5$  earthquakes that have occurred in Italy since 1900. The gray scale indicates the distance (km) to the 4<sup>th</sup> station detecting the P-waves. In its current station configuration, and assuming  $V_p \approx 6.0$  and no data transmission delays, the figure shows that it possible to provide early warning estimates ranging from less than 4 s along most of peninsular Italy to several seconds in northern Italy (NE-Italy and in parts of Lombardy and Piedmont). The plot shows, for example, that early warning for the Irpinia region could be done in a matter of a few seconds whereas for the Friuli area more than 16 s would be necessary to provide a first location. This result stresses the importance of real-time data exchange among different networks and institutions.

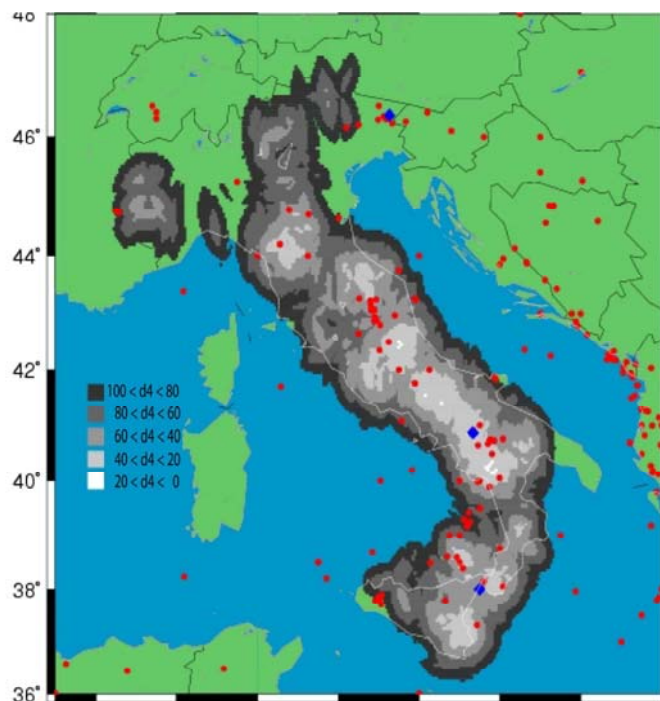


Figure 3.15 Map of the Italian territory showing the potential for early warning using ElarmS. White and light grey color areas indicate places where ElarmS would be capable to provide early warning determinations of location and magnitude within a few seconds.

### ***Web-portals***

INGV, UniGe and University of Trieste developed web portals where it is possible to access most of the results of the analysis obtained in the project.

The INGV published the data on the web site <http://earthquake.rm.ingv.it>. For each event, the following products are determined in near real-time:

- epicentral map with the stations used for the location;
- map of the catalogued epicenters and centroid moment tensors;
- web publication of the Time Domain Moment Tensor (TDMT) and of the Quick Regional Centroid Moment Tensor (QRCMT) if available;
- web publication of the PGA and PGV ShakeMap;
- availability of the *shape file* of the shakemap for ground motion representation using GIS;
- availability of the tar archive file of the SAC event waveforms;
- parse the information provided by the seismic center and from the CNT data-base (DB) to 'retrieve' the information about the earthquake and publish it.

All this information is inserted within a unique event directory and a DB is populated. This DB is also accessed by GoogleMap for additional plotting or for information retrieval.

In the web portal are also inserted the reviewed TDMT and QRCMT solutions and the procedure has been designed to contemplate possible updates of the products presented above up to one week after the event (e.g., revised locations, shakemaps). In Figure 3.16, some screen-shots of the developed INGV web portal are shown.

The UniGeo also publishes automatically a web page with all the information regarding automatic procedures on <http://www.dipteris.unige.it/geofisica/AutoLoc.php>. This page contains the epicentral map, the location and its quality, the list of towns closer to the epicentre, some ground-motion parameters (the PGA and PGV values for each station), the magnitude (MI), and a figure with the waveforms, and the automatic picks. In case the event is important, a button can be hit to go to the ShakeMap (it requires a login username and password). The xml files to build the ShakeMap can be downloaded by an authorized user, and are also automatically emailed to INGV. The automatic procedures also allows the (1) sending of e-mails (to a selected e-mail addresses), including all location parameters and the link to the web page (<http://www.dipteris.unige.it/geofisica/AutoLoc.php>) and (2) sending of SMS reporting the hypocentral coordinates, magnitude, the closest town and other useful information.

In Figure 3.17, screen-shot of UniGe web portal is shown.

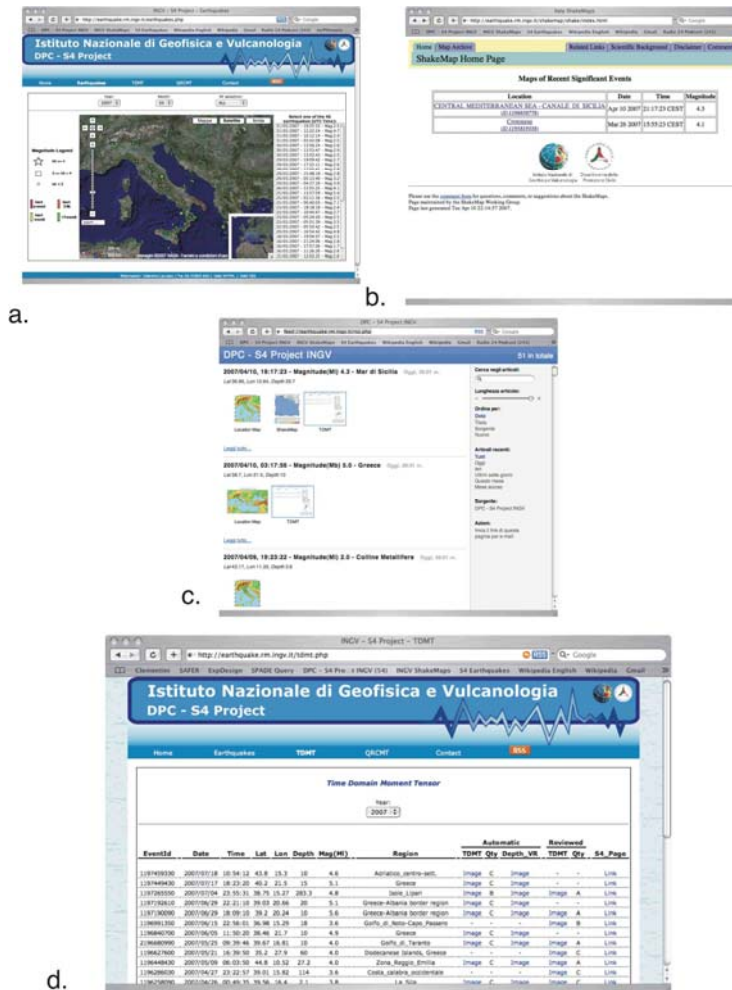


Figure 3.16. Screenshots of the project web portal developed by INGV during the project. a.) Page showing the earthquake locations using the software GoogleMap; b.) INGV ShakeMap page; c.) RSS access to the information within the portal; d.) index of the Time Domain Moment Tensors for the  $M > 3.5$  earthquakes.

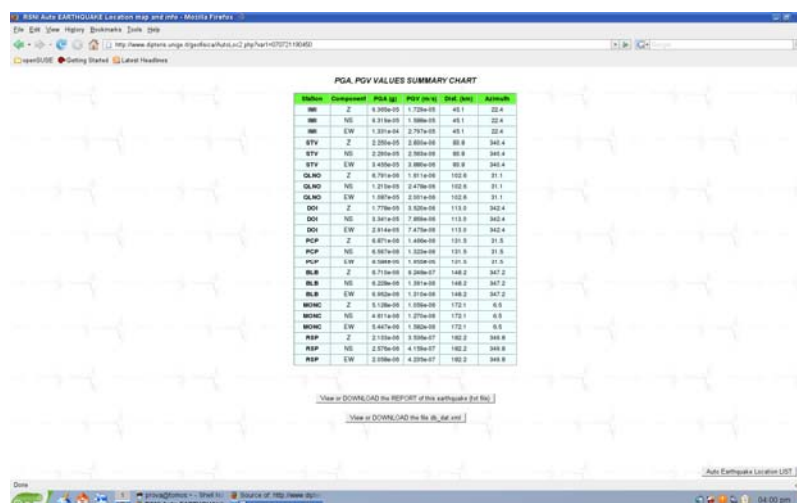


Figure 3.17. Screenshots of the project web portal developed by UniGe during the project: page showing ground motion parameters.

### *Real time automated methods development for the definition of macroseismic field maps*

Starting from January 2007, the macroseismic questionnaire has been deeply modified both for kind of questions and for elaboration methods. It is available at the web address: <http://terremoto.rm.ingv.it>. (Figure 3.18)

An important difference with the previous method is that now the questionnaire is directed to single persons, having adapted the M.C.S. and E.M.S. macroseismic scales.

Considering the experience gathered with the old questionnaire (on line since 1997), we can show that people induced an overestimation of the damages, when compiling a questionnaire. This was due to the fact that old questions were referring to whole groups of people feelings and reported by the compiler (the compiler was considered expert and able to test large area effects). For this reason original Mercalli effects were set and considered as averaged over large people groups. It is clear that a single internet questionnaire compiler has an intuitive estimation of effects and damages over a large area, often driven by fear and emotive reasons. To overcome this effect we have modified the original M.C.S. and E.M.S. macroseismic scales into the new W.M.C.S. and W.E.M.S. macroseismic scales: the letter W indicates the web origin of information.

The statistical methods used to analyze the questionnaires have been adapted to the new scales and the filters to detect errors in compilation have been strengthened.

Starting from the end of June a completely automated procedure is running. For every earthquake, each single questionnaire can be recorded after compilation. It is analyzed and a degree for each of the two web macroseismic scales is assigned. If it passes the reliability tests it constitutes information that it will be displayed into macroseismic maps. Such maps are rescaled to fit all data into a range due to the earthquake magnitude. This procedure is activated in real time and the graphical results, along with data listings, are available to a dedicated web page (<http://terremoto.rm.ingv.it/index.php?page=list>). In particular produced maps represent: felt intensities into W.M.C.S. scale, felt intensities into W.E.M.S. scale, and felt sound effects. These three maps are in jpg format. The first one (W.M.C.S. scale intensities) is also offered into kmz format: it can be visualized with the Google Earth program. This allows a variable representation scale and each intensity point has additional information such as the number of questionnaires that produced that value. Values presented into geographic maps are also available into ASCII format for downloading.

Obtained data, although produced by people with no specific technical experience, give a good and reasonable representation of macroseismic intensities in real time. A large number of information can be collected, processed and stored including data from events with low magnitude. This class of events did not receive attention prior the activation of this automated system for cost reasons.

In conclusions the whole procedure allows in real time the collection, analysis and visualization of effects on people and urban structures from earthquakes. Regarding high magnitude events the method complete in real time the information obtained by specialized personnel. For low-medium magnitude events the method is the sole source of information.

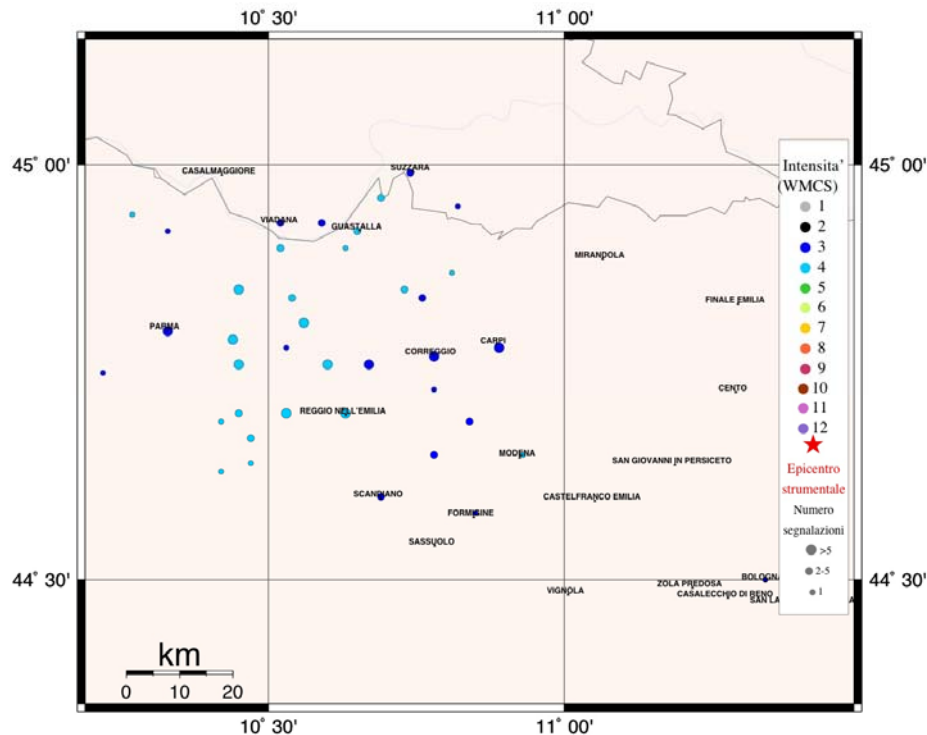


Figure 3.18. Earthquake of May 9 2007,  $M_I=4.0$ , deep=27.2 km, U.T.C. time: 06:03:50. Preliminary map of macroseismic intensities in WMCS scale. 334 compiled questionnaires at the web address: <http://terremoto.rm.ingv.it>.

### *Space-temporal seismic hazard*

The algorithm developed during the project provides the users with quantitative estimates of the probability of occurrence of new earthquakes on specific areas of the target territory. The algorithm avails of the earthquake data detected by the Italian National seismic network. The software adopted for the estimation of the space-temporal seismic hazard is based on epidemic models of the ETAS type (*Epidemic Type Aftershock Sequence*) (Console *et al.*, 2001; 2003; 2005; 2006; 2007). In epidemic models each event can be either inducing to another earthquake or induced by a previous one. The expected seismicity rate in any particular point of the target area for a given threshold value can be determined through the contribution of all the previous events using a kernel function that involves: magnitude, distance and time of occurrence of every previous events. The magnitude distribution assumed follows the Gutenberg-Richter law. The parameters used by the software have undergone a first phase of training using the INGV data set so that to obtain a maximum likelihood estimates of the parameters. The time span for training is from July 1987 to December 2005 for  $M>2.0$  earthquakes. It has been used the statistical software ZMAP (Wiemer and Wyss, 1994) used at ETH Zurich to verify the data completeness.

Since January 2006, the procedure described above has been tested on the server called “wood” dedicated to the project. The goal is to determine the occurrence probability of new medium to large size events detected in real time by the INGV seismic monitoring center. The results are displayed as time-dependent maps showing every 5 minutes both the expected rate density of  $M>4.0$  earthquakes overall Italy, given as events/day/km<sup>2</sup>, and the probability of ground motions larger than 0.01 g in areas of the size of 100 x 100 km in the

next 24 hours, around the zone of maximum expected rate density. In order to verify the results of the predictions, it has been used the statistical method ROC (Relative Operative Characteristics) known also as Molchan diagram. This method is also used to assess the meteorological forecasts. In essence it addresses the capability of the model to predict or to generate false alarms. The results obtained in this study show that the ETAS model is capable to obtain predictions some hundreds of times more accurate than a purely random model.

### ***Determination of the damage caused by seismic events***

Remote sensing techniques have revealed themselves a suitable monitoring tool for disaster management since they provide a quick detection of land changes in wide areas, especially in remote areas or where the infrastructures are not well developed to ensure the necessary communication exchanges. A limitation for an operational use is the availability of the images in time to manage the crisis. This is a key point for Civil Protections who need a fast and draft overview of the epicentral area, quick information relative to the extension and distribution of damages, and the evaluation of infrastructure (roads, bridges) conditions. A single satellite can provide access time to a specific site in the order of some days. At the moment the use of any type of data (satellites) available and an integration of those data is mandatory to increase the chance to collect information on time. In the near future (years) the implementation of satellite constellations may reduce the access time with the same sensor to 12 hours, as in the case of the Italian COSMO-SkyMed system, based on X-band high resolution (few meters) radars.

For this purpose we have exploited in our research both data provided by active microwave sensors, such as high resolution (tens of meters or less) Synthetic Aperture Radar (SAR), and data from optical sensors working in the visible and infrared bands with spatial resolution ranging from medium (tens of meters) to very high resolution (1 meter or less).

In particular, SAR is widely used in environmental studies due to its characteristics which allow a fairly synoptic view in almost completely weather and time independent conditions, as opposed to optical sensors affected by cloud cover limitations. Multi-temporal observations from SAR can be used to detect urban changes either looking at the image intensity changes, as in the case of optical images, but also taking advantage from the information on the phase of the returned signal. This is specific of the radar technique and in particular of the interferometric SAR (InSAR).

The project activities has been developed following two different guidelines: first of all an analysis of some case studies has been carried out to understand and quantify the sensitivity of the different types of remotely sensed data to urban damages. Successively, based on such experience, few methodologies to generate products with operational applications have been investigated.

We have exploited intensity correlation and the InSAR complex coherence as SAR features to recognize changes on the surface caused by an earthquake. These two features hold different information concerning changes in the scene. The complex coherence is prevalently influenced by the phase difference between radar returns, a distinctive parameter measured by a coherent sensor. It is particularly related to the spatial arrangement of the scatterers within the pixel and thus to their possible displacements. Conversely, the intensity correlation is more related to change in the magnitude of the radar return.

The interaction of the SAR signal with the urban structures has been studied within this project in order to understand the phenomenon that affect the radar backscattering, in addition to surface changes we want to detect. A temporal series of SAR images, concerning the city of Rome, has been analysed for modelling the response of buildings and the influence of urban settlements characteristics on the backscattered signal. In particular, the model takes

into account three different effects on SAR coherence in urban unchanged areas: temporal baseline, perpendicular baseline and track orientation difference between the two interferometric acquisitions. Such model has been conceived to correct the above mentioned effects, thus enabling to detect structural changes even from interferometric pairs with different baselines and track orientation.

The potential of medium and very high resolution optical data has been also investigated. Medium resolution images have been used for classifying automatically surface changes in conjunction with SAR data, considering also the comparable pixel dimension. For this purpose we have considered two earthquakes as test beds: Izmit (Turkey) in 1999 and Bam (Iran) in 2003. In the Izmit case the combination of SAR and IRS panchromatic optical data allowed us to apply automatic procedures for damage classification, reaching the 90% of correct classification. In this case, it has also been demonstrated the possibility to significantly improve the results taking advantage of the change detection potential of the InSAR complex coherence combined with optical data. The correlation with damage level observed in situ has been also demonstrated for the optical change image and SAR intensity correlation when data are aggregated within homogeneous regions (such as blocks of buildings) and this is shown in Figure 3.19. Also for the Bam case study, the combined use of SAR and optical data reached 77% of correct classification, confirming the complementarity of optical and microwave techniques. The apparently lower quality of the Bam result originates from the large spatial baseline of the SAR image pairs and the moderate resolution of the optical data (ASTER satellite with ground resolution of 15 m respect to Izmit case where the collected IRS images with ground resolution of 5 m).

In the Adapazari case, the experience made in the previous cases has been used to test the capability to generate a product useful for civil protection rescue activities. Based on the results of the Izmit and Bam case studies, a procedure to create a damage map has been attempted using only satellite data. The SAR intensity correlation has been used as a unique feature to generate the damage map. Three damage levels (low, medium and high) have been identified, each one corresponding to three thresholds defined on the intensity correlation values. The latter have been calculated within regions extracted from a ground truth map provided by the Kandilli Observatory and Earthquake Research Institute (KOERI) of Turkey. Concerning high resolution optical image, they can in principle provide information on collapse of a single building or part of it. However, the information content could be affected by differences in the acquisition time, geometry, and changes in the sight observation angle. The presence of shadows, variation in sun illumination and geometric distortions are critical both for multispectral and panchromatic data, and they may prevent using automatic change detection procedures. Therefore the visual inspection approach is still the most used to produce a realistic and reliable inventory of damages. We had this kind of situation for Al Hoceima (Morocco) and San Giuliano (Italy) earthquakes. Concerning Al Hoceima, the analysis of damages in the urban areas hit by the earthquake was performed using multispectral high resolution (~1 m pan-sharpened) images acquired by the Ikonos satellite. The dataset was composed by one pre- and one post-seismic scene. Due to the light different looking angle and sun illumination between the two Ikonos acquisitions, geometric and radiometric distortions were present, affecting also buildings and manufactures looking. The damage visual detection was focused on Al Hoceima and Imzourene cities and has demonstrated that the identification of single individual buildings from the available dataset was possible at least by visual interpretation, identifying a couple of damage classes (total collapses and partially damaged structures).

The main limitation for the San Giuliano test case was the absence of any satellite high resolution pre-seismic image. As pre-seismic data an aerial colour photo of the village has been used, whereas one post-seismic high resolution satellite image was available provided by

EROS-1A satellite (one meter resolution). Although the two images were very much different, the identification of three different levels of change has been possible. Total collapses and strong damages have been observed even though a large number of false alarms were present (undamaged areas considered as strongly changed). In this case the reason was the lack of homogeneity among data sets and the difference in sun illumination.

Despite of the mentioned problems, high resolution optical data can potentially detect collapse of single buildings. The objective is to develop specific techniques making change detection quick and reliable with respect to simple visual interpretation. The experience gained from San Giuliano and Al Hoceima test cases has provided us with significant guidelines for developing automatic techniques. In particular, it suggested us to extract from the image, before applying any change detection algorithm, all the man made structures to map the potentially damaged area, thus avoiding the false alarms caused by shadow and transitory targets (for example cars), in particularly in those regions where a detailed cartography is not available. To do this it becomes necessary to integrate the spectral information carried out by the images (radiance in different spectral bands) with others features describing the geometry of the objects within the scene. More sophisticated classification algorithms are also needed to manage those information. For this aim, morphology operators have been used to extract features from the original image that give information about the distribution and geometry of the objects, whereas neural network classifiers have been exploited to improve the extraction of urban settlements. The test case for this exercise was the Bam earthquake, using two panchromatic Quickbird images (60 cm of ground resolution) available before and after the event. The results of the automatic change detection procedure are shown in Figures 3.20 and 3.21, where we can see the potential of this kind of techniques, especially to detect partially damaged structures. In particular, Figure 3.20 represents a possible product where the damage are identified as red areas. Figure 3.21 shows some details pointing out the capability of the technique to discriminate between shadows and actual settlement changes. This type of product can be conceived as a quick look at the damages, indicating the areas which are worth to better investigate either by image photointerpretation or by carrying out a ground survey, when possible.

We cannot claim to have investigated all possible spectrum of data type, urban settlement conditions and techniques, but the project has provided a quite realistic view of what remote sensing can offer for this application and which methods and sensors worth to be further developed in the future. The experience of this project has been summarized in Table 3.1 where a list of possible damage products are shown, spanning different ground scales and obtainable with different satellite data. Those products can be valuable for managing different phases of the crises, and especially mitigation of the effect in the course of the event and precise inventory of the damage in the post-event phase.

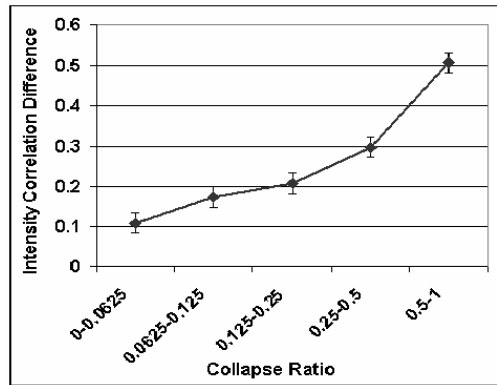
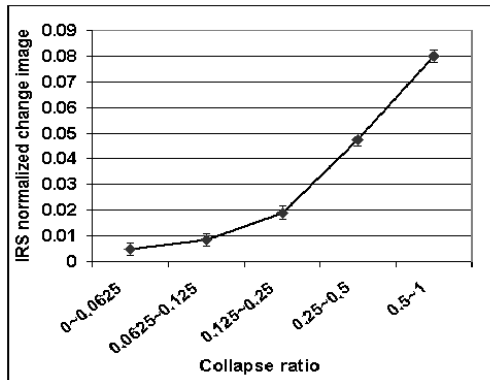


Figure 3.19 : a) IRS normalized

change (i.e., difference between pre-seismic and post-seismic images) averaged over the surveyed areas as function of the corresponding collapse ratio; b) Pre-seismic and co-seismic intensity correlation difference averaged over each surveyed area as function of the corresponding collapse ratio.

| <i>Product</i>                           | <i>Description</i>   | <i>Tools</i>                                    | <i>Scale</i>                    |
|--|--|---|---------------------------------|
| <b>Potential damage snapshot</b>         | Prompt overview of potentially damaged area (only qualitative)           | Medium/high res. OPT & SAR                      | Medium, tens to hundreds meters |
| <b>Damage level at district scale</b>    | Damage level (i.e., collapse ratio) estimated on homogeneous urban areas | medium/high res. OPT & very-high res. OPT & SAR | District, block of buildings    |
| <b>Collapsed/heavy damaged buildings</b> | Identification of single buildings collapsed or heavily damaged          | Very-high res. OPT                              | Single building                 |

Table 3.1: Resume of possible earthquake damage detection products derived from remote sensing data



Figure 3.20: Map of damaged buildings (in red) for the Bam case study derived from a pair of Quickbird images.

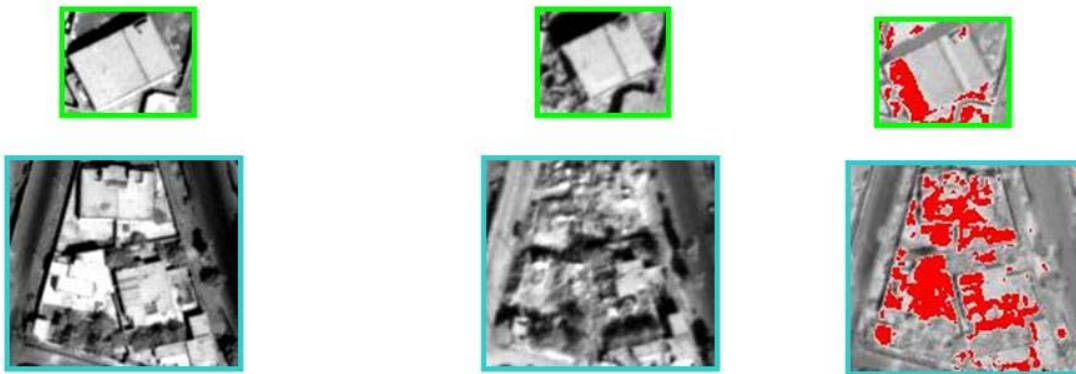


Figure 3.21: Details of Quickbird images before (left panel) and after (middle panel) the earthquake and the resulting damage map (right panel) where the successful discrimination between shadow and damages can be perceived.

- **Task 4 – Predictive relationships for the ground motion**

UR2, UR4, UR5 were all involved in activities of Task 4. After the meeting with the International Review Committee, at the end of the first year of the project, we were asked to start coordinating the activities of Task 4. The idea was to have a single set of predictive relationships to be used for producing ShakeMaps.

At some point during the first year of activities, during a meeting with the Reviewers, we faced the problem of which predictive relationship to be used for the national ShakeMaps, because it is clear that the ground motion induced by moderate events ( $M_w < 5.5$ ) is not correctly estimated by strong-motion equations. The problem has been solved in the US by calibrating an ad-hoc set of equations called Equations based only on strong-motion data from large events may be inadequate for predicting the ground motion induced by small events. In the ShakeMap context, for example, the issue was solved by deriving a specific predictive equation for small earthquakes in California. We stress the importance of the predictive capabilities for moderate-sized earthquakes, since the model by Atkinson and Silva (2000) (which is representative of an entire class of equations) tends to overpredict the shaking at M4 and 5 (see Malagnini et al., 2007, their Figures 12 and 13).

For official use in the California ShakeMap, a specific predictive relationship was developed for modeling the small events, through a multistage regression performed on data from hundreds of earthquakes in the magnitude range between  $M_w$  3.0 and  $M_w$  5.5, each recorded at many stations. The ShakeMap Small Regression (ShakeMap manual, p.148) is a modified form of the attenuation relationship for small events described in Wald et al. (1999), obtained on an extended version of the event database (to 2002). The Small Regression is used in the California ShakeMap as the default regression for events with magnitude below 5.3. For completeness of information, we must mention that, in northern California, the equation by Boatwright et al. (2003) is also implemented for both small and large earthquakes ("Large\_seg" and "Small\_seg" modules in the ShakeMap package). The working group decided that the correct approach would have been to use weak-motion-based equations for events up to a threshold of  $M_w = 5.5$ . Beyond that value, we would switch to strong-motion-based ones, like Sabetta and Pugliese (1996) or Ambraseys et al. (1998).

In order to make use of our in-house predictive relationships for the ground motion, we decided to write a specific module that would have treated them as a table of the following parameters, as a function of distance (one value for each km) and of moment magnitude (one value for each 0.1 increment of  $M_w$ ): pga, pgv, psa(3sec), psa(1.0 sec), and psa (3.0 Hz). The results by Malagnini et al. (2002) were tabulated to be used into the ShakeMap package, together with the ones by Malagnini et al (2000) for the Apennines, and the ones by Morasca et al. (2005) for the northwestern Italy. As done for the hazard map of Italy produced by INGV in 2004, the Italian territory was divided into six main areas: Apennines, Northern Sicily, Southern-Eastern Sicily, Northwestern Italy, Calabrian Arc. The Apennine results were applied also to Northern Sicily, the Northeastern Italy ones applied also to Apulia and Southern and Eastern Sicily, and the Northwestern Italy results applied also to the Calabrian Arc region. For each earthquake occurring within the Italian territory, of  $M_w < 5.5$ , the predictive relationship pertaining to the area where the epicentre is located is used for computing the ground motion. See Figure 4.1 for the exact definition of the attenuation regions.

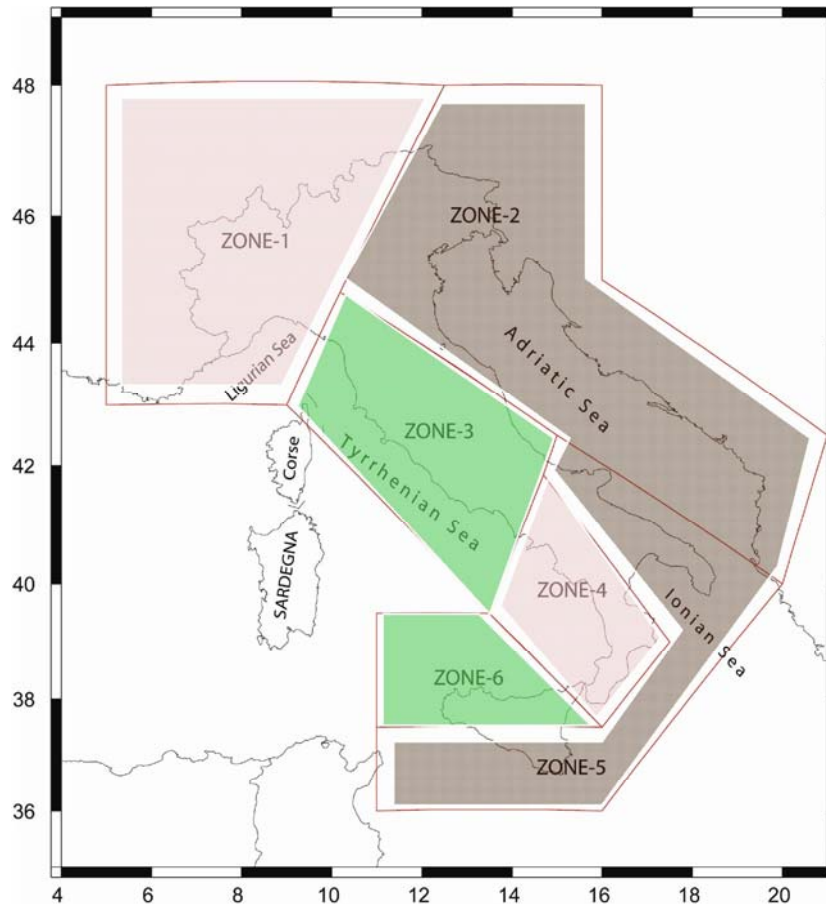


Figure 4.1: Map of the six attenuation regions used for applying the attenuation relationships also used for the national hazard map of 2004.

Other studies were carried out by the URs involved in Task 4, and UR5 (Costa) computed ground motion relationships as a function of distance and magnitude using data from the RAF database. An inter-RU project was also developed under the supervision of Giovanni Costa. The aim of this sub-project was to carry out a 2-D tomography of Northern Italy, after the integration of data sets from the networks maintained by the UniGe, by the University of Trieste, and by OGS-CRS.

The RU of Trieste University, of UniGe and of INGV of Milano participated to the research group. Some meeting has been organized in Trieste, Milano and Genova to organize the activities and to exchange experiences about using different techniques. In particular, researchers of the University of Genova, with experience in using the coda Mw computation and Q attenuation tomography, went to Trieste to teach the use of the code and to organize a common dataset. Researcher of the RU of the University of Trieste went to Genova for the same reasons.

In the last year of activity, data coming from the Friuli Venezia Giulia broadband network (NE Italy BB network) and from the strong motion regional network (Friuli Venezia Giulia Accelerometric Network, RAF) has been merged with the existing data sets of northwestern Italy (RSNI, INGV-CNT, INGV-MI, ARSO, SDS-net etc.) of the last 30 years (612 waveforms recorded since 1976 with  $3.5 < ML < 6.3$ , maximum epicentral distance 100 km). Ground motion relations have been computed for Northern Italy using the integrated dataset. The relations are computed for PGA and PGV selecting the vertical and the largest horizontal component. The same relations have been computed also for the acceleration response spectra, Arias (Arias, 1970) and Housner intensity (Housner, 1952). Strong motion duration

(Vanmarcke and Lai, 1980) has been also computed and the respective attenuation relationships derived (see above, and also the project report of RU5).

The calibration of station correction (Mayeda e Walter, 1996 and Mayeda et al., 2003) has been started for the stations of northeastern Italy. The calibration of the Friuli Venezia Giulia stations will permit the coda Mw computation also in this region. We hope to extend this calibration to the Slovenian and Austrian networks. The results obtained for the first 2 stations (TRI and VINO) has been compared with the Mw obtained using the real-time procedure developed at DST applying the methodology described in Andrews (1986). This methodology uses the Brune spectrum and the corner frequency and is applied to the S waves. The dataset and the stations calibration will permit also to realize the attenuation tomography of the region of the Alps Dinarides junction. A PhD student is working on this at DST.

The inter-station project did not go beyond the creation of some important interactions and personal contacts that will be useful for future work, mostly because of the strong resistance to share data sets between different institutions. What described is an attitude that apparently permeates the entire Italian seismological community. One of the goals of the S4 project was the creation of a modern attitude for the Italian seismologists towards data sharing, especially if such data sets come from permanent regional networks. With respect to the fulfilment of this specific goal, we failed. As a recommendation for future projects, we suggest funding specific efforts just for the permanent integration of different data sets, and for the creation of web-based interfaces for the effective distribution of real-time waveforms.

One important part of the activities of RU2 was devoted to experiment how the new, regionalized, weak-motion-based predictive relationships for the ground motion could be used to predict the shaking induced by large events. Also, part of the experimentation was on estimating absolute site effects at the sites of the stations used in the regional regressions (Figure 4.2). This would have allowed the prediction of the ground motion at specific site in the NEHRP (or EuroCode) classification. Data for these research activities were provided by the Berkeley Digital Seismic Network (BDSN). Figure 4.3 shows results of the predictions at moderate magnitude, whereas Figure 4.4 shows predictions for the Loma Prieta event (Mw ~ 7, well above the top of the magnitude range used for the California regressions). Results have been published under the auspices of this project by Malagnini et al. (2007).

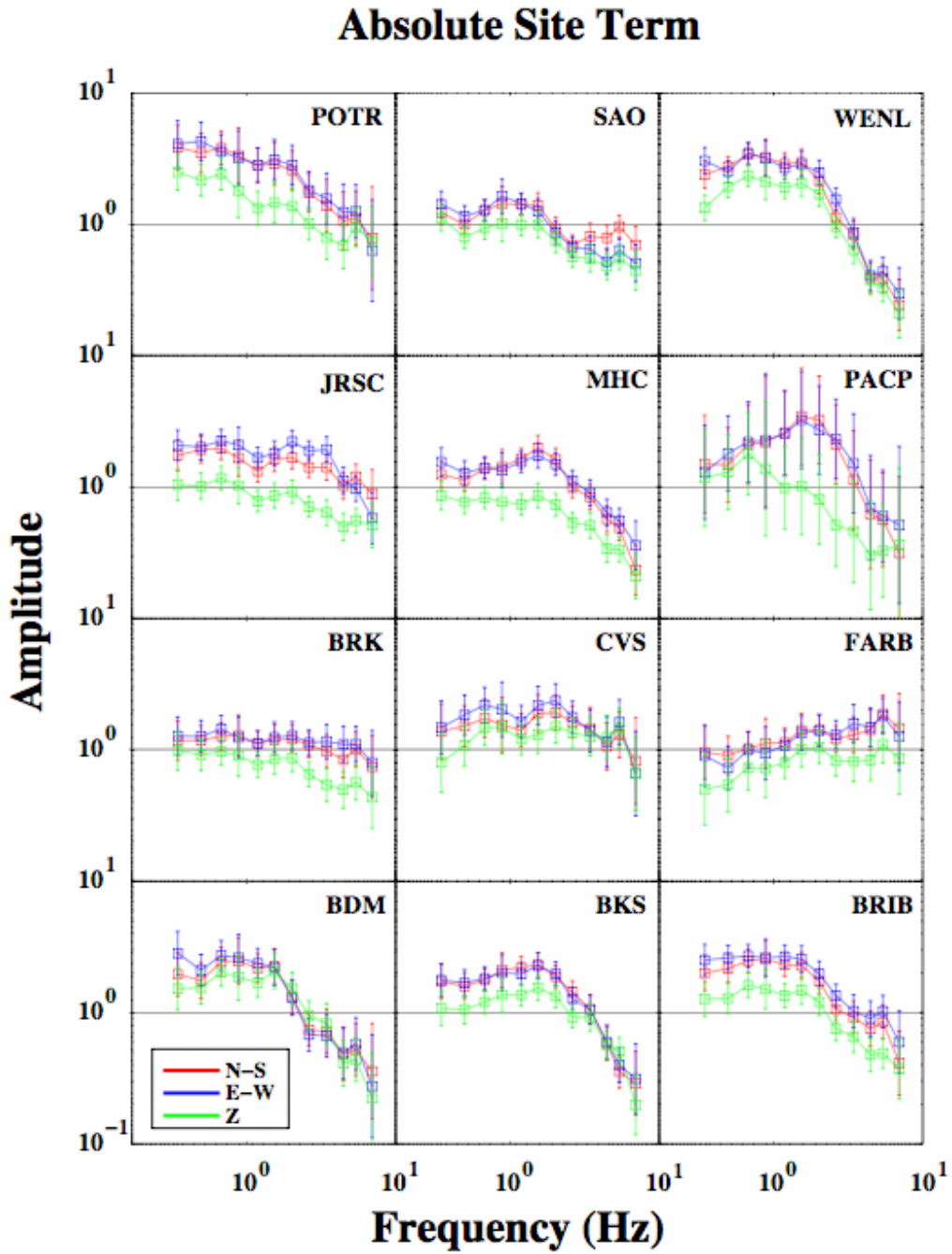


Figure 4.2: Absolute site terms for the stations of the Berkeley Digital Seismic Network: BDM, BKS, BRIB, BRK, CVS, FARB, JRSC, MHC, POTR, SAO, WENL, and PACP (N-S component, red, E-W component, blue, vertical, green).

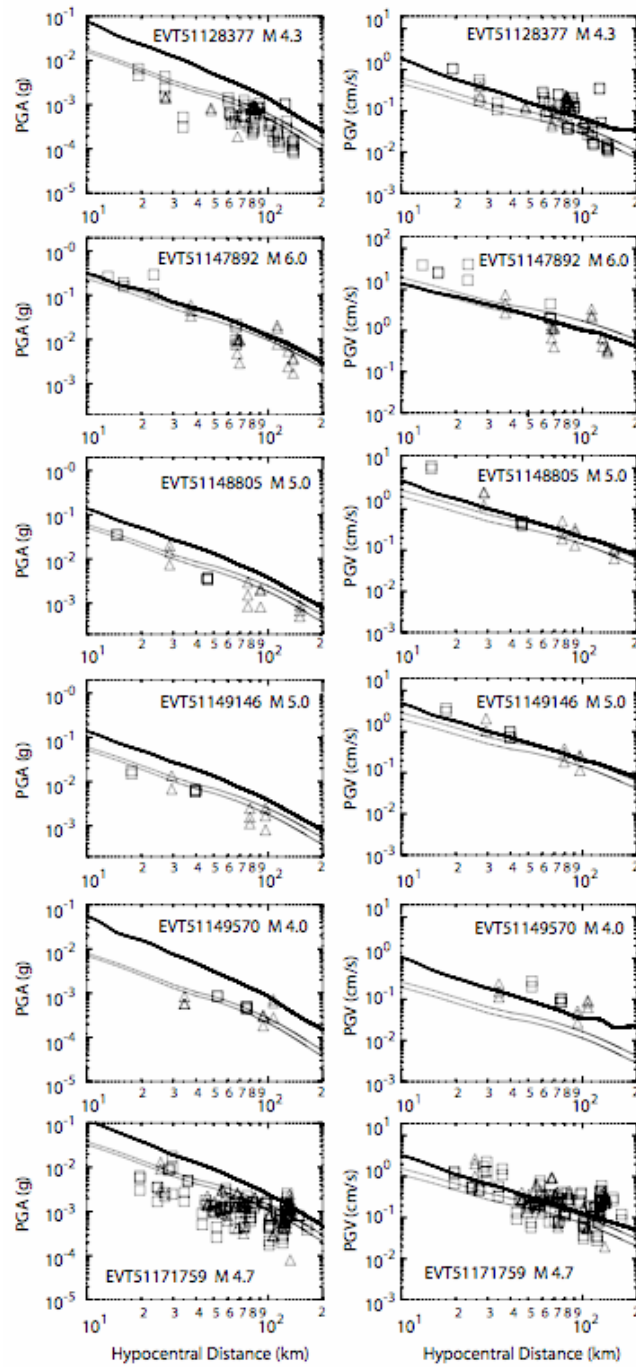


Figure 4.3: Left frames: Peak Ground Acceleration (PGA, in units of g) observed during the events listed in Table 1 (NEHRP C-class sites, squares, and NEHRP D-class sites, triangles), compared to predictions made using the model developed in this study (thin lines) for the corresponding two NEHRP classes. Thick lines represent the predictions obtained using Atkinson and Silva (2000) (AS2000) (Generic Rock Site, BC-boundary). Since AS2000 are relative to firmer site conditions, predictions for NEHRP C- and D-class sites would be amplified with respect to the presented thick lines. Right frames: Peak Ground Velocity (PGV, in units of cm/s) for the same events, for C- and D-class sites, compared with our predictions (thin lines), and with AS2000's ones (thick lines). As for the PGA's plots, AS2000's predictions are relative to the Generic Rock Site (NEHRP BC-boundary).

Loma Prieta M 7  $\Delta\sigma=15$  MPa,  $\kappa_0=0.035$  sec

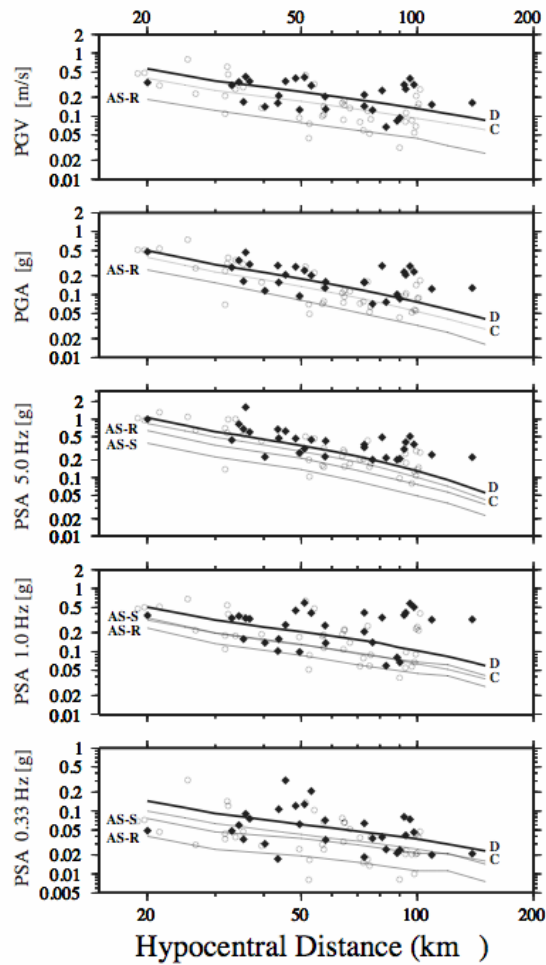


Figure 4.4: Predictions of ground shaking for the  $M_w$  7.0 Loma Prieta earthquake. Solid symbols are those from NEHRP class D sites, whereas clear symbols refer to measurements from NEHRP class C sites. Our predictions are shown as C (thin line) and D (thick line), whereas the ones from AS2000 are labeled AS-S and AS-R (soil and rock sites, respectively). Predictions are for: i) horizontal peak ground velocity (in m/s, top frame); ii) horizontal peak ground acceleration (second top frame, in units of g); iii) horizontal spectral accelerations at three reference frequencies (in units of g): 0.33 Hz, 1.0 Hz, and 5.0 Hz (bottom three panels). All our results were computed relative to the generic rock site term by Boore and Joyner (1997), integrated with the high-frequency filter  $\exp(-\pi\kappa_0f)$ ,  $\kappa_0=0.035$  sec.

The detailed knowledge of the attenuation of the seismic spectra, and of the absolute site terms (Figure 4.2), allowed the development for the BDSN of an automatic tool for the computation of  $M_w$ . Such tool works well in the entire magnitude range of the investigated data set, and includes all the available information about the network and the monitored region (see Figure 4.5).

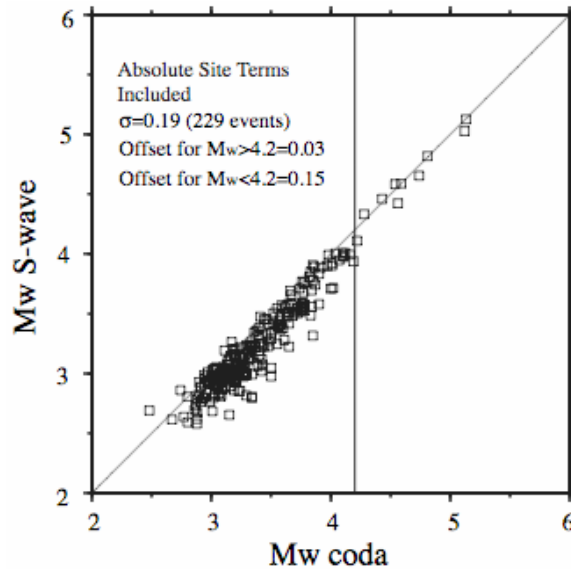


Figure 4.5: The results shown above were obtained using the code developed by Bodin et al. (2004) for the automatic computation of the moment magnitude, given  $g(r)$ ,  $Q(f)$ ,  $\kappa_0$ , and  $T(r)$  obtained from the regional study on excitation and attenuation of the ground motion. The attenuation model is given in Equation (1), with the geometric spreading and the parameter  $Q(f)$  described in the text.. Other parameters in the code are listed in the text. Duration used is the one at 1.75 Hz ( $T=\text{const.}=7$  sec for  $r < 70$  km;  $T=0.01*r$  for  $r > 70$  km,  $r$  in km). The coda-wave moment magnitudes represented our reference estimates. Y-axis: automatically obtained S-wave  $M_w$ 's, computed by correcting the observed spectra for the regional attenuation (path and absolute site terms), X-axis: "ground-truth", coda-based  $M_w$ 's, computed by Mayeda et al (2005). A residual adjustment of 0.03 magnitude units would be needed to perfectly match (in an L-1 sense), the ground-truth values. For smaller magnitudes ( $M_w < 4.2$ ), scatter is larger and a residual adjustment of 0.15 magnitude units is found.

The same kinds of tools were produced also for the Abruzzo seismic network that used to be maintained by SSN, and now is being re-instrumented and run by INGV (See Figures 4.6 and 4.7). The absolute sites were meant to be used for comparisons with theoretical site terms obtained from in-situ shear-wave velocity measurements carried out at Castelli (CAST) and Barisciano (BARI). These comparisons were unsuccessful because the boreholes could not reach the underlying bedrocks.

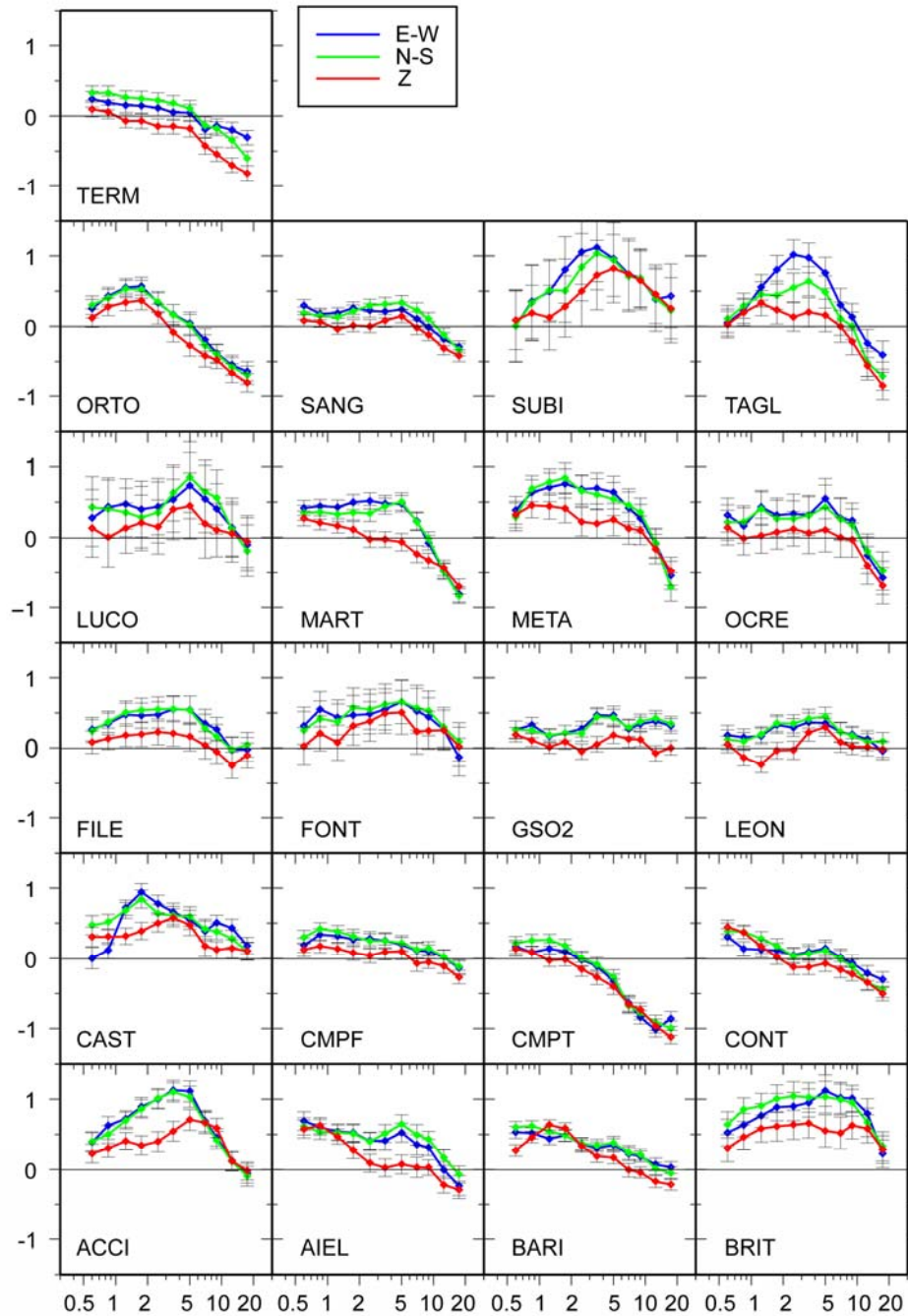


Figure 4.6: Absolute site terms for the stations of the Abruzzo network (blue: E-W component, green: N-S component, red: vertical component).

The picture on the magnitude tool for the Abruzzo network shows how well the method works at very low magnitudes, allowing the compilation of a catalog of instrumental earthquakes with no magnitude ambiguities. The large scatter at the higher end is due to the fact that the network was a short-period one, and so the S/N ratios at the lower frequencies may be a problem. The 1-to-1 correspondence between the absolute coda magnitude and the automatic  $M_w$  one for the seismicity of the low-end is a result of the excellent S/N ratios at high frequencies that is necessary to estimate the moment-rate spectral plateaus.

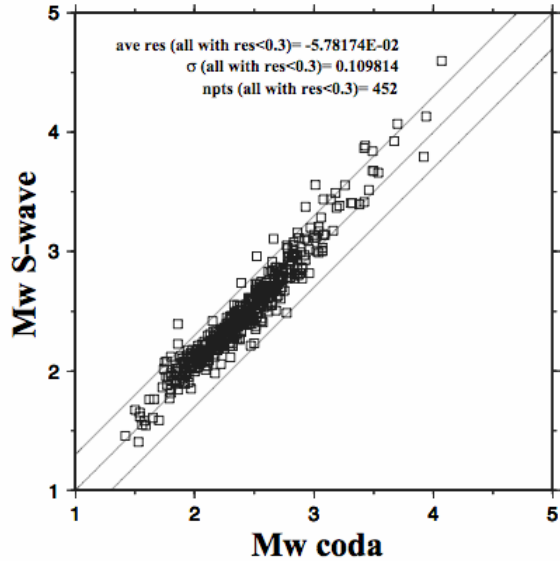


Figure 4.7: Same as Figure 4.4, for 452 events recorded by the Abruzzo network.

### ***Strong Motion Attenuation Relations***

Attenuation relationships (PGA; PGV; SA at 0.3, 1.0 and 3.0 s) have been computed by UR5 using mainly waveforms contained in the RAF database. Such database, maintained by DST, contains 570 three-component high-quality waveforms related to 362 seismic events occurred in NE Italy, Austria and Slovenia. The magnitude range is  $1.0 \leq M \leq 5.6$  and epicentral distances less than 400 km. Several high-magnitude events, occurred in the past in NE Italy and Slovenia, were considered, their waveforms being taken from the ESD database (Ambraseys et al., 2002). We chose 17 events with  $M \geq 4.5$ , the strongest one ( $M_w = 6.5$ ) being the Friuli May 6, 1976 earthquake. The dataset was also merged with observed data recorded by RSNI, INGV-CNT, INGV-MI, ARSO, SDS-net etc. in the last 30 years, resulting in a total of 612 waveforms recorded since 1976 with  $3.5 < M_L < 6.3$ , with a maximum epicentral distance of 100 km.

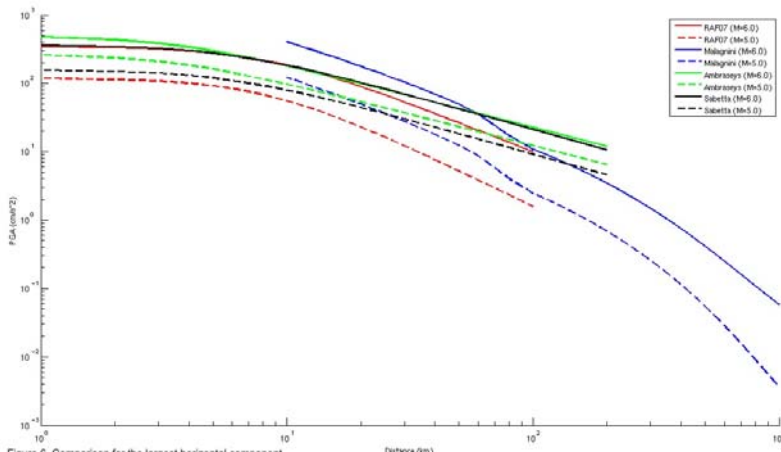


Figure 4.8: Comparison of different attenuation relations for the largest horizontal magnitude (Malagnini considers the horizontal median). Comparisons are carried out at  $M_w 5.0$  and  $M_w 6.0$ .

The relations are computed for PGA (Figure 4.8) and PGV after selecting the vertical and the largest horizontal component of the ground motion. The same relations have been computed also for the acceleration response spectra at the 12 periods ranging between 0.04 s and 2.0 s and for pseudo-velocity response spectra at the 14 periods ranging between 0.04 s and 4.0 s. Arias (Arias, 1970) and Housner intensity (Housner, 1952) and the strong motion duration (Vanmarcke and Lai, 1980) have been also computed and the respective attenuation relationships derived (Figure 4.9). different magnitude scales have been used by UR5: the ML (INGV bulletin or CPTI04 catalogue) and the Mw derived from empirical relations (Gasperini et al., 2004). The sites classification was based on EC8 and the geological information of the 1:500.000 Italian Geological Map. Two ground motion models proposed by Sabetta and Pugliese (1987; 1996) and Ambraseys et al. (2005) have been tested. The random effects model (Abrahamson and Youngs, 1992; Joyner and Boore, 1993) has been applied to estimate the earthquake-to-earthquake and record-to-record components variance. The results have been compared to the models proposed by Sabetta and Pugliese (1987; 1996) and Ambraseys et al. (2005).

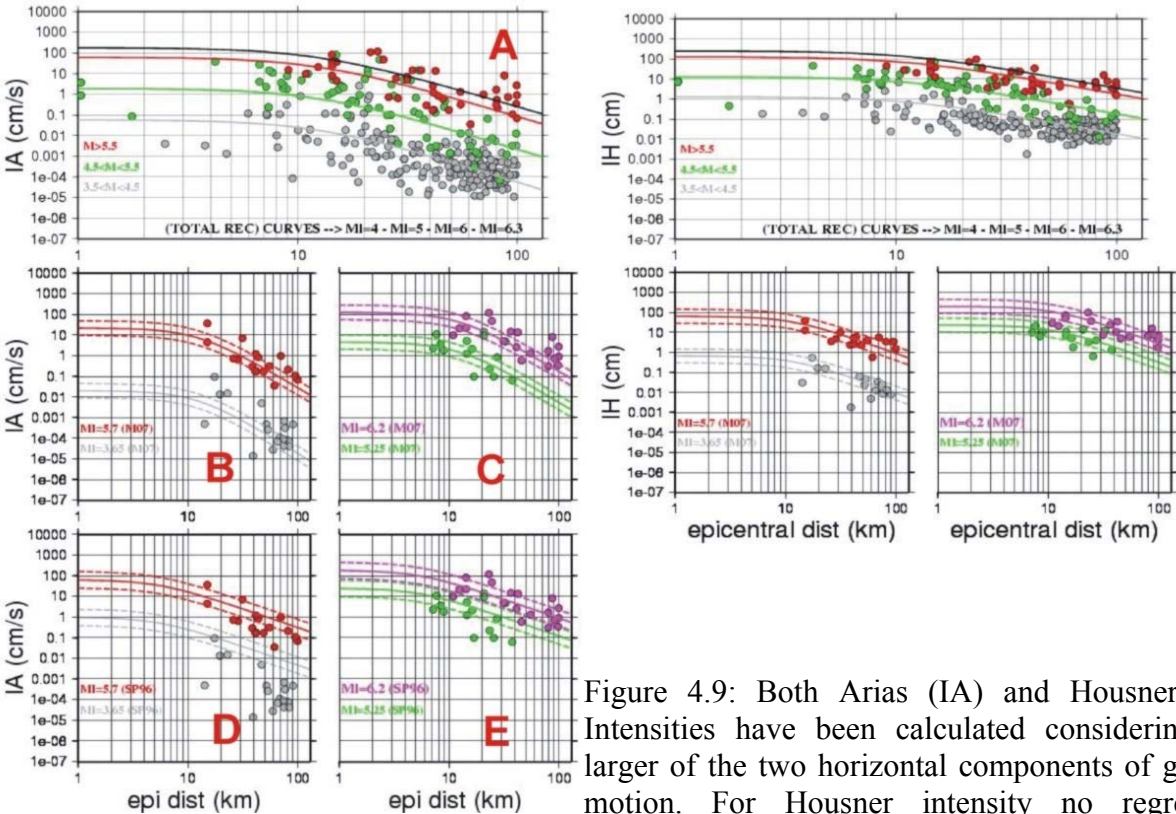


Figure 4.9: Both Arias (IA) and Housner (IH) Intensities have been calculated considering the larger of the two horizontal components of ground motion. For Housner intensity no regression coefficients (in order to make comparison) are at present available.

## Energy Scaling

We designed a new method for studying source scaling that exploits the stability of coda-based moment-rate spectra (Mayeda and Walter, 1996, Mayeda et al., 2003). A spectral ratio technique was implemented during the last year of this project by Luca Malagnini and Kevin Mayeda. Results for the Hector Mine seismic sequence, where we could use data of excellent quality, that spanned a large magnitude range, were published by Mayeda et al. (2007). By computing spectral ratios, we eliminated path and site contributions. Moreover, the coda spectral measurements are particularly stable and accurate, so that we could eliminate large uncertainties in spectral ratios, for example the ones shown for similar reasons by Izutani and Kanamori (2001). In this report we show the spectral ratios between the Hector Mine mainshock and six of its aftershocks. Since the shape of each spectral ratio is determined by the moments of the two earthquakes, by their two corner frequencies, and by the scaling properties of the seismic sources, a best-fit algorithm was written by Luca Malagnini and applied to the six ratios of Figure 4.10 to obtain information on the  $M_0$ - $f_c$  scaling, as shown in Figure 4.11. For the Hector Mine seismic sequence, we found that the best fitting model corresponded to a reference event of Mw 5.0 with an apparent stress of 0.1 MPa and a scaling parameter, ( $\psi$ ), of 0.25, in good agreement with previous studies using independent methods. Similar scaling plots are shown in Figures 4.12 and 4.13 for the multiple mainshock/aftershocks sequences of Colfiorito and San Giuliano.

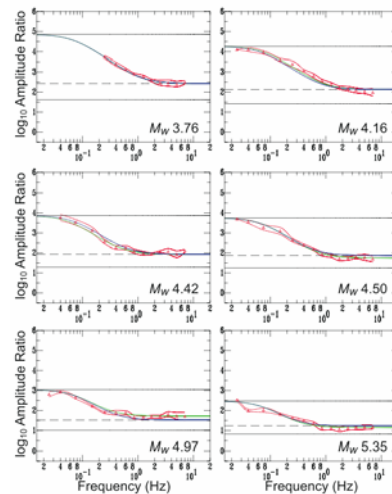


Figure 4.10: Spectral ratios for the Hector Mine mainshock relative to 6 aftershocks. In each figure, we show the low and high frequency asymptotes from equation 1 of Mayeda et al. (2007) as solid black horizontal lines and dashed lines represent the case when  $p = 1.5$ . The average for each band is shown by red triangles and red lines represent  $\pm 1s$ . Blue lines represent the best fitting MDAC spectral ratios that fit all 6 ratios simultaneously, whereas the green lines represent the case when each ratio was fit individually. We find that the best fitting model corresponds to a reference event of Mw 5.0 with an apparent stress of 0.1 MPa and a scaling parameter, ( $\psi$ ), of 0.25, in good agreement with previous studies using independent methods.

## Hector Mine Scaling

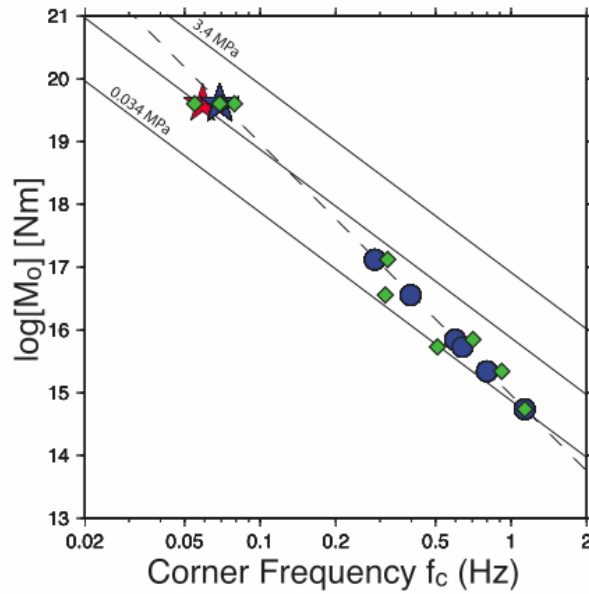


Figure 4.11: Inferred corner frequency based on a simultaneous fit to all 6 ratios (blue circles for aftershocks and blue star for the mainshock). Green diamonds are for the case when the fitting was performed individually, allowing different estimates of the mainshock corner frequency. Red star is the teleseismic estimate of the mainshock from Venkataraman et al. [2002]. Solid lines represent  $f^{-3}$  scaling which is required for self-similarity and dashed line represents best fitting scaling of  $f^{-4}$ .

## San Giuliano

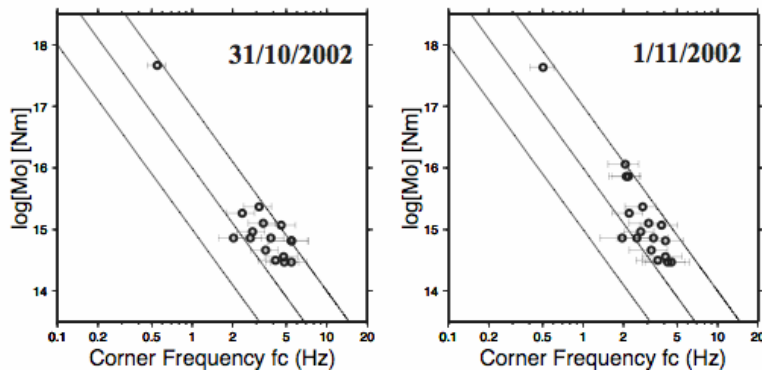


Figure 4.12: Same as in Figure 4.11, for the two mainshocks of San Giuliano, and a number of recorded aftershocks. Solid lines represent  $f_c^{-3}$  scaling.

## Colfiorito

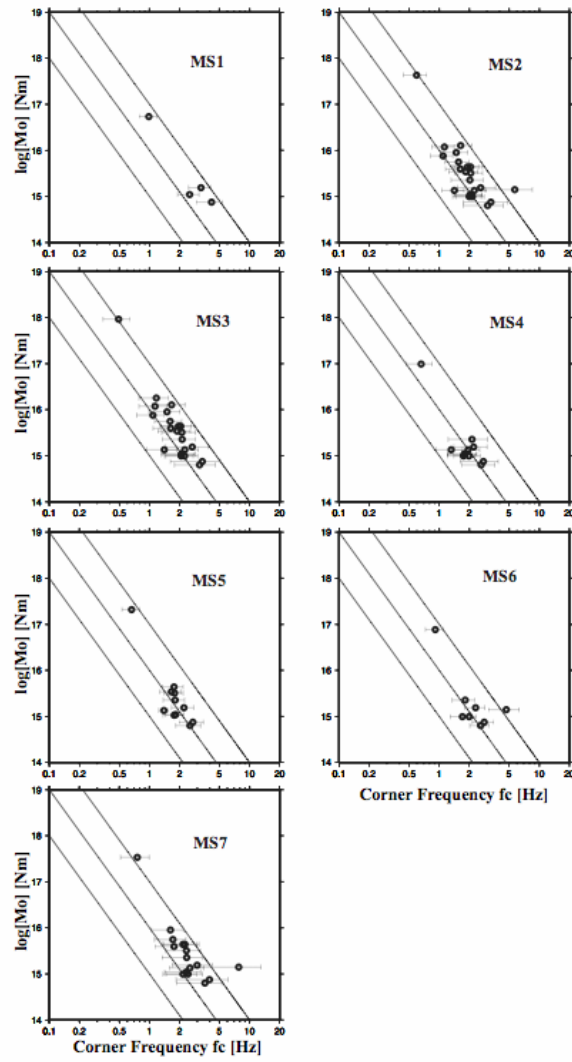


Figure 4.13: Same as in Figure 4.11 and 4.12, for the seven main events of the Colfiorito seismic sequence of 1997-1998. Solid lines represent  $f_c^{-3}$  scaling.

- **Task 5 Site effects**

ShakeMaps are generated by using data recorded at the seismic/accelerometric stations of the regional networks involved. After being corrected for site response (i.e., brought down to the bedrock), the recorded parameters (PGA, PGV, SA's) need to be propagated over the rest of the region that was hit by the earthquake, wherever direct observation of ground shaking are not available. After such propagation, in order to be "brought back to the surface", the local effect of the shallow geology ought to be applied to the ground motion parameters.. Corrections at the seismic/accelerometric stations may be done on the ground of detailed, in-situ, geophysical surveys, or simply by using a database of the shallow geology (a GIS object describing the spatial distribution of the Eurocode 8 – EC8 - site classes). At all points where the ground motion is not directly measured, site corrections are applied by using the EC8 site classification of each point on the map, whose effects are superimposed to the bedrock ShakeMaps. Our project delivered a national map of the shallow geology at the 1:100.000 scale (Figure 5.1a). Regionally, the RU's interested in the seismic monitoring used more detailed regional maps (Figure 5.1b,c).

Task 5 was of interest for all RU's, except for RU6 (Pierdicca). The most important project within the Task was the compilation of a map at the national scale with detailed information about site conditions, in terms of the EC8 classification. Differences between the EC8 and the NEHRP classifications can be easily seen by comparing Tables 4.1 and 4.2.

Another important set of activities was about the evaluation of the best rapid method for estimating site amplifications, to be applied to a large number of stations in a future effort of site classification to be done at the national scale. With respect to this topic, one important part of Task 5 was about the absolute calibration of a number of site terms of greater interest, and their investigation using borehole measurements. By comparing the different results, we would have been able to judge the level of performance of non-invasive techniques against ones that would require expensive drilling. Figure 4.5 shows absolute site terms derived through the application of a sophisticated seismicological technique. Unfortunately, funds devoted to drilling boreholes were sufficient only for a few tens of meters in depth for each of the two sites chosen (Barisciano and Castelli, of the Aquila seismic network), where we found a velocity inversion. The bedrock could not be reached at any of the sites, and so a theoretical transfer function could not be computed for comparison with the empirical results. Comparisons between results from several non invasive methods and those from a theoretical modeling based on the borehole velocity profile have been produced at a test site in Valmontone (Figure 5.2).

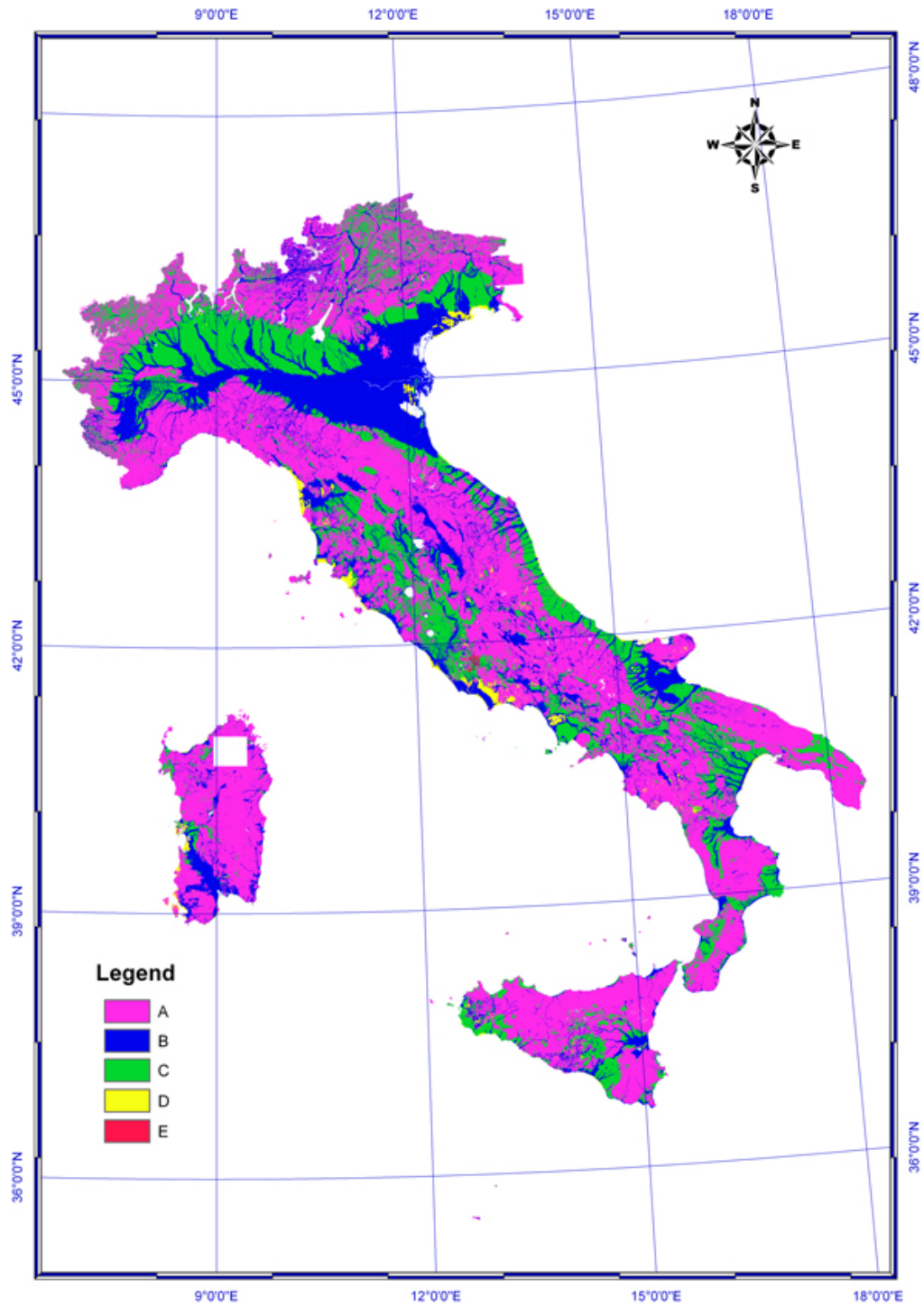


Figure 5.1a: Map of the shallow geology on the Italian region. Classification was done according to the EC8 provision (See Table 4.1 for the values of  $V_s$  averaged over the first 30 meters from the free surface).

| <b>Ground type</b> | <b>Description of stratigraphic profile</b>   | <b><math>V_{S,30}</math> (m/s)</b> |
|--------------------|---|------------------------------------|
| <b>A</b>           | <i>Rock or other rock-like geological formation, including at most 5 m of weaker material at the surface</i>  | <b>&gt; 800</b>                    |
| <b>B</b>           | <i>Deposits of very dense sand, gravel, or very stiff clay, at least several tens of m in thickness, characterised by a gradual increase of mechanical properties with depth</i>  | <b>360 – 800</b>                   |
| <b>C</b>           | <i>Deep deposits of dense or mediumdense sand, gravel or stiff clay with thickness from several tens to many hundreds of m</i>  | <b>180 – 360</b>                   |
| <b>D</b>           | <i>Deposits of loose-to-medium cohesionless soil (with or without some soft cohesive layers), or of predominantly soft-to-firm cohesive soil</i>  | <b>&lt;180</b>                     |
| <b>E</b>           | <i>A soil profile consisting of a surface alluvium layer with <math>v_s</math> values of type C or D and thickness varying between about 5 m and 20 m, underlain by stiffer material with <math>v_s &gt; 800</math> m/s</i> | -----                              |

Table 5.1: Lithotypes described in the original legend of the 1:100,000 Italian Geological Map of Figure 5.1, grouped into the five categories A, B, C, D and E from EC8.

#### NEHRP site classification

| <b>Ground type</b> | <b>Description of stratigraphic profile</b>   | <b><math>V_{S,30}</math> (m/s)</b> |
|--------------------|---|------------------------------------|
| <b>A</b>           | <i>Hard rock</i>  | <b>&gt; 1500</b>                   |
| <b>B</b>           | Firm to hard rock   | <b>760 – 1500</b>                  |
| <b>C</b>           | Dense soil, soft rock   | <b>360 -- 760</b>                  |
| <b>D</b>           | Stiff soil  | <b>180 -- 360</b>                  |
| <b>E</b>           | Soft clays  | <b>&lt;180</b>                     |
| <b>F</b>           | Special study soils, e.g., liquefiable soils, sensitive clays, organic soils, soft clays > 36 m thick | -----                              |

Table 5.2: Site categories in the NEHRP Provisions (Martin, 1994).

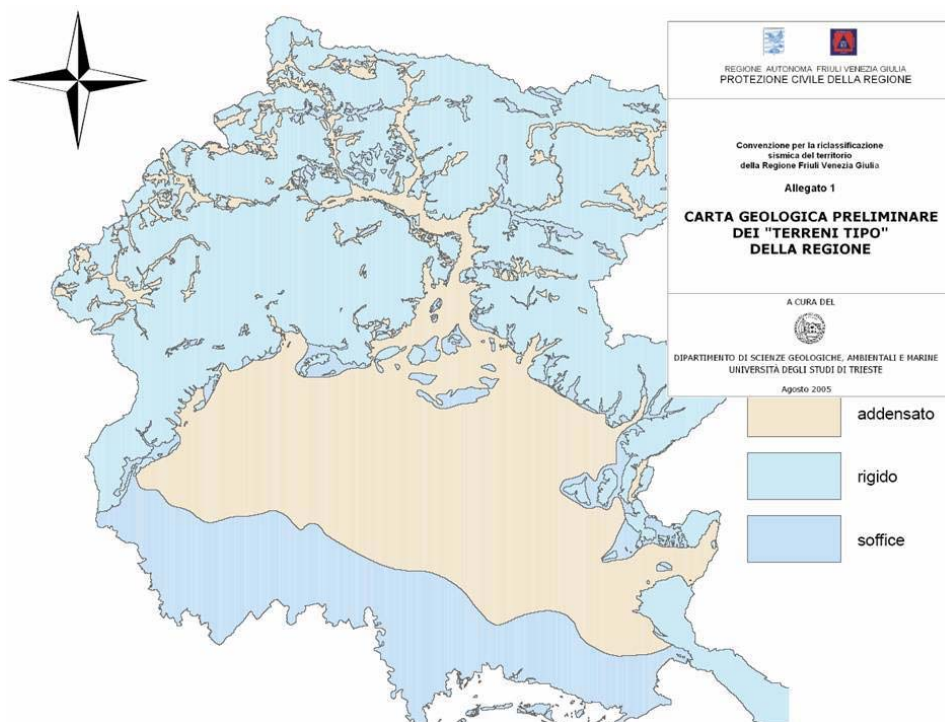


Figure 5.1b: Map of the geological classification for the Friuli-Venezia Giulia region done by the "Dipartimento di Scienze Geologiche, Ambientali e Marine dell'Università di Trieste"; the soil is classified as bedrock, stiff soil and soft soil. Classification is based on values of  $V_s30$ : "rigido" means 700 m/s; "addensato" means 500 m/s; "soffice" means 300 m/s.

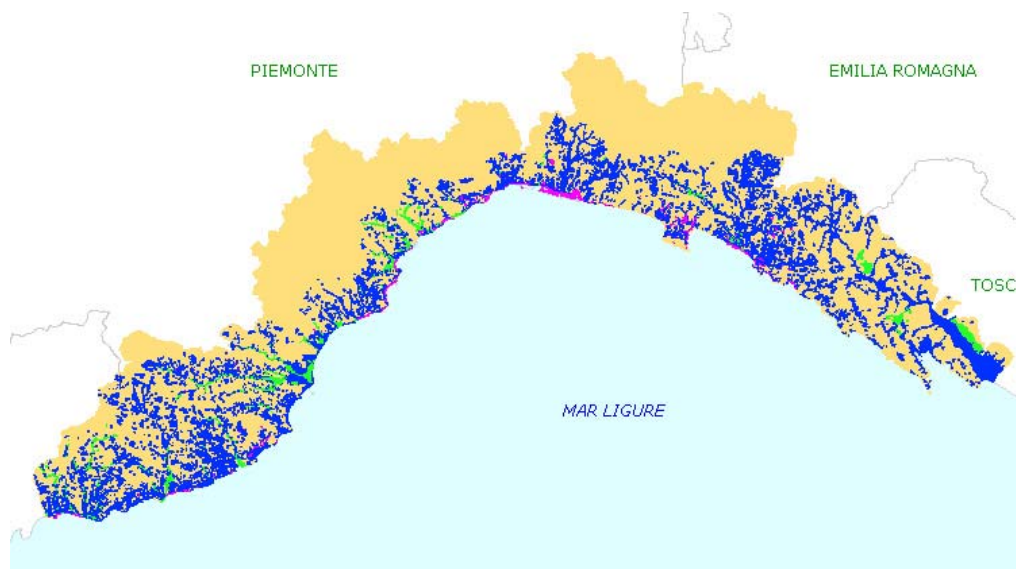


Figure 5.1c: Map of the geological classification for the Liguria region used by RU4 (University of Genova) for the generation of their ShakeMaps; the soil is classified as bedrock ( $V_s > 750$  m/s); stiff soil ( $V_s 360-750$  m/s); soft soil (180-360 m/s), and very soft soil ( $L < 180$  m/s).

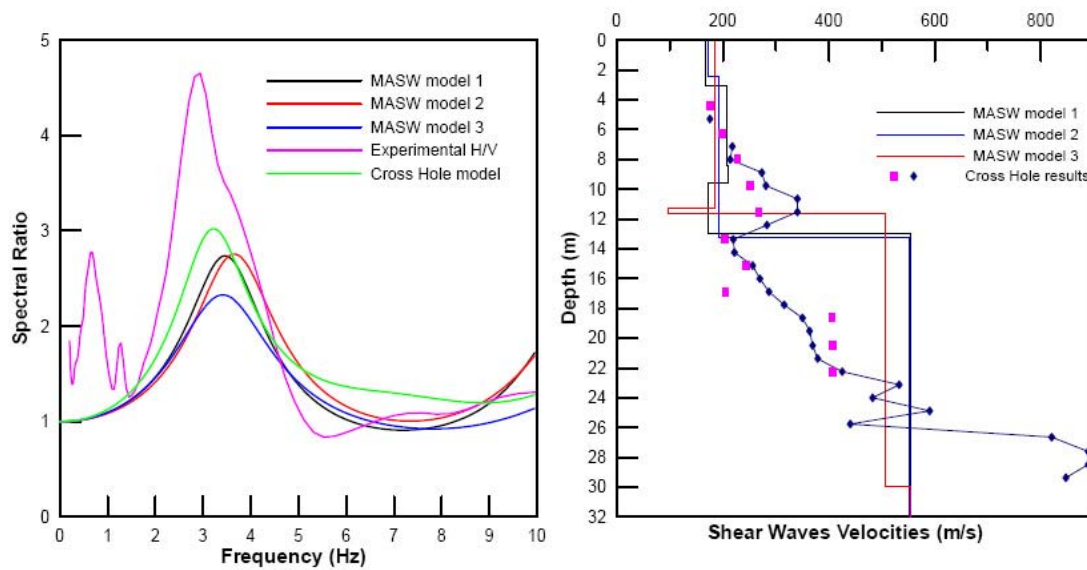


Figure 5.2: Surface analyses for Valmontone site. (A) Comparison between MASW models, H/V ratio, and Cross-hole data. (B) Comparison between shear waves velocity measured by Cross-hole and MASW models.

Different geology maps were used by the different RU's involved in Task 5. The national map was developed at INGV (RU1, Michelini), but different regional GIS' were used by RU5 (Costa) and by RU4 (Spallarossa) for their own ShakeMaps.

Other important activities were carried out within Task 5: RU3 (OGS-CRS) focused their efforts in on estimating the maximum reduction of the standard deviation,  $\sigma$  associated to predictive relationships. Their conclusions were that the reduction of  $\sigma$  may be obtainable by using either a proper site classification, or the H/V spectral ratios (HVSRS) computed from microtremors, although the use of a soil classification is often unsatisfactory, since it has only marginal effects. Researchers of RU3 have investigated on the subject by analyzing the residual from a ground motion relation for 399 values of PGA in the strong motion range (magnitude between 5 and 7.6) collected at 142 sites in Europe and the Middle East (Bragato, 2007). By applying cluster analysis to the residual they found that site effects contribute to 33% of the total  $\sigma$ , a proportion that is much higher of what found by Lee et al. (1998) in California. On the one hand, there is the theoretical possibility of reducing  $\sigma$  by 23% using only 3 categories. On the other hand, the available geological classification into 3 soil categories, chosen according to  $V_{s30}$  (soft soil, stiff soil and rock) gives no reduction of  $\sigma$ , a result similar to what found in USA for similar soil classifications (e.g., Lee and Anderson, 2000). The main conclusion of the work by RU 3 is that, in Europe, site classification could help reducing  $\sigma$ , but the current classification is inadequate, and alternative classifications should be developed.

RU3 assessed the possibility of characterizing site effects in ground motion relations using HVSRS from noise recordings. For such analysis, seismic noise was recorded at 9 accelerometric stations that were active during the 1976 Friuli seismic sequence, and spectral ratios were computed (Barnaba et al., 2006). For each station, the average ratio was computed between 1 and 8 Hz (HVSRS1-8). With the exception of one station (BUI), which experienced liquefaction effects, HVSRS1-8 is well correlated ( $R=0.78$ ) with the average station residuals

of  $\log(\text{PGA})$  computed for a ground motion relation valid for the area (Fig. 5.2).

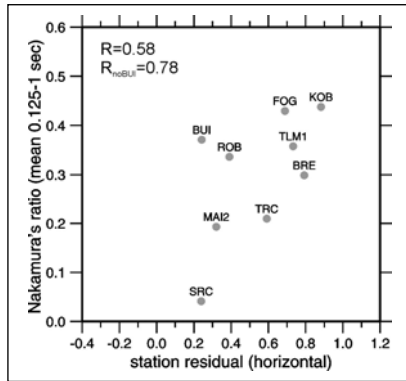


Figure 5.2: Correlation between the average station residual from ground motion relation (PGA) and the logarithm of the average HVSRs between 1 and 8 Hz computed from noise recordings at the accelerometric stations of the 1976 Friuli sequence (Barnaba et al., 2006)

Using the available PGA values and excluding station BUI, the following ground motion relation was obtained:

$$\log(\text{PGA}) = c_1 + c_2 M + c_3 \log(r) + c_4 \text{HVSRI-8}$$

for three magnitude classes (4-5, 5-6 and  $>5.8$ , including 67, 37 and 22 observations, respectively) and compared the resulting  $\sigma$  with that obtained without site correction. We found that the inclusion of the HVSR term has maximum effect at low magnitudes, for which  $\sigma$  reduces by 23%; it is still useful at intermediate magnitudes (reduction of  $\sigma$  by 14%), while its impact is marginal for magnitudes greater than 5.8 (reduction by 8%). Though the data are too scarce to draw firm conclusions, the analysis gives a useful indication about the range of applicability of the technique.

One of the sites with high amplification (Tolmezzo/Ambiesta dam, TLM1 in Figure 5.3) was studied into detail in the framework of the SEISMOVALP project cited above. The study (Barnaba et al., 2007) includes spectral analysis of the 1976 strong motion recordings, near-surface S-wave profiling by surface wave analysis and the azimuthal analysis of HVSRs. The results attribute the observed amplification to the relief and its interaction with the nearby dam-reservoir system.

Site effects at RAF stations were also studied at RU 5. A result is shown in Figure 5.4.

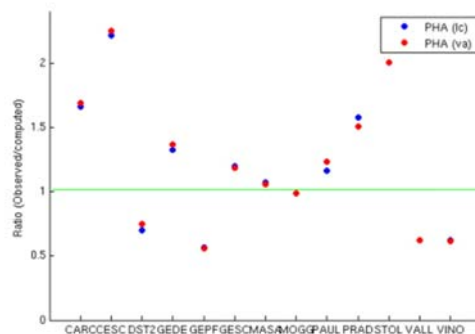


Figure 5.4: Mean value of the ratio between computed and observed PHA for the stations of the RAF. la= largest component of the ground motion (NS or EW); va=vectorial addition.

At the sites of the Berkeley Digital Seismic Network, in order to test the quality of the absolute site terms shown in Figure 4.5, we compared them against independently determined magnitude residuals. Local magnitude residuals were computed for all the stations used in this study (for the details of their computation, the reader is referred to Appendix 2 by Malagnini et al., 2007). All the magnitude residuals,  $-\delta ML(H)$  (N-S and E-W), and  $-\delta ML(V)$  (vertical) are plotted in different colors in Figure 5.5. The visual inspection of the eight frames indicate that, although all the frequencies up to 2.5 Hz show a good degree of correlation, the linear trend of the data set of 1.25 Hz is characterized by the best linear correlation (1.25 Hz is the corner frequency of the Wood-Anderson seismometer). This is in good agreement with the value of the median dominant frequency on which the  $M_L$ 's of the events in the used data set are computed ( $f_d=1.3\pm 0.3$  Hz). The central frequency of 1.75 Hz also shows an excellent correlation. The results shown in the figure are similar to the ones described by Mayeda et al. (1991), who performed a similar analysis on coda-based spectral measurements. Correlation deteriorates beyond 2 Hz, and finally breaks down at  $f=3.5$  Hz. Higher sampling frequencies (not shown in this picture) show no correlation at all.

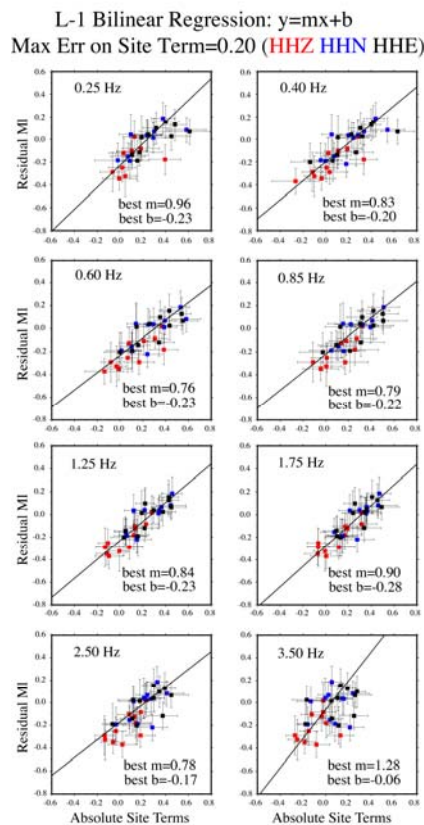


Figure 5.5: Correlation between the absolute site terms obtained at some of the central sampling frequencies, and the  $M_L$  residuals (not a function of frequency).  $M_L$  residuals were obtained by multiplying the  $M_L$  adjustments of Table A2.1 of Malagnini et al. (2007) by  $-1$ . Each frame shows all the data points with error bars on both the x- and y- axes. A bilinear regression is performed, in the L-1 sense, at each central frequency. The best parameters of the linear functions are indicated for each frequency. Note: station PACP of the Berkeley Digital Seismic Network was not included due to lack of data. The colors indicate the

component of the ground motion, as explained in the picture's title.

Finally, Table 5.3 presents a prototype form for station classification (in Italian). The form was developed by RU4, and was used for routine operations.

| Scheda geologico-geomorfologica delle stazioni sismiche della Rete Sismica |  |
|--|--|
| Nome della Stazione  | VINM   |
| Localizzazione   | Località Vinca –Chiesetta della Madonna - Fivizzano (MS)   |
| Elemento C.T.R.  | 249060   |
| Latitudine (WGS84)   | 44N0847  |
| Longitudine (WGS84)  | 10E0913  |
| quota  | 710 m.s.l.m.   |
| rilievo in sito  | l'area è collocata piede del corpo di frana in prossimità di un salto morfologico; la frana è costituita da materiale proveniente dalla creste rocciose soprastanti e presenta granulometria non classata con trovanti di dimensioni metriche. La frazione granulare prevalente è cementata per la presenza di materiale calcareo come principale costituente della frana  |
| Unità Litologico-Tecnica / Litologia                                       | U.L.T. C1<br>Detriti e discariche di cava soprastanti la Formazione di Vinca (S.G.I., 1970, Foglio 96 Massa)   |
| morfologia   | la frana, che risulta essere quiescente e/o in parte stabilizzata, è collocata in corrispondenza di un gradino morfologico di probabile origine glaciale collocato lungo un versante dall'acclività elevata ( superiore a 45°) che diminuisce bruscamente al piede della nicchia di distacco principale del corpo franoso. La presenza di una nicchia così estesa può essere ricondotta a superfici scollamento tettonico che interessano le formazioni geologiche costituenti i versanti soprastanti il corpo di accumulo |
| distanza dalla prima rottura significativa di pendio                       | la Chiesetta è ubicata a circa 50 m dal gradino morfologico glaciale ben evidente, in corrispondenza del quale si passa da una pendenza di circa 10°-15° relativa alla frana a valori molto elevati superiori a 50° fino all'alveo del torrente Lucido   |
| presenza di acque superficiali   | accumuli franosi come questo, che presentano assente o scarsissima frazione fine interstiziale, hanno un comportamento permeabile per porosità con coefficienti estremamente elevati mentre il basamento roccioso sottostante risulta essere praticamente impermeabile: la presenza di una falda sub superficiale è facilmente ipotizzabile considerato il continuo apporto dal versante roccioso soprastante e la forte presenza di acqua alla base del corpo di frana  |
| presenza di frane  | il corpo di frana su cui è ubicata la stazione sismica ha un estensione di alcuni Km <sup>2</sup> e su di esso si sviluppa l'intero centro abitato del paese di Vinca; gli spessori massimi sono nell'ordine delle decine di metri mentre in corrispondenza della stazione tali spessori sono ridotti a qualche metro  |
| prove in situ  | MASW - Sismica a rifrazione con strumentazione a 24 canali   |
| Vs 30  | 920  |
| Fenomeni di amplificazione   | Dal punto di vista geologico-stratigrafico non sono state individuate le condizioni per la presenza di effetti di sito (Sito Tipo A = roccia) anche se le condizioni morfologiche potrebbero portare a effetti di sito topografici   |

Table 5.3: Classification of seismometric station VINM. The station is classified as rock, without evidence of significant site effects of 1-D nature. 2-D effects, however, could not be ruled out due to a sharp slope disruption in the immediate vicinity of VINM.

3. Eventuali difficoltà maggiori incontrate e conseguenti modifiche di indirizzo, ecc. (*max 4 pagine*)

4. Presentazione dei deliverables, per singoli deliverable (*max 6 pagine*)

## **Deliverables:**

### **RU1 (INGV-CNT)**

---

**Deliverable:** Procedure for genetic algorithm inversion of waveforms and traveltimes

**Description:** Code for the inversion of waveform and arrival time data to determine 1-D velocity models.

**Nature:** unix scripts and fortran codes

**Contact:** Hongyi Li, Alberto Michelini, INGV, Roma, [hongyi.li@ingv.it](mailto:hongyi.li@ingv.it), [alberto.michelini@ingv.it](mailto:alberto.michelini@ingv.it)

**Availability:** at the reported contact

---

**Deliverable:** Procedure for the determination of group velocities from ambient seismic noise

**Description:** several bash scripts and fortran codes for the evaluation of the continuous data cross-correlations and the determination of group velocities

**Nature:** unix shell scripts

**Contact:** Fabrizio Bernardi and Hongyi Li, INGV, Roma, [fabrizio.bernardi@ingv.it](mailto:fabrizio.bernardi@ingv.it), [hongyi.li@ingv.it](mailto:hongyi.li@ingv.it)

**Availability:** at the reported contact

---

**Deliverable:** Procedure for real-time moment tensor determination

**Description:** several bash scripts and fortran codes for the evaluation of the moment tensor solutions using the broadband data of the Italian Seismic network

**Nature:** unix shell scripts

**Contact:** Laura Scognamiglio and Elisa Tinti, INGV, Roma, [laura.scognamiglio@ingv.it](mailto:laura.scognamiglio@ingv.it), [elisa.tinti@ingv.it](mailto:elisa.tinti@ingv.it)

**Availability:** at the reported contact

---

---

**Deliverable:** Procedure for near real-time finite fault determination

**Description:** scripts to run the finite source inversion code by Dreger and Kaverina (2000)

**Nature:** unix shell scripts

**Contact:** Elisa Tinti and Laura Scognamiglio, INGV Roma, elisa.tinti@ingv.it, laura.scognamiglio@ingv.it

**Availability:** at the reported contact

---

**Deliverable:** web interface for moment tensor solution review

**Description:** Interface to promptly review the automatic moment tensors

**Nature:** XML script

**Contact:** Matteo Quintiliani, matteo.quintiliani@ingv.it

**Availability:** At the reported contact

---

**Deliverable:** project web portal

**Description:** This deliverable allows publication of the results of the project. It consists of several unix scripts and PHP programs designed to populate the pages of the project web portal

**Nature:** bash unix scripts, PHP scripts, GMT package, HTML

**Contact:** Valentino Lauciani, valentino.lauciani@ingv.it

**Availability:** At the reported contact

---

**Deliverable:** Software for ShakeMap feeding

**Description:** Changes of earthworm module *localmag* in order to produce input for ShakeMap software

**Nature:** C code

**Contact:** Matteo Quintiliani, INGV, quintiliani@ingv.it

**Availability:** Within *Earthworm v7.1* <http://www.isti2.com/ew/>

---

**Deliverable:** Automatic control of ShakeMap Software at INGV

**Description:** Daemon for monitoring the event locations, automatic generation of shakemaps and web page publication

**Nature:** Shell scripts

---

**Contact:** Matteo Quintiliani, INGV, quintiliani@ingv.it

**Availability:** CVS Server cvs.rm.ingv.it

---

**Deliverable:** Filling Nanometrics gaps in near real time

**Description:** Added a feature to naqs\_plugin (SeisComp) in order to fill gaps in near realtime.

**Nature:** C code

**Contact:** Matteo Quintiliani, INGV, quintiliani@ingv.it

**Availability:** CVS Server cvs.rm.ingv.it

---

**Deliverable:** Nanometrics Data Completeness

**Description:** Off-line procedure to complete archived Nanometrics data. Procedure requests missing data by the "Data Access Protocol"

**Nature:** C, Perl code, shell scripts

**Contact:** Matteo Quintiliani, INGV, quintiliani@ingv.it

**Availability:** CVS Server cvs.rm.ingv.it

---

**Deliverable:** **msdc** (miniseed data completeness)

**Description:** procedure for filling waveform gaps in miniseed data archives

**Nature:** unix shell script

**Contact:** Stefano Pintore, stefano.pintore@ingv.it

**Availability:** At the reported contact

---

**Deliverable:** porting of the SeisComp seedlink-slarchive software on the INGV-GAIA data logger

**Description:** software to obtain miniseed data streams on the INGV built data loggers

**Nature:** C and XML languages

**Contact:** Stefano Pintore and Leonardo Salvaterra, stefano.pintore@ingv.it,  
leonardo.salvaterra@ingv.it

**Availability:** At the reported contact

---

**Deliverable:** Early warning procedure

**Description:** Procedure to run the ElarmS early warning package

---

**Nature:** C and Fortran language codes and unix shell scripts

**Contact:** Marco Olivieri, marco.olivieri@ingv.it

**Availability:** At the reported contact

---

**Deliverable:** SAC to Shakemap data feeding

**Description:** Off-line procedure to extract peak ground motion parameters from SAC event waveforms

**Nature:** unix and perl shell scripts

**Contact:** Alberto Michelini, alberto.michelini@ingv.it

**Availability:** At the reported contact

---

**Deliverable:** Med calculation

**Description:** Off-line procedure to determine Energy-Magnitude Duration

**Nature:** unix shell scripts and SeisGram2k program

**Contact:** Anthony Lomax, alomax@free.fr

**Availability:** At the reported contact

---

**Deliverable:** Mwp calculation

**Description:** Off-line procedure to determine Mwp (i.e., moment magnitude from broadband P-arrival phases) from Seed volumes available through ORFEUS or IRIS peak data management centers

**Nature:** unix and perl shell scripts

**Contact:** Alberto Michelini, alberto.michelini@ingv.it

**Availability:** At the reported contact

---

**Deliverable:** ISESD to Shakemap data feeding

**Description:** Off-line procedure to extract peak ground motion parameters from Internet-Site for European Strong-Motion Data

**Nature:** unix and perl shell scripts

**Contact:** Alberto Michelini, alberto.michelini@ingv.it

**Availability:** At the reported contact

---

---

**Deliverable:** NLL real-time

**Description:** procedure to feed the NLLoc location program in near real-time using the automatic picks of the INGV backnet-locator system.

**Nature:** unix and perl shell scripts

**Contact:** Alberto Michelini, [alberto.michelini@ingv.it](mailto:alberto.michelini@ingv.it)

**Availability:** At the reported contact

---

**Deliverable:** near real time ETAS implementation

**Description:** procedure to determine at 5 minutes interval maps of seismic hazard.

**Nature:** unix shell scripts, fortran codes and GMT

**Contact:** Alberto Michelini, [alberto.michelini@ingv.it](mailto:alberto.michelini@ingv.it)

**Availability:** At the reported contact

---

**Deliverable:** geologic map with soil class differentiation

**Description:** geologic map classified in five different categories starting from the 1:100,000 Italian geological map (Servizio Geologico Nazionale).

**Nature:** ASCII file has been elaborated with ArcInfo software

**Contact:** Marco Moro, [marco.moro@ingv.it](mailto:marco.moro@ingv.it)

**Availability:** At the reported contact

---

**Deliverable:** SAC waveforms event data

**Description:** procedure to convert native TWF format INGV data in SAC tar archives.

**Nature:** unix shell scripts, fortran and C codes

**Contact:** Remo Moro and Franco Mele, [remo.moro@ingv.it](mailto:remo.moro@ingv.it) [f.mele@ingv.it](mailto:f.mele@ingv.it)

**Availability:** At the reported contact

---

## **RU2 (INGV-Roma1)**

---

**Deliverable:** Preliminary study on cross-correlation of broadband ground noise and joint inversion of group velocity dispersion curves with receiver functions.

**Description:** Gathering of a data set of interstation Green's functions and of a data set of receiver functions at a number of available broadband stations

**Nature:** Codes, data, cross-correlation results

**Contact:** , INGV-Roma, [malagnini@ingv.it](mailto:malagnini@ingv.it)

**Availability:** At the reported contact

---

**Deliverable:** Web Pages to collect data on effects of earthquakes (Did you feel it?), and to show results with maps and data.

**Description:** Two main pages constitute the subject. The first page is the questionnaire used to collect info on effects felt after an earthquake. In the second page a map shows the results of elaboration in graphic and numeric output. The system is automatic and works in real time (updating time ca. 10 minutes).

**Nature:** Web code, elaboration programs code, maps and data files.

**Contact:** Valerio De Rubeis, INGV-Roma, [derubeis@ingv.it](mailto:derubeis@ingv.it)

**Availability:** <http://terremoto.rm.ingv.it/>  
<http://terremoto.rm.ingv.it/index.php?page=lis>

---

**Deliverable:** Predictive relationships for the ground motion from weak-motion data: extrapolation to strong-motion level.

**Description:** Study on wave propagation in the San Francisco Bay Area: source, absolute site, and propagation terms

**Nature:** Publication and codes.

**Contact:** Luca Malagnini, INGV-Roma, [luca.malagnini@ingv.it](mailto:luca.malagnini@ingv.it)

**Availability:** At the reported contact.

---

**Deliverable:** Automatic evaluation of moment magnitudes.

**Description:** Automatic code for the calculation of Mw in the San Francisco Bay Area.

**Nature:** Codes.

**Contact:** Luca Malagnini, INGV-Roma, [luca.malagnini@ingv.it](mailto:luca.malagnini@ingv.it)

**Availability:** At the reported contact.

---

**Deliverable:** Predictive relationships for the ground motion from weak-motion data in Central Apennine.

**Description:** Study on wave propagation in the Central Apennine: source, absolute site, and propagation terms

**Nature:** Data, empirical laws, and codes.

**Contact:** Laura Scognamiglio, INGV-Roma, [laura.scognamiglio@ingv.it](mailto:laura.scognamiglio@ingv.it)

**Availability:** INGV, Rome.

---

**Deliverable:** Predicted ground motion parameters for the Central Apennines.

**Description:** Based on the predictive relationship developed for the Central Apennines, we have computed peak ground acceleration (pga), peak ground velocity (pgv), and pseudospectral acceleration (psa) for magnitude between 2.5 and 7.5, and hypocentral distances in 10 – 1000 km range.

**Nature:** PGA, PGV and PSA (0.3, 1.0 and 3.0 sec) tables.

**Contact:** Aybige Akinci, INGV-Roma, [akinci@ingv.it](mailto:akinci@ingv.it)

**Availability:** INGV, Roma.

---

**Deliverable:** Automatic evaluation of moment magnitudes.

**Description:** Automatic code for the calculation of Mw in the Central Apennine.

**Nature:** Codes.

**Contact:** Luca Malagnini, INGV-Roma, [luca.malagnini@ingv.it](mailto:luca.malagnini@ingv.it)

**Availability:** At the reported contact.

---

**Deliverable:** Predicted ground motion parameters for the Western Alps.

**Description:** Based on the predictive relationship developed for the Western Alps, we have computed peak ground acceleration (pga), peak ground velocity (pgv), and pseudospectral acceleration (psa) for magnitude between 2.5 and 7.5, and hypocentral distances in 10 – 1000 km range.

**Nature:** PGA, PGV and PSA (0.3, 1.0 and 3.0 sec) tables.

**Contact:** Aybige Akinci, INGV-Roma, [akinci@ingv.it](mailto:akinci@ingv.it)

**Availability:** INGV, Roma.

---

**Deliverable:** Predicted ground motion parameters for the Eastern Alps.

**Description:** Based on the predictive relationship developed for the Eastern Alps, we have computed peak ground acceleration (pga), peak ground velocity (pgv), and pseudospectral acceleration (psa) for magnitude between 2.5 and 7.5, and hypocentral distances in 10 – 1000 km range.

**Nature:** PGA, PGV and PSA (0.3, 1.0 and 3.0 sec) tables.

---

**Contact:** Aybige Akinci, INGV-Roma, akinci@ingv.it

**Availability:** INGV, Roma.

---

**Deliverable:** Predictive relationships for the ground motion in Calabrian Arc from weak-motion data.

**Description:** A frequency dependent propagation term containing both anelastic, and elastic attenuation parameters.

**Nature:** Data, empirical laws, and codes.

**Contact:** Sebastiano D'Amico, INGV-Roma, damico@ingv.it

**Availability:** INGV, Roma.

---

**Deliverable:** Waveforms database for the Southern Apennines

**Description:** Data set of weak-motion waveforms for Southern Apennines.

**Nature:** Data

**Contact:** Sebastiano D'Amico, INGV-Roma, damico@ingv.it

**Availability:** INGV, Roma.

---

**Deliverable:** Waveforms database for Northern Sicily

**Description:** Database consists in velocity waveforms from 392 earthquakes recorded in Sicily by seven three component digital stations (INGV Seismic Network, and Mednet network) located in the region from October 2005 to May 2007. These events have magnitude ranging from  $M_I=1.0$  to  $M_I=4.2$ , epicentral distances comprised between few kilometers to about 300 km, and they have maximum depth around 50 km.

**Nature:** Data

**Contact:** Sebastiano D'Amico, INGV-Roma, damico@ingv.it

**Availability:** INGV, Roma.

---

**Deliverable:** Source Energy Scaling

**Description:** Method for studying self-similarity in source radiation processes: calibration of the codes and application to Hector Mine (California) seismic sequence

**Nature:** Codes, publications

**Contact:** Luca Malagnini, INGV Roma 1, luca.malagnini@ingv.it

**Availability:** At the reported contact

---

**Deliverable:** Source Energy Scaling

**Description:** Method for studying self-similarity in source radiation processes: application to

---

Colfiorito seismic sequence

**Nature:** Results  
**Contact:** Luca Malagnini, INGV Roma 1, [luca.malagnini@ingv.it](mailto:luca.malagnini@ingv.it)  
**Availability:** At the reported contact

---

**Deliverable:** Source Energy Scaling  
**Description:** Method for studying self-similarity in source radiation processes: application to San Giuliano seismic sequence  
**Nature:** Results  
**Contact:** Luca Malagnini INGV Roma 1, [luca.malagnini@ingv.it](mailto:luca.malagnini@ingv.it)  
**Availability:** At the reported contact

---

**Deliverable:** Tables of rheological parameters and stratification derived from 40 rheological profiles

**Description:** The table is divided in two parts: rheological parameters, and information about the stratification. These tables can be used with the friction law, and with dislocation creep power-law to reproduce the rheological profiles at the 40 locations where such profiles have been computed.

**Nature:** Tables of results

**Contact:** Salvatore Barba, INGV-Roma, [barba@ingv.it](mailto:barba@ingv.it)

**Availability:** INGV, Roma.

---

**Deliverable:** National geologic map at 1:100.000 scale modified according to the EC8 soil classes.

**Description:** A geologic map with soil class differentiation has been elaborated starting from the 1:100.000 Italian geological map (Servizio Geologico Nazionale). Geologic units have been unified in five different classes A, B, C, D, E according to the EuroCode8 provisions, EC8, after Draft 6, January 2003, on the base of the ground acceleration response.

**Nature:** GIS project, raster and vectorial maps, and database files.

**Contact:** Marco Moro, INGV-Roma, [moro@ingv.it](mailto:moro@ingv.it).

**Availability:** INGV, Roma.

---

**Deliverable:** Monograph of investigated recording sites.

**Description:** Description of the seismic recording site including: geographical information, stratigraphic description, geotechnical and seismological data.

**Nature:** Power Point presentation.

**Contact:** Giuliano Milana, INGV-Roma, [milana@ingv.it](mailto:milana@ingv.it).

---

**Availability:** INGV, Roma.

---

## **RU3 (OGS-CRS)**

---

**Deliverable:** Low-cost accelerometric network

**Description:** Prototype low-cost accelerometric network implemented at Tolmezzo with real-time connection to OGS/CRS and INGV/DPC

**Nature:** hardware/software system

**Contact:** Pier Luigi Bragato, OGS/CRS-Udine, [pbragato@inogs.it](mailto:pbragato@inogs.it)

**Availability:** seedlink connection over IP

---

**Deliverable:** Implementation of ShakeMap for NE Italy

**Description:** Prototype software system for production of ShakeMaps with data from OGS seismic stations in NE Italy

**Nature:** software system

**Contact:** Pier Luigi Bragato, OGS/CRS-Udine, [pbragato@inogs.it](mailto:pbragato@inogs.it)

**Availability:** At the reported contact

---

**Deliverable:** Implementation of the MT inversion software for NE Italy

**Description:** Prototype software system for MT inversion with data from OGS seismic stations in NE Italy

**Nature:** software system

**Contact:** Pier Luigi Bragato, OGS/CRS-Udine, [pbragato@inogs.it](mailto:pbragato@inogs.it)

**Availability:** At the reported contact

---

**Deliverable:** Noise recordings at the 1976 accelerometric stations

**Description:** Noise recordings and HVSRs computed for 9 accelerometric stations that recorded the 1976 Friuli seismic sequence.

**Nature:** Data files and technical report in electronic format

**Contact:** Pier Luigi Bragato, OGS/CRS-Udine, [pbragato@inogs.it](mailto:pbragato@inogs.it)

**Availability:** At the reported contact

---

---

**Deliverable:** Code for estimate an optimal site classification, OPTSITECLASS  
**Description:** Code for estimate the contribution of site variability to the overall standard deviation of a ground motion relation.  
**Nature:** Code for Linux system  
**Contact:** Angela Saraò, OGS/CRS-Udine, [asarao@inogs.it](mailto:asarao@inogs.it)  
**Availability:** At the reported contact

---

**Deliverable:** Structural model of NE Italy  
**Description:** Structural model for different areas in NE Italy used for the computation of the Green functions in MT inversion  
**Nature:** Data files  
**Contact:** Angela Saraò, OGS/CRS-Udine, [asarao@inogs.it](mailto:asarao@inogs.it)  
**Availability:** At the reported contact

---

**Deliverable:** MT solutions for recent earthquakes in NE Italy  
**Description:** Data file with the main parameters of the MT solutions for recent earthquakes in NE Italy.  
**Nature:** Data file  
**Contact:** Angela Saraò, OGS/CRS-Udine, [asarao@inogs.it](mailto:asarao@inogs.it)  
**Availability:** At the reported contact

---

## RU4 (University of Genova)

---

**Deliverable:** Automatic evaluation of moment magnitudes.  
**Description:** Automatic code for the calculation of Mw in the Western Alps and Northern Apennines.  
**Nature:** Codes.  
**Contact:** Paola Morasca, Dip.Te.Ris.-Genova, [alpocc@dipteris.unige.it](mailto:alpocc@dipteris.unige.it)  
**Availability:** At the reported contact.

---

**Deliverable:** Energy-moment scaling in the Western Alps and Northern Apennines.

---

**Description:** Based on coda waves calibration study, we derived a relationship between radiated energy and seismic moment for two regions: Western Alps and Northern Apennines.

**Nature:** Energy-moment relationship.

**Contact:** Paola Morasca, Dip.Te.Ris.-Genova, alpocc@dipteris.unige.it

**Availability:** At the reported contact.

---

**Deliverable:** Synthetic coda envelope parameters, frequency-dependent path and site correction parameters calibrated for coda waves in the Western Alps and Northern Apennines.

**Description:** Coda waves calibration studies yielded synthetic coda envelope parameters and a set of path and site correction parameters to be applied on coda waves to estimate stable seismic source parameters for the Western Alps and Northern Apennines

**Nature:** Synthetic coda envelope parameters and frequency-dependent path and site correction tables.

**Contact:** Paola Morasca, Dip.Te.Ris.-Genova, alpocc@dipteris.unige.it

**Availability:** At the reported contact.

---

**Deliverable:**  $M_W$  and  $E_R$  estimates for 1283 earthquakes occurred in the Western Alps and Northern Apennines.

**Description:** Based on the coda waves calibration studies in the Western Alps and Northern Apennines, we derived stable source spectra and hence source parameters such as  $E_R$  and  $M_W$  for 1283 earthquakes.

**Nature:** Tables of source parameters for 1283 earthquakes.

**Contact:** Paola Morasca, Dip.Te.Ris.-Genova, alpocc@dipteris.unige.it

**Availability:** At the reported contact.

---

**Deliverable:** 1D and 3D crustal models in North - Western Italy

**Description:** Study on the mono dimensional and three dimensional seismic velocity structure of the north – western part of Italy based on a selected and reliable dataset of earthquake locations and P and S phase arrival times.

**Nature:** Data and publications

**Contact:** Davide Scafidi, Dip.Te.Ris. - Università di Genova, scafidi@dipteris.unige.it

**Availability:** At the reported contact

---

## **RU 5 (University of Trieste)**

---

---

|                      |   |
|----------------------|---|
| <b>Deliverable:</b>  | Integrated shake map system for Antelope users.   |
| <b>Description:</b>  | Integrated software for event location, parameters extraction and real-time shake map computation running on Antelope system. |
| <b>Nature:</b>       | Integrated software   |
| <b>Contact:</b>      | Costa Giovanni, DST Univ. Trieste, <a href="mailto:costa@units.it">costa@units.it</a>   |
| <b>Availability:</b> | at the Dip. Scienze della Terra, University of Trieste (DST)  |

---

|                      |   |
|----------------------|---|
| <b>Deliverable:</b>  | Prototype of Matlab code for the real time Mw computation   |
| <b>Description:</b>  | Matlab code for the calculation moment magnitude Mw computation using real-time data (antelope system). |
| <b>Nature:</b>       | Code for Antelope (BRTT)-Matlab system  |
| <b>Contact:</b>      | Costa Giovanni, DST Univ. Trieste, <a href="mailto:costa@units.it">costa@units.it</a>                   |
| <b>Availability:</b> | at the Dip. Scienze della Terra, University of Trieste (DST)  |

---

|                      |   |
|----------------------|---|
| <b>Deliverable:</b>  | Datascope RAF strong motion database (1993-2006).                                     |
| <b>Description:</b>  | Strong motion database of the Friuli Venezia Giulia Accelerometric Network.           |
| <b>Nature:</b>       | Digital data  |
| <b>Contact:</b>      | Costa Giovanni, DST Univ. Trieste, <a href="mailto:costa@units.it">costa@units.it</a> |
| <b>Availability:</b> | at the Dip. Scienze della Terra, University of Trieste (DST)                          |

---

|                      |  |
|----------------------|--|
| <b>Deliverable:</b>  | Attenuation relationships (PGA, PGV, PGD, PSA Arias, Housner) for the Alps Dinarides contact and for North Italy.  |
| <b>Description:</b>  | RAF strong motion database, ISES strong motion database, RSNI, INGV-CNT, INGV-MI, ARSO, SDS-net etc. have been used to obtain attenuation relationships (PGA, PGV, PGD, PSA Arias, Housner) for the Alps Dinarides contact and for North Italy |
| <b>Nature:</b>       | Research publications  |
| <b>Contact:</b>      | Costa Giovanni, DST Univ. Trieste, <a href="mailto:costa@units.it">costa@units.it</a>  |
| <b>Availability:</b> | at the Dip. Scienze della Terra, University of Trieste (DST)   |

---

|                      |   |
|----------------------|---|
| <b>Deliverable:</b>  | Prototype of shake map WEB site.  |
| <b>Description:</b>  | WEB site prototype for the shake map publication.                                     |
| <b>Nature:</b>       | WEB site  |
| <b>Contact:</b>      | Costa Giovanni, DST Univ. Trieste, <a href="mailto:costa@units.it">costa@units.it</a> |
| <b>Availability:</b> | at the Dip. Scienze della Terra, University of Trieste (DST)                          |

---

---

|                      |   |
|----------------------|---|
| <b>Deliverable:</b>  | Accelerometric stations site monographies.                          |
| <b>Description:</b>  | Site monographies and EUROCODE classification for the RAF stations. |
| <b>Nature:</b>       | Reports   |
| <b>Contact:</b>      | Costa Giovanni, DST Univ. Trieste, costa@units.it                   |
| <b>Availability:</b> | at the Dip. Scienze della Terra, University of Trieste (DST)        |

---

## **RU6 (University of Rome – Pierdicca)**

---

|                      |  |
|----------------------|--|
| <b>Deliverable:</b>  | Method to generate “Potential damage snapshot” product from Earth observation data                               |
| <b>Description:</b>  | Prompt overview of potentially damaged area (only qualitative) (application product)                             |
| <b>Nature:</b>       | Procedure description by flow chart and/or pseudo code   |
| <b>Contact:</b>      | Nazzareno Pierdicca, Dept. Electronic Engineering - Sapienza University of Rome, nazzareno.pierdicca@uniroma1.it |
| <b>Availability:</b> | At the reported contact  |

---

|                      |  |
|----------------------|--|
| <b>Deliverable:</b>  | Method to generate “Damage level at district scale” product from Earth observation data                          |
| <b>Description:</b>  | Damage level (i.e., collapse ratio) estimated on homogeneous urban areas (application product)                   |
| <b>Nature:</b>       | Procedure description by flow chart and/or pseudo code   |
| <b>Contact:</b>      | Nazzareno Pierdicca, Dept. Electronic Engineering - Sapienza University of Rome, nazzareno.pierdicca@uniroma1.it |
| <b>Availability:</b> | At the reported contact  |

---

|                      |  |
|----------------------|--|
| <b>Deliverable:</b>  | Method to generate “Collapsed/heavy damaged buildings” product from Earth observation data                             |
| <b>Description:</b>  | Identification of single buildings collapsed or heavily damaged from very-high resolution images (application product) |
| <b>Nature:</b>       | Procedure description by flow chart and/or pseudo code   |
| <b>Contact:</b>      | Nazzareno Pierdicca, Dept. Electronic Engineering - Sapienza University of Rome, nazzareno.pierdicca@uniroma1.it       |
| <b>Availability:</b> | At the reported contact  |

---

**Deliverable:** InSAR coherence model in urban areas

**Description:** Empirical law relating the Interferometric SAR coherence to spatial baseline, temporal baseline and azimuth difference between satellite tracks (research product)

**Nature:** Regressive law coefficient

**Contact:** Nazzareno Pierdicca, Dept. Electronic Engineering - Sapienza University of Rome, nazzareno.pierdicca@uniroma1.it

**Availability:** At the reported contact

---

## **RU 7 (University of Rome, Cardarelli)**

---

**Deliverable:** training of UR7 about equipment device source SBS42 and SBS66

**Description:** meeting and short course in the manufacturing industry of the sparker source SBS42 and SBS66

**Nature:** operative ability to use the equipment in the field survey.

**Contact:** Prof. Ettore Cardarelli, "Sapienza" l'Università di Roma, [ettore.cardarelli@uniroma1.it](mailto:ettore.cardarelli@uniroma1.it)

**Availability:** at Dept. ITS, via Eudossiana, 18 – 00184 Roma

---

**Deliverable:** test and upgrading of the device source SBS66.

---

**Description:** test in Valmontone site, planning and construction of waterproof case of compass\_senso of the device source SBS66.

**Nature:** improved unit compass\_sensor

**Contact:** Prof. Ettore Cardarelli, "Sapienza" l'Università di Roma, [ettore.cardarelli@uniroma1.it](mailto:ettore.cardarelli@uniroma1.it)

**Availability:** at Dept. ITS, via Eudossiana, 18 – 00184 Roma

---

**Deliverable:** records of P and S waves in Valmontone site (RM)

**Description:** tomography map of P waves and S waves log

---

**Nature:** digital files of records and results

**Contact:** Prof. Ettore Cardarelli, “Sapienza” l’Università di Roma, [ettore.cardarelli@uniroma1.it](mailto:ettore.cardarelli@uniroma1.it)

**Availability:** at Dept. ITS, via Eudossiana, 18 – 00184 Roma

---

**Deliverable:** records of P and S waves in Barisciano site (AQ)

**Description:** tomography map of P waves and S waves log

**Nature:** digital files of records and results

**Contact:** Prof. Ettore Cardarelli, “Sapienza” l’Università di Roma, [ettore.cardarelli@uniroma1.it](mailto:ettore.cardarelli@uniroma1.it)

**Availability:** at Dept. ITS, via Eudossiana, 18 – 00184 Roma

---

**Deliverable:** records of P and S waves in Castelli site (TE)

**Description:** tomography map of P waves and S waves log

**Nature:** digital files of records and results

**Contact:** Prof. Ettore Cardarelli, “Sapienza” l’Università di Roma, [ettore.cardarelli@uniroma1.it](mailto:ettore.cardarelli@uniroma1.it)

**Availability:** at Dept. ITS, via Eudossiana, 18 – 00184 Roma

---

**Deliverable:** records of P and S waves in Gubbio (PG) site 1 and site 2

**Description:** P and S waves log

**Nature:** digital files of records and results

**Contact:** Prof. Ettore Cardarelli, “Sapienza” l’Università di Roma, [ettore.cardarelli@uniroma1.it](mailto:ettore.cardarelli@uniroma1.it)

**Availability:** at Dept. ITS, via Eudossiana, 18 – 00184 Roma

---

**Deliverable:** records of P and S waves in Valle dell’Aterno site (AQ)

---

**Description:** tomography map of P waves and S waves log

**Nature:** digital files of records and results

**Contact:** Prof. Ettore Cardarelli, “Sapienza” l’Università di Roma, [ettore.cardarelli@uniroma1.it](mailto:ettore.cardarelli@uniroma1.it)

**Availability:** at Dept. ITS, via Eudossiana, 18 – 00184 Roma

---

#### 5. Riferimenti Bibliografici (max 3 pagine)

Abrahamson, N.A., Youngs, R.R., (1992). Bull Seism. Soc. Am. 82, 505-510.

Allen R.V., 1978: Automatic Earthquake recognition and timing from single traces; Bull. Seism. Soc Am., Vol. 68, No. 5, pp 1521-1532

Ambraseys, N.N., Smit, P., Sigbjornsson, R., Suhadolc, P., Margaris, B., (2002). Internet-Site for European Strong-Motion Data, European Commission, Research-Directorate General, Environment and Climate Programme.

Ambraseys, N.N., Douglas, J., Sarma, S.K., Smit, P.M., (2005). Bull. Earthq. Eng. 3, 1-53.

Arias, A., (1970). A measure of earthquake intensity. In: Seismic Design of Nuclear Power Plants, R. Hansen (Editor), M.I.T. press, Cambridge.

Barnaba C., Bragato P.L. and Romanelli M., 2006. Acquisizione ed elaborazioni H/V di misure di rumore ambientale nei siti della Rete Temporanea ENEL-ENEA del 1976-77, OGS report Rel. OGS 2006/67-CRS 12.

Barnaba C., Priolo E., Vuan A. and Romanelli M., 2007. Site effect of the strong-motion site at Tolmezzo-Ambiesta dam in northeastern Italy, Bull.Seism.Soc.Am. 97, 339-346.

Bernard P., and A. Zollo, 1989, The Irpinia (Italy) 1980 earthquake: detailed analysis of a complex normal faulting, J. Geophys. Res. 94, 1631-1647.

Bodin P., Luca Malagnini L and Aybige Akinci (2004). Ground-Motion Scaling in the Kachchh Basin, India, Deduced from Aftershocks of the 2001  $M_w$  7.6 Bhuj Earthquake, Bulletin of the Seismological Society of America, Oct 2004; 94: 1658 - 1669.

Boore, D. M. and W. B. Joyner (1997). Site amplifications for generic rock sites, *Bull. Seism. Soc. Am.*, v. 87, p. 327-341.

Bragato P.L., 2007. Optimal site classification for empirical ground-motion relations, submitted to Bull.Seism.Soc.Am.

Bressan G., 2005. Modelli di velocità 1D dell’Italia nord-orientale, OGS report Rel. OGS 2005/20-CRS 5.

Chini M., F. Pacifici F., Emery W.J N. Pierdicca, (2006) “A comparison between statistical and neural network approaches within a common processing scheme for detecting urban changes from high resolution image of Rocky Flats”, *Submitted to IEEE Transaction on Geosciencie and Remote Sensing*.

Chini M., Bignami C., Stramondo S. And N. Pierdicca (2006). "Uplift and subsidence due to the December 26th, 2004, Indonesian earthquake and tsunami detected by SAR data". *Accepted for publication in the International Journal of Remote Sensing*.

Console, R. and M. Murru (2001), A simple and testable model for earthquake clustering, *J. Geophys. Res.*, 106, 8699-8711.

Console, R., A.M. Lombardi, M. Murru and D. Rhoades (2003), Bath's law and the self-similarity of earthquakes, *J. Geophys. Res.*, 108 (B2), 2128, doi: 10.1029/2001JB001651.

Console, R., M. Murru, and A.M. Lombardi (2003), Refining earthquake clustering models, *J. Geophys. Res.*, 108, 2468, doi: 10.1029/2002JB002130.

Console, R., M. Murru, and F. Catalli (2005), Physical and stochastic models of earthquake clustering, *Tectonophysics*, 417, 141-153.

Console, R., D.A. Rhoades, M. Murru, F.F. Evison, E.E. Papadimitriou and V.G. Karakostas (2006), Comparative performance of time-invariant, long-range and short-range forecasting models on the earthquake catalogue of Greece, *J. Geophys. Res.*, 111, B09304, doi:10.1029/2005JB004113.

Console, R., M. Murru, F. Catalli, and G. Falcone (2007), Real time forecasts through an earthquake clustering model constrained by the rate-and-state constitutive law: Comparison with a purely stochastic ETAS model, *Seismological Research Letters*, 78, 49-56.

Cocco, M. and F. Pacor, 1993, The rupture process of the 1980 Irpinia, Italy, earthquake from the inversion of strong motion waveforms, *Tectonophysics*, 218, 157-177.

Douglas J., Aochi H., Suhadolc P., Costa G. (2007). The importance of crustal structure explaining the observed uncertainties in ground motion estimation. *Bull. Earthquake Engineering* 5:17-26.

Dreger, D. S. (2003). TDMT\_INV: time domain seismic moment tensor inversion, *International Handbook of Earthquake and Engineering Seismology*, W.H.K. Lee, H. Kanamori, P.C. Jennings, and C. Kisslinger (Editors), Vol B, 1627 pp.

Dreger D.S., and Helmberger D.V. (1993). Determination of source parameters at regional distances with 3-component sparse network data, *J. Geophys. Res.*, 98, 8107-8125.

Dreger D., and Kaverina A., 2000, Seismic remote sensing for the earthquake source process and near-source strong shaking: A case study of the October 16, 1999 Hector mine earthquake, *J. Geophys. Res.*, 27 (13), 1941-1944.

Furlanetto E., Costa G., Suhadolc P., Palmieri F. (2007) Gravimetric characterization of the Gemona (NE Italy) alluvial fan for site estimation, submitted to *Near Surface Geophysics*.

Gasparini, P., Gruppo di lavoro per redazione della mappa di pericolosità sismica prevista dall'ordinanza PCM 3274 del 20 Marzo 2003 (2004). *Catalogo dei terremoti CPTI2 - App. 1 al rapporto conclusivo*, open file report., 1-29.

Gentili, S., 2006. Identificazione delle sequenze di aftershock nelle Alpi nord-orientali, OGS report Rel. OGS 2006/71-CRS 15.

Gentili S. and Bressan G., 2007. The aftershock sequences in the Friuli - Venezia Giulia region and western Slovenia in the last thirty years. OGS report Rel. OGS 2007/16-CRS 5.

Housner, G.W., (1952). Spectrum intensities of strong-motion earthquakes. In: *Proc. Symp. on Earthquake and Blast Effects Structures*, C. M. Feigen (editors), Univ. California, Los Angeles, 21-36.

Lahr J.C., 1979: Hypoellipse: a computer program for determining local earthquake parameters, magnitude, and

first motion pattern, U.S. Geol. Surv., Open File Rep. 79-431 pp.

Lomax A., Curtis, A. (2001). Fast, probabilistic earthquake location in 3D models using oct-tree importance sampling, *Geophys. Res. Abstr.*, **3**, 955.

Lee, Y., and Anderson J.G., 2000. Potential for improving ground-motion relations in southern California by incorporating various site parameters, *Bull. Seism. Soc. Am.* **90**, S170–186.

Lee, Y., Zeng Y. and Anderson J.G., 1998. A simple strategy to examine the sources of errors in attenuation relations, *Bull. Seism. Soc. Am.* **88**, 291-296.

Lomax A., 2005: A Reanalysis of the hypocentral location and related observations for the great 1906 California Earthquake - *Bull. Seism. Soc. Am.*, **95**, 861-877.

Lomax A., Curtis, A. (2001). Fast, probabilistic earthquake location in 3D models using oct-tree importance sampling, *Geophys. Res. Abstr.*, **3**, 955.

Lomax, A., Virieux, J., Volant, P. and Berge C. (2000). Probabilistic earthquake location in 3D and layered models: introduction of a Metropolis – Gibbs method and comparison with linear locations, in *Advances in Seismic Event Location*, C. H. Thurber and N. Rabinowitz (Editors), Kluwer, Amsterdam, 101-134.

Lomax A., Zollo A., Capuano P. e Virieux J., 2001: Precise, absolute earthquake location under Somma-Vesuvius volcano using a new 3D velocity model - *Geophys. J. Int.*, **146**, 313-331.

Izutani Y. and Kanamori, H. (2001), Scale-dependence of seismic energy-to-moment ratio for 33 strike-slip earthquakes in Japan. *Geophys. Res. Lett.* **28**, 20, 4007-4010.

Malagnini L., K. Mayeda, R. Uhrhammer, A. Akinci, and R. B. Herrmann (2007). A Regional Ground-Motion Excitation/Attenuation Model for the San Francisco Region, *Bulletin of the Seismological Society of America*, **97**(3): 843 - 862.

Malagnini L., Aybige Akinci, Robert B. Herrmann, Nicola Alessandro Pino, and Laura Scognamiglio (2002). Characteristics of the Ground Motion in Northeastern Italy, *Bulletin of the Seismological Society of America*, **92**: 2186 - 2204.

Malagnini L., Robert B. Herrmann, and Massimo Di Bona (2000). Ground-Motion Scaling in the Apennines (Italy), *Bulletin of the Seismological Society of America*, **90**: 1062 - 1081.

Mayeda, K., S. Koyanagi, and K. Aki (1991). Site amplification from S-wave coda in the long Valley Caldera region, California, *Bull. Seism. Soc. Am.*, **81**, 2194-2213.

Mayeda, K. M., and W. R. Walter (1996), Moment, energy, stress drop, and source spectra of western U.S. earthquakes from regional coda envelopes, *J. Geophys. Res.*, **101**, 11,195 – 11,208.

Mayeda, K., Hofstetter, A., O'Boyle, J.L., Walter, W.R., (2003), *Bull. Seismol. Soc. Am.* **93**, 224–239.

Mayeda, K., R. Gök, W. R. Walter, and A. Hofstetter (2005), Evidence for non-constant energy/moment scaling from coda-derived source spectra, *Geophys. Res. Lett.*, **32**, L10306, doi:10.1029/2005GL022405.

Mayeda, K., L. Malagnini, and W. R. Walter (2007), A new spectral ratio method using narrow band coda envelopes: Evidence for non-self-similarity in the Hector Mine sequence, *Geophys. Res. Lett.*, **34**, L11303, doi:10.1029/2007GL030041.

Morasca P., Mayeda K., Malagnini L. and Walter W.R., 2005a: Coda-derived source spectra, moment magnitudes and energy-moment scaling in the Western Alps; *Geophys. J. Int.*, **160** (1), 263-275.

- Morasca, P., Mayeda, K., Gök, R., Malagnini, L., Eva C. (2005). A break in self-similarity in the Lunigiana-Garfagnana region (Northern Apennines). *Geophysical Research Letters* Vol. 32, No. 22, L2230110.1029/2005GL024443.
- Morasca, P., L. Malagnini, A. Akinci, D. Spallarossa, and R.B. Herrmann (2006). Ground-Motion Scaling in the Western Alps, *Journal of Seismology*, Vol. 10, pp. 315-333.
- Olivieri, M., R. M. Allen, and G. Wurman (2007). The potential for Earthquake Early Warning in Italy using ElarmS, *Bull. Seism. Soc. Am.*, submitted.
- Piatanesi A., A. Cirella, P. Spudich and M. Cocco, 2007, A global search for earthquake kinematic rupture history: Application to the 2000 western Tottori, Japan earthquake, *J. Geophys. Res.*, in press.
- Pondrelli, S., A. Morelli, G. Ekström, S. Mazza, E. Boschi, and A. M. Dziewonski, 2002, European-Mediterranean regional centroid-moment tensors: 1997-2000, *Phys. Earth Planet. Int.*, 130, 71-101, 2002
- Pondrelli S., A. Morelli, and G. Ekström, European-Mediterranean Regional Centroid Moment Tensor catalog: solutions for years 2001 and 2002, *Phys. Earth Planet. Int.*, 145, 1-4, 127-147, 2004.
- Pondrelli, S., S. Salimbeni, G. Ekström, A. Morelli, P. Gasperini and G. Vannucci, The Italian CMT dataset from 1977 to the present, *Phys. Earth Planet. Int.*, [doi:10.1016/j.pepi.2006.07.008](https://doi.org/10.1016/j.pepi.2006.07.008), 159/3-4, pp. 286-303, 2006.
- Rovelli A., O. Bonamassa, M. Cocco, M. Di Bona and S. Mazza, 1988, Scaling laws and spectral parameters of the ground motion in active extensional areas in Italy, *Bull. Seism. Soc. Am*
- Sabetta, F., Pugliese, A., (1987). *Bull. Seism. Soc. Am.* 77, 1491-1513.
- Sabetta, F., Pugliese, A., (1996). *Bull. Seism. Soc. Am.* 86-2, 337-352.
- Saraò A., 2007. Feasibility study of automatic moment tensor determination at CRS. OGS report Rel. OGS 2007/60-CRS 16.
- Sean R. Ford, Douglas S. Dreger, Kevin Mayeda, William R. Walter, Luca Malagnini, and William S. Phillips. Regional Attenuation in Northern California: A Comparison of Five 1-D Q Methods. *Bull. Seim. Soc. Am.* (2007), submitted.
- Shapiro N. M., M. Campillo (2004), Emergence of broadband Rayleigh waves from correlations of the ambient seismic noise, *Geophys. Res. Lett.*, 31, L07614, [doi:10.1029/2004GL019491](https://doi.org/10.1029/2004GL019491).
- Shapiro N. M, Campillo, M., Stehly, L. and M. H. Ritzwoller (2005), High resolution surface wave tomography from ambient seismic noise, *Science*, 307, 1615-1617.
- Sleeman, R., and T. v. Eck (1999). Robust automatic P-phase picking: an on-line implementation in the analysis of broadband seismogram recordings, *Phys. of the Earth and Planet. Int.*, 113, 265-275.
- Somerville, P.G., K. Irikura, R. Graves, S. Sawada, D. Wald, N. Abrahamson, Y. Iwasaki, T. Kagawa, N. Smith, and A. Kowada, Characterizing crustal earthquake slip models for the prediction of strong ground motion, *Seism. Res. Lett.*, 70, 59-80, 1999.
- Spallarossa D., Ferretti G., Bindi D., Augliera P. e Cattaneo M. (2001): Reliability of earthquake location procedures in heterogeneous areas: synthetic tests in the South Western Alps, Italy, *Phys. Earth Plan. Int.*, 123
- Spallarossa D., Bindi D., Augliera P. and M. Cattaneo (2002a). An MI scale in Northwestern Italy, *Bull. Seism. Soc. Am.* Vol. 92, 2205-2216 pp.
- Stramondo S., Bignami C., Chini C., Pierdicca N. And A. Tertulliani (2006) "The radar and optical remote sensing for damage detection: results from different case studies". *International Journal of Remote Sensing*, Volume 27, N. 20, 20 October, 2006.

- Vanmarcke, E.H., Lai, S.P., (1980). *Bull. Seism. Soc. Am.* 70, 1293-1307.
- Venkataraman, A., L. Rivera, and H. Kanamori (2002), Radiated energy from the 16 October 1999 Hector Mine earthquake: Regional and tele- seismic estimates, *Bull. Seismol. Soc. Am.*, 92, 1256 – 1265.
- Wald, D.J., Quitoriano, V., Heaton, T.H., Kanamori, H., (1999a). *Earthquake Spectra* 15, 557-563.
- Wald, D.J., Quitoriano, V., Heaton, T.H., Kanamori, H., Scrivner, C.W., Worden, C.B., (1999b). *Earthquake Spectra* 15,537-555.
- Wald, D. J., Worden, C. B., Quitoriano, V., and K. L. Pankow (2006). ShakeMap® Manual, technical manual, users guide, and software guide, available at <http://pubs.usgs.gov/tm/2005/12A01/pdf/508TM12-A1.pdf>, 156 pp.
- Wells D.L. and K.J. Coppersmith, 1994, New empirical relationships among magnitude, rupture length, rupture width, rupture area, and surface displacement, *Bull. Seism. Soc. Am.*, 84 (4): 974-1002.
- William R. Walter, Kevin Mayeda, Luca Malagnini, and Laura Scognamiglio. Regional body-wave attenuation using a coda source normalization method: Application to MEDNET records of earthquakes in Italy. *Geophys. Res. Lett.*, May 2007, Vol. 34, No. 10.
- Wiemer, S., and M. Wyss (1994), seismic quiescence before the Landers (M=7.5) and Big Bear (M=6.5) 1992 earthquakes, *Bull. Seismol. Soc. Am.*, 84, 900-916.
- Zhu, L., and Kanamori, H. (2000), Moho depth variation in southern California from teleseismic receiver functions: *J. Geophys. Res.*, no. B2, p. 2969-2980.

